ARC FLASH HAZARDS ANALYSIS

by

ZHENYUAN ZHANG

Presented to the Faculty of the Graduate School of

The University of Texas at Arlington in Partial Fulfillment

of the Requirements

for the Degree of

DOCTOR OF PHILOSOPHY

THE UNIVERSITY OF TEXAS AT ARLINGTON

December 2015

Acknowledgements

I would like to express deep gratitude to my supervising professor, Dr. Wei-Jen Lee for his guidance, encouragement, patience, and support throughout my entire doctoral program at the University of Texas at Arlington. He encouraged me to not only grow as an electrical engineer but also grow as independent and creative thinker. Also, I would like to take this opportunity to convey my sincere gratitude to Dr. Lee for extending his support and guidance leading me to complete this dissertation. I am blessed to have adviser like him.

I would like to thank my doctoral dissertation committee members: Dr. William E. Dillon, Dr. Rasool Kenarangui, Dr. David A. Wetz, and Dr. Ali Davoudi. Thanks for their valuable and detailed instruction, suggestions and review.

I would also like to thank for the members of the Energy Systems Research Center. Thank for all of their helps and the friendship in last six and half years. They are not only the team members in my researches but also bring me laugh, happiness, and inspirations during the stressful graduate life. Also, I want to express my great thanks to Mr. Lydon Lee, who helps me a lot on the dissertation revision.

I wish to thank for all the Steering Committee and Technical Advisory Committee members of IEEE/NFPA collaboration on arc flash phenomena research project. Thank for their support and valuable suggestions and guidance throughout the project. It is my great honor to be a part of the team.

Finally, I would dedicate my dissertation to my parents. Their support, encouragement, patience and unwavering love were serving as my continued source of inspiration for the tenure of my doctoral degree. Without them, this work would never have been accomplished.

November 20, 2015

Abstract

ARC FLASH HAZARDS ANALYSIS

Zhenyuan Zhang, PhD

The University of Texas at Arlington, 2015

Supervising Professor: Wei-Jen Lee

Annually more than 2000 workers are admitted to hospital burn centers for extensive injuries caused by arc flash accidents. Arc flash incidents occur when unintended electric current flows through air, superheating the air and causes an explosion. Recognizing the significant threat posed by arc flash hazards, IEEE and NFPA have joined forces on an initiative to support research and additional testing to increase the understanding of the arc flash phenomena.

Accurately represent all the real applications for arc flash events are very difficult, not only because of their random complex nature, but also because a large number of uncertain variables involved. Several areas of the arc flash phenomena need further research and testing validation. In order to have a precise arc flash hazards assessment, approximately 2000 arc flash experiments had been conducted, which are crossed extensive range of system voltage, bolted fault current, electrodes gap width, arc initiative configuration and enclosure dimensions.

This dissertation has reviewed the testing methodology, test equipment design and modeling process for arc flash hazards analysis. The research and testing focused on, but will not be limited to (a) the development of physics and engineering-based modeling for arc flash thermal hazards, and (b) design and testing for non-thermal hazards, such as light, pressure and sound.

Based on the works of the dissertation, sets of assessment equations and approaches have been proposed for arc flash thermal and non-thermal hazard analysis. The results of this dissertation will provide information to help more accurately predict the hazards associated with high energy arcing faults, thereby improving electrical safety standards and providing practical safeguards for employees in the work place.

Table of Contents

List of Illustrations

List of Tables

Chapter 1

Introduction

1.1 Introduction of arc flash phenomenon

According to the records, approximately 5 to 10 arc flash explosions occur on the electrical related job every day in the United States. On Average, 4000 non-disabling and 3600 disabling electrical contact causes injuries, and over 2000 workers are sent to burn centers with arc flash related burn injuries every year [1]. Though electrical incidents represent a relatively small percentage of all work related incidents, they are disproportionately fatal and may result in extended hospitalization and rehabilitation, especially for thermal hazards from arc flash.

Arc flash occurs when an electric current passes through an air gap between electrified conductors, or from the energized conductor to the ground, when the insulation or isolation is not sufficient to withstand the applied voltage.

Arcing faults are sometimes initiated when cheap meters, lacking adequate insulation for the available energy levels, explode during troubleshooting. Environmental contaminants such as metallic dusts, vermin, and forgotten articles or tools can also lead to the development of arcing faults. Arcing faults are known to develop in aging equipment, especially when they are not properly maintained and inspected. Arcing faults can also be unintentionally initiated when workers drop a tool or wire, which provides a temporary path between two energized phases or between the phase and the ground.

While the arc flash event itself may only last couple of cycles, the results can be lasting, ranging from superficial burns to debilitating injury, and even to death.

1.2 Overview of arc flash hazards

During the arcing event, the current creates successive and repulsive magnetic force, which dramatically expended plasma cloud. The cloud is driven outward of

electrode tips, and then pushes the molten materials ejected off the tips along with the cloud flow. Moreover, when the arc is being established, the current begins to ionize the air, then releases massive quantities of heat after the ionization process. Huge heated gases may combine with vaporized conductors and expel them out through the explosion. With arcs continually forming, electrical energy is kept to be converted into extremely hazardous energy forms. Figure 1-1 illustrates the forms of arcing hazards mechanism. Personnel hazards due to the release of energy generated by an arc event may include: immense heat, large volumes of toxic gases, molten droplets, sound, pressure, and extremely intense light, which all affect personnel.

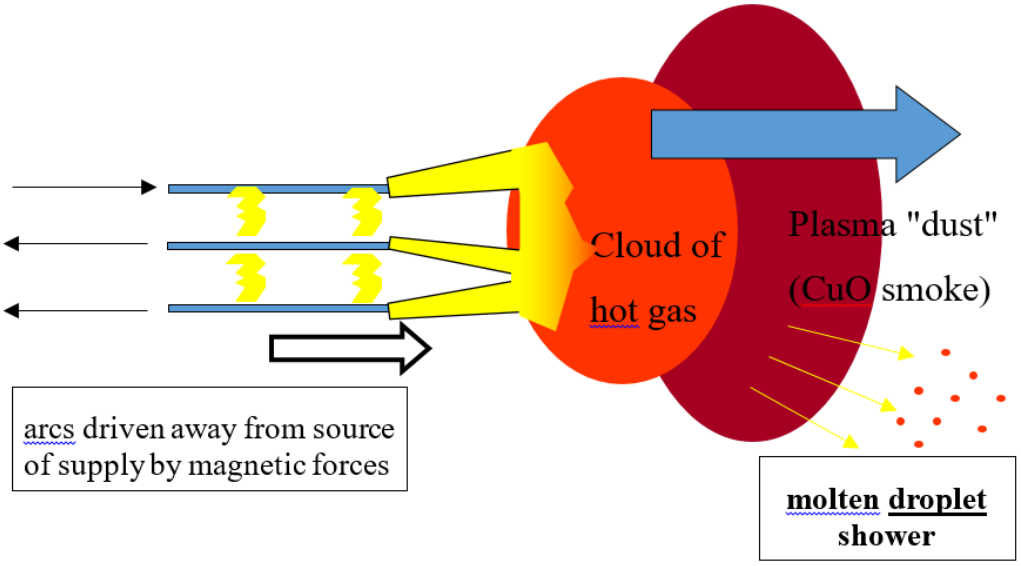

Figure 1-1 Arc flash behaviors and hazards formed mechanism [2]

- Burn

The extremely high temperature levels of the plasma or gas produced by arc event may result in severe burns. The melted solid metal fragments or superheated steam can cause secondary or even third degree burns. Also, high temperature may start a fire on clothes and gloves. Flames can cause all types of burns, and in certain severer

condition, carbonization may happen. Figure 1-2 shows the burning hazards on equipment and personnel caused by arc flash.

Figure 1- 2 Arc flash burning on equipment and personnel [3]

- Ejected materials

The ejection of metal particles or loose parts of equipment itself caused by arc blast may result in severe injuries to parts of a human body, such as eyes, head and chest. The materials expelled due to the explosion produced by arc may penetrate the weak parts of a human body [4].

- Blast and pressure waves

When an arcing fault is initiated, the gases expand rapidly in the vicinity of the arc. The blast pressure can also cause severe injures for humans. The intense blast pressure generated by an arc flash can be dangerous. Severely air pressured waves with propel force in the surrounding area can blow workers off their feet or knock them off ladders, and even wound the human body with projectile parts. Figure 1-3 shows the blast during an arc flash test.

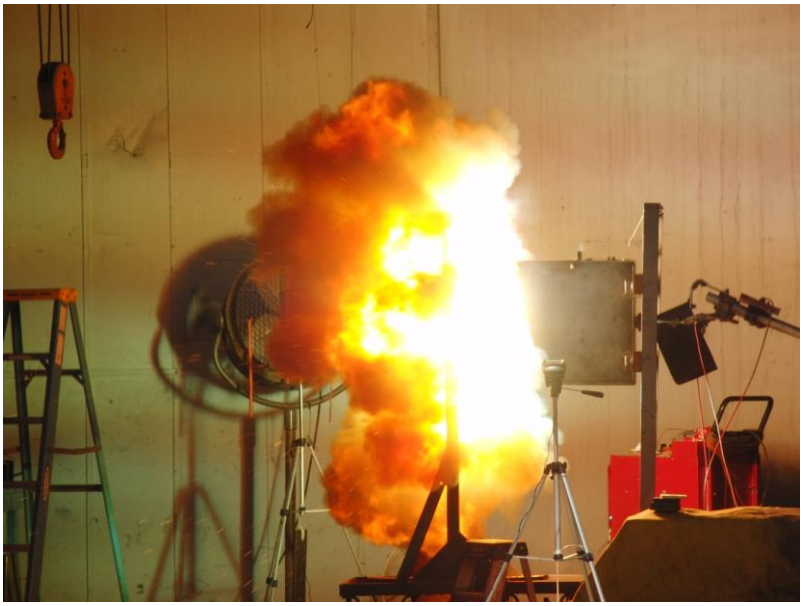

Figure 1- 3 Arc blast of arc flash event

- Intense light

The intense light generated by an arc flash can be dangerous; eye injuries account for about 4.2 percent of all arc flash related injuries [5]. Temporary blindness due to sudden bright light, known as flash blindness, is a common occurrence. High-intensity light in the visible, infrared (IR), and ultraviolet (UV) spectrums can damage important structures such as the cornea or retina.

- Intense sound

During the arc event, the blast makes intense and huge sound, which may cause permanent hearing loss. During recent arc tests involving arc currents from 5 to 30 kA, all sound pressures measured over 140 dB at a distance of 10 feet from the arc [6].

- Toxic gases and vapors

The fumes produced by burnt insulating materials or vaporized metal can be toxic. During the burning process, particles, dusts and solid substances can suspend in the air, which is also fatal to inhalation.

Those hazards due to arc flash are the typical part of the picture for overall worker safety. NFPA 70E, provides a hazard risk analysis procedure flowchart. It implies that each establishment must perform a number of tasks and establish training and safety procedures that should be implemented for workers' safety.

1.3 Research motivation

The safety of both personnel and equipment when performing tasks on energized equipment is a growing concern. Due to the dangerous nature of arc flash hazard conditions, work is being done to establish industry standards for personal protective equipment (PPE) when electrical hazards are present.

As in the earlier editions of NFPA 70E, the 2004 Edition has included a table [Table 130.7(C) (9)] that provides a qualitative assessment of the arc flash hazard risk based on worker task. Although the qualitative task based determination of risk is still approved by the latest version of the NFPA 70E, it is valid only within the given boundaries. For applications outside of those boundaries, a growing concern about arc flash injury has led to an increased demand for more exacting methods of predicting arc flash risks.

First published in 2002, IEEE 1584, "Guide for Performing Arc Flash Calculations", has become the predominant method in the industry for performing arc flash calculation studies. This guide provides detailed incident energy and arc current calculation methods based upon around 300 data set from the lab testing [7].

Although the 1584 model was shown to fit the data well, concern has arisen on how well the IEEE 1584-2002 can predict the arcing current and the incident energy associated with "real-world" arcing faults and other possible configurations. Since the models in IEEE 1584-2002 are developed from statistic relationships recorded through limited arc testing designed to simulate real arcing currents and incident energy levels,

they are only valid within the range of measured data. Besides, a statistical analysis is not truly based on physical observation, it may introduce incorrect relationships which do not really exist or may obscure fundamental phenomena.

Thus, the existing equations may not completely describe known arc flash behaviors when variables or combination of variables relationships fall outside the test range. For example, the limited test configurations defined by IEEE 1584 are not fully covered by the equipment conditions or fault occur position. In addition, from the modeling side, discontinuities occurs at 1000V threshold separating low voltage systems from medium voltage systems.

Other anomalies are pointed out at the research articles authored by D. Sweeting and R. Wilkins [8] [9] [10].

Recognizing the weakness and limitations of IEEE 1584-2002, Institute of Electrical and Electronics Engineering (IEEE) and National Fire Protection Association (NFPA) have joined forces on an initiative to support research and additional testing to increase the understanding of the arc flash phenomena. In particular, these efforts are intend to predict the hazards associated with arc faults and the accompanying arc blasts in order to provide practical workplace safeguards.

Although the works from this research are mainly focuses on the modeling of thermal hazards related arcing current and arcing energy, the non-thermal effects of the arc blast, including blast pressure, sound and visible light are also studied through proper tests and measurement. In the 2005 NFPA/IEEE Research and Testing Planning Committee (RTPC) report, David Wallis analyzed 454 public OSHA records on investigations involving electric arcs, non-thermal injuries were reported in 7.3% of the remaining 424 records involving electrical faults [5].

In previous records and researches, the testing approaches and measurement device reliability are limited by the destructive environments for arc flash tests, and also by dynamic nature of arc itself. The inaccurate measurement results, such as light intensity or pressure intensity, are quite doubt by public. From this IEEE/NFPA arc flash research project, the well-defined testing approaches and well-designed measurement system are established to ensure the accuracy of data recording. The test results of this research will provide information to help more accurately predict the hazards associated with high energy arc flash to improve electrical safety standards and provide safeguards for employees in the work place.

1.4 Research objective

Arc flash analysis requires an extensive understanding of power system, electronics, electromagnetic effects, plasma flow properties and magneto hydrodynamics, at extremely high current, voltage and energy, which make the research a highly complex situation.

Though the most effective way to protect workers from arc flash hazards is to de-energize the circuit before attempting to work on or near the exposed conductors, some works must be performed on energized equipment or environment. When those works under an electrified system, an electrical hazard analysis must be conducted, which will determine such as the voltage level for personnel exposed, arc flash incident energy estimation, safety protection boundary defined.

Generally, the purpose of arc flash analysis is to assess potential arc flash hazards and the corresponding risk of injury. This analysis is necessary to address the highly specific and complex physics and engineering aspects of arc flash events in order to provide useful, reliable guidelines for use in actual practice across a broad range of different electrical equipment and work environments.

In developing improved arc flash hazard assessment processes, it is important to understand the various essential factors, such as bolted fault current and electrode gap width, and how they combine to produce highly unpredictable and highly dynamic arc flash incidents. Additionally, it is critical to understand how these hazards can be quantified, in order to provide guidelines and procedures that promote the greatest possible level of overall workplace and environmental safety.

To address these issues, arc flash hazards analysis in thermal part of this dissertation is trying to model arcing currents, incident energy and protection boundary, which can be used to classify the arc flash thermal risk and determine personal protective equipment (PPE) level for those personnel who may be exposed in a potential arc flash event. These models may base on physics-empiric with statistic aided, in order to provide deeper and more precise insight to understand the characteristic of arc flash.

In non-thermal hazards part, the proper and durable measurement schemes are designed and implemented to achieve accurate and reliable measurement. These studies pave the road for both qualitative and quantitative arc flash hazards analysis and estimation.

1.5 Dissertation overview

In this dissertation, two parts of work could be categories: arc flash thermal hazards modeling, and non-thermal hazards measurement.

In thermal hazards modeling, this dissertation described testing methodology and modeling process. The identified areas of the thermal hazard related work include but not limited to:

- Curial parameter identification
- Equipment configuration analysis
- Arcing current modeling

- Incident energy modeling
- Arc flash protection boundary calculation

This effort will include the development of physics and empiric based models on both arcs in the open air and inside the enclosures commonly found in electrical systems, such as switchgear, motor control centers and power panels.

In non-thermal hazards part, the works will focus on arc blast pressure, sound and light hazards. The identified area of non-thermal hazards include but it is not limited to:

- Non-thermal arc flash hazards description and analysis
- Specified measurement equipment design for light hazard, pressure hazard and sound hazard
- Non-thermal hazard testing and measurement approach validation

These non-thermal measurement work tries to overcome the limitation of the traditional approaches and to increase the reliability and accuracy of the testing. It will provide a feasible way to perform arc flash hazards measurement in different arc flash occurrence environments.

Chapter 2

Review on arc flash researches

2.1 Nature of arcing phenomena

An electric arc is an electrical breakdown of the resistance of air or gas, which can occur where there is sufficient voltage in an electrical system and a path to lower voltage, or ground. Figure 2-1 shows the breakdown phenomenon when arc happens in the air.

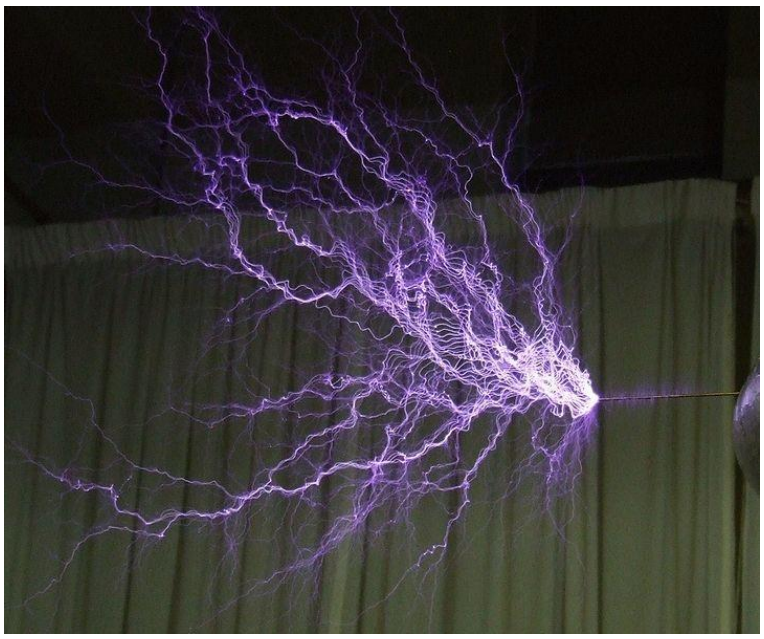

Figure 2- 1 Electrical breakdown in the air [11]

An arc flash is a rapid energy release which can cause excessive heat exposure and serious burn injuries. The results of this violent event may cause destruction of equipment, fire, and injury, which may not only be fatal to the worker but also to nearby personnel. Such burns are typically second or third degree in nature and may cause death within few days of the accident. The safety of both personnel and equipment in arc flash exposure environments is a growing concern. According to Electrical Safety

Foundation International (ESFI), electrical hazards cause more than 3000 deaths and 4000 injuries per year in the United States alone [12]. Figure 2-2 shows an arcing event in a test cell.

Figure 2- 2 Destructive arc blast in test cell [13]

Sustained arcing sometimes begins with an initial sputtering that heats the electrodes and carbonizes the nearby insulation. Arcs can self-sustain or re-ignite every half cycle; the re-ignition is accompanied by a popping sound as a current is conducted through ionized air. Even 208V systems can sustain three phase arcs because the phase shift allows for the arc space to remain ionized when one arc current passes through current zero [14]. During the recent test conducted by IEEE/NFPA collaborative arc flash research team, laboratory tests have produced arcs sustained for RMS supply voltages as low as 208V at 2.5kA.

In the past, industry and standard association, such as IEEE, NEC, OSHA and UL, have put lots of effort to design prevalent standards tried to cover every aspects of

electrical system. However, arc flash hazard was not a direct consideration into the scope before. With the increasing concern on serious arc flash hazards, industry is heading toward to mitigate the arc flash hazards, as it is detrimental to worker safety. This opens another era of the power system safety design, analysis, and calculations.

2.2 Arc initiation

Arc may be initiated in several ways. In power systems, arcs may form through “glow to arc” transitions. The glow state is characterized by a large voltage drop and low current flow in the cathode region. The release of electrons from the cathode initiated the transition from the glow to the arc, which is characterized by a smaller voltage drop and larger current flow in the cathode region [15]. Figure 2-3 illustrates the shape of the static voltage/current characteristic for transitions through several discharges until an arc is formed, and the specific voltage and current magnitudes differ with conditions.

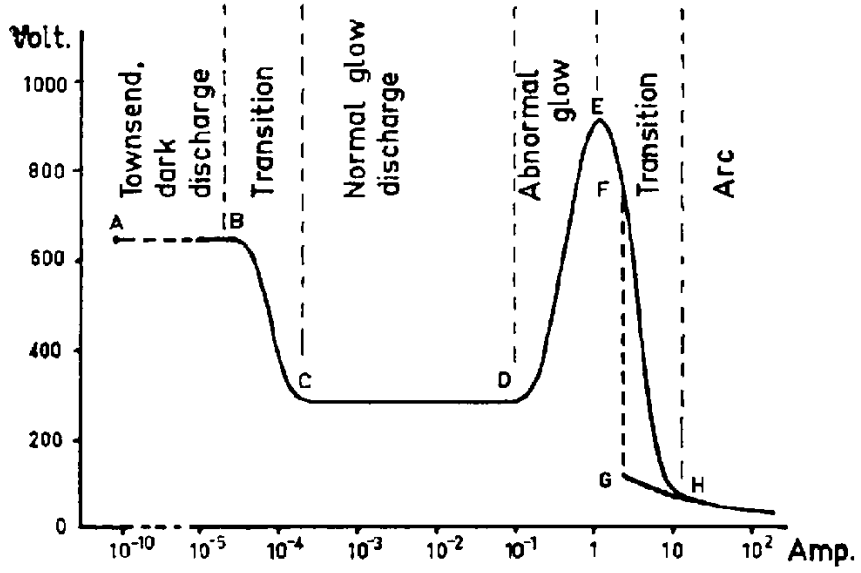

Figure 2- 3 Arc transition [15]

Moreover, arc can also result from a spark discharge. The discharge is initiated when the voltage between two electrodes is sufficient to break down the air or gas in

some particular environment [15]. The breakdown of voltage and the rise in current for an arc are displayed in Figure 2-4.

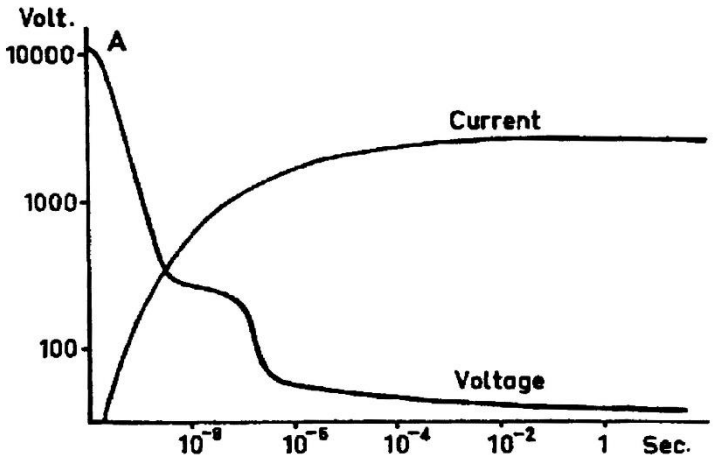

Figure 2- 4 Arc formation from spark discharge (at 1 atm) [15]

2.3 Arc regions and arc column

An arc is an electrical discharge flowing between two electrodes through air. The voltage drop across the cathode region must provide the minimum ionizing potential of the air. An arc can be divided into three general regions: the cathode (negative electrode) region, the anode (positive electrode) region, and the positive column or plasma. These regions are illustrated in Figures 2-5.

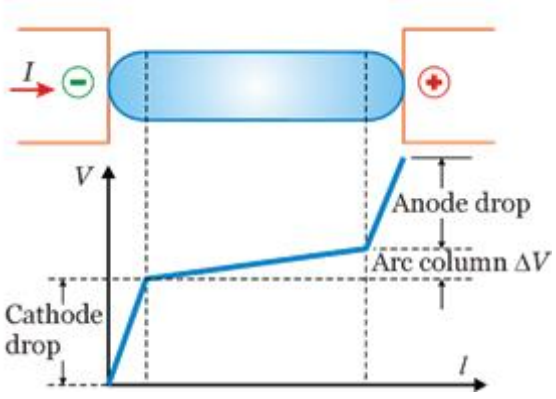

Figure 2- 5 Distribution of arc voltage

The voltage drop of the cathode region is comprised of the cathode fall and the drop in the cathode boundary layer. Generally, the cathode falls between 8 and 20 V over a region of 1 to 10 μm [16]. From the geometry viewpoint, the voltage drop in the anode region is divided in a similar manner and varies. The anode fall is generally between 1 to 12 V over a region of approximately 1 μm [16]. The voltage gradient across the positive column always in a uniform trend [17], but it depends on the length of the arc and the magnitude of the arc current.

The cathode and anode regions can be subdivided as shown in Figure 2-6. In the cathode's contraction zone, the current density varies from the current density at the positive column on one end to a density which almost equals the cathode density at the other end. The temperatures in the cathode's contraction zone may be between the temperatures found in the positive column and the cathode fall region, or they may actually exceed the temperatures in the positive column due to the increased density of charge carriers because of the contraction [16].

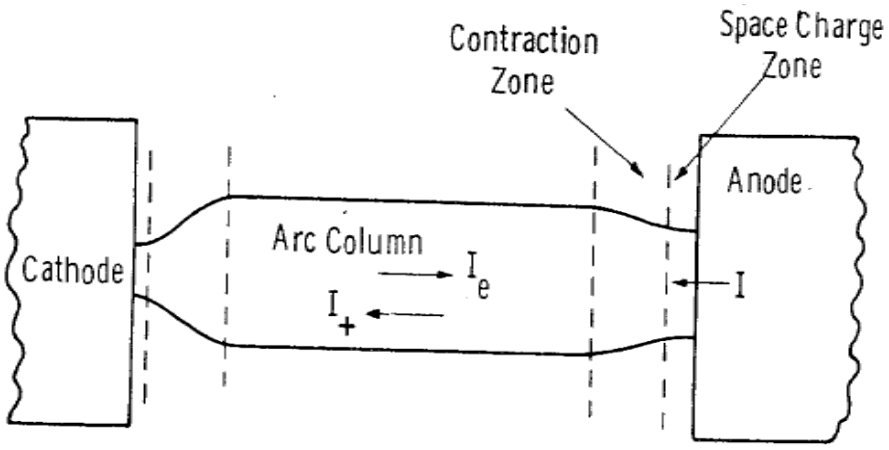

Figure 2- 6 Contraction and space charge zones [18]

Energy balance must be preserved at the electrodes and in the positive column. The cathodic energy remaining after ion bombardment and electron emission is primarily

released by vaporizing the cathode material [19]. Electrodes reach vaporization temperatures as quickly as 1 μs [20]. The anode also balances the energy input through vaporization of electrode material. For arc currents greater than 30 A, the electrodes also lose energy by radiation outward from the surface; furthermore, the radiation losses associated with copper or steel electrodes are much more significant than carbon electrodes [21].

2.4 Incident energy and heat transfer

2.4.1 Incident energy

Incident energy is electrical energy convert into heat, which could be transferred from arc blast to personnel or nearby equipment. It likes other forms of energy, is an integration over a period of time, such as the arc duration (arc duration is estimated from the calculated arc current and the response time of the overcurrent protective device).

Heat level of an arcing event is quantified by the temperature rise in copper calorimeters at a given distance from an arcing point. The energy absorbed by the calorimeters (Based upon the specifications of ASTM 1959) is the heat transferred from the arc by radiation, conduction, and convection. Each degree rise in calorimeter temperature (Celsius) is converted to incident energy (cal/cm^2) by a multiplier of 0.135 cal/cm^2. From the previous investigations, copper calorimeters absorb at least 90% of the incident energy, which is assumed to equal to incident energy.

An incident energy level of 1.2 cal/cm^2 (5.0 J/cm^2) has been established as the level of 50% chance to cause a second degree burn in human tissue. To adequately protect a worker from thermal injury during an arcing fault, Personal Protective Equipment (PPE) must exceed the potential incident energy to which a worker might be exposed. Incident energy calculations are also used to determine the flash protection

boundary distance where the available incident energy is 1.2 cal/cm^2; outside this boundary, PPE is not required.

2.4.2 Personal protective equipment

Personal Protective Equipment (PPE) is required equipment wear to minimize exposure to serious workplace injuries and illnesses. PPE may include gloves, safety glasses, shoes, hard hats, vests and body suits. NFPA 70E categorizes PPE in five different levels. These are shown in Table 2-2.

Table 2- 1 Protective Clothing Characteristics [22]

Hazard Category	Clothing Description	Range of Incident Energy	Arc Rating of PPE
0	Non-melting, flammable materials, that is, untreated cotton, wool, rayon, or silk, or blends of these materials	0 ≤ E ≤ 1.2	N/A
1	Arc-rated clothing, minimum arc rating of 4 cal/cm^2	1.2 < E ≤ 4	4 cal/cm^2
2	Arc-rated clothing, minimum arc rating of 8 cal/cm^2	4 < E ≤ 8	8 cal/cm^2
3	Arc-rated clothing selected so that the system rating meets the required minimum arc rating of 25 cal/cm^2	8 < E ≤ 25	25 cal/cm^2
4	Arc-rated clothing selected so that the system rating meets the required minimum arc rating of 40 cal/cm^2	25 < E ≤ 40	40 cal/cm^2

The maximum incident energy for which PPE is specified is 40 cal/cm^2. Standard does not provide a reference guideline for higher incident energy levels. However, it may

encounter energy levels much higher than 40 cal/cm^2 in actual electrical systems, especially in medium and high voltage systems.

In 2012, NFPA 70E gave detailed PPE description for hazard risk categories [22]. This was based on developing a clothing system meeting a specific tested cal/cm^2 level and comprised of arc rated materials. Natural fiber clothing like cotton, wool, and silk are still allowed but cannot add to the protection level because of risk of ignition. Additionally, from the guide, PPE rating cannot be achieved by wearing multiple layers of clothes, which means more layers of PPE cannot be used to increase the arc rating of clothing. For example, one layer of PPE clothing is rated as 2 cal/cm^2, and another layer is rated as 4 cal/cm^2, and when a person wears them together, the total PPE rating does not add to 6 cal/cm^2. When more than one layers are used, the total system must be tested to obtain the total arc rating.

2.4.3 Heat transfer

Heat can be transferred by conduction, convection, and radiation [23] [24] [25]. With radiative heat transfer, heat can be transmitted from the source to the receiver through a vacuum, or air, at a temperature lower than either the source or the receiver, such as infrared heaters.

Thermal radiation is a significant component of the measured incident energy, especially when the test configuration follows vertical, parallel electrodes. However, the arc moves randomly away from the electrode axis, and the calorimeters placed uniformly around the test setup in a circle experience different levels of heat [26]. When an arc is initiated in an open-front test enclosure, some radiant energy hitting the sides and the back of the enclosure is reflected and transmitted out the front. Due to this situation, the incident energy of arc flash with enclosure is higher than for a similar arc initiated in open air [27]. Figure 2-7 explains this phenomenon.

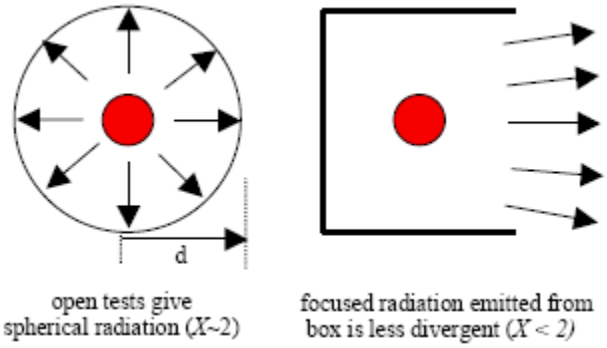

Figure 2- 7 Effect of Box for Arc Flash Incident Energy Exposure [28]

Previous researches for open air arc models, such as IEEE 1584, have demonstrated a difference between incident energy with enclosure and without enclosure. However, those previous researches did not quantify the difference of incident energy in various enclosure size and shape.

Convection is the transfer depends on the surface area through which the heat transfer takes place. In some types of arc testing, convective heating is a significant component of the incident energy measured by calorimeters. For example, an arc flash tests with either horizontal, parallel electrodes pointing directly towards the calorimeters, or with a vertical electrode setup, but an insulate barrier is placed on the bottom of enclosure. At the arc initiation time period, the heat at the calorimeters is radiation. After a few milliseconds, the magnetic force associated with the plasma jets drive the plasma cloud with its flow of convective heat toward the calorimeters. Recent research has demonstrated that protective clothing fabrics performed at only 50% of their arc ratings when exposed to the large convective heating component of arcs initiated from horizontal or barrier tests [2].

2.5 Review on previous arc flash hazards analysis researches

2.5.1 Stoll curve

Alice Stoll and Maria Chianta conducted burn injury research on “sailors, pigs and rats” in the late 1950s and early 1960s at the Aerospace Medical Research Department, Naval Air Development Center. It is reported that sailors of the U.S. Navy volunteered to be burned on their forearms for a weekend pass. Stoll and Chianta used heat exposures on human and animal skin to determine the level of heat energy that would create a second-degree burn [29].

For their work, they defined a second degree burn as the point at which a blister forms which is the point at which the outer layer of human skin, the epidermis, is destroyed. Damage to the skin depends not only on the cumulative incident energy but also on the rate of heat transfer, as shown in Figure 2-8.

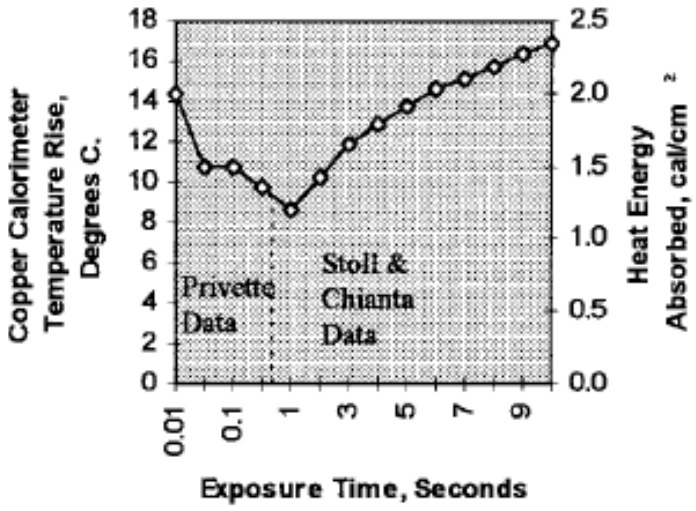

Figure 2- 8 “Stoll Curve” - Heat Energy required for Second-Degree Burn [30]

The Stoll and Chianta data was presented in 1969 and was later used to create the “Stoll curve”, which quantifies the level of heat and the duration of time required for a

second degree burn for a wide range of exposure conditions. The range covers a high level of heat for a short time period to a low level of heat for a much longer time period.

As early as December 1970, the Occupational Safety and Health Act required that each employer recognize hazards that are causing or likely to cause death or serious physical harm to his employees. In 1976 the National Fire Protection Association (NFPA) formed a new electrical standards development committee at the request of OSHA to develop an electrical safety standard. Three years later, NFPA 70E, Standard for Electrical Safety Requirements for Employee Workplaces, was first published; it serves as the foundation for electrical safety practices in the United States today. It was not till late 1995 that the NFPA 70E added words acknowledging arc flash as an electrical hazard.

2.5.2 Ralph Lee's equations

In 1982 Ralph Lee presented "The Other Electrical Hazard: Electrical Arc Blast Burns," the first paper to quantify the potential burn hazards from arc flash incidents. Ralph Lee's equations estimated the three phase arc flash incident energy based on the maximum power calculation [31].

From his work, incident energy could be achieved by two separate equations, one for 600V above, another is below 600V. The models fitted into bolted fault current from 16kA to 50kA, and minimum 18 inches distance from arcing point to measurement point. He also considered the different condition in open air system and arc in 20 inches cubic box.

Lee's work made the engineering community aware of the occurrence of arc flash incidents in the workplace and their associated thermal and pressure hazards. Although thermal burns usually represents the greatest harm, arc flash can also cause a severe injury from blast pressure.

2.5.3 Arc flash testing and modeling in mid-1990s

Much of the earlier arc flash testing was performed in single phase condition. Research focused on quantifying electrical parameters, assessing system damage or protecting the electrical system from damage. Due to the growing awareness in the 1990s that electrical arc flashes account for a significant number of electrical injuries, the arc testing focus expanded to quantifying incident energy, fabric testing, and determining the PPE needed to protect workers from arc flash hazards. Testing was done to quantify the reduction in incident energy associated with current limiting and overcurrent protective devices. The recognition of the arc flash hazard in the 1995 edition of NFPA 70E was the beginning of standards formally addressing this additional electrical hazard. The 2000 edition of NFPA 70E introduced the Hazard Risk Category classification system, which was developed for FR fabric and PPE selection to protect against the thermal effects of arc flash.

In 2000 Richard L. Doughty, Thomas E. Neal and H. Landis Floyd II published "Predicting Incident Energy to Better Manage the Electric Arc Hazard on 600V Power Distribution Systems" [32]. This paper included the results of 25 three phase arc tests conducted at 600V and presented separate open-air and enclosure incident energy equations based on bolted-fault current, arc duration and distance to the arc. These equations have been included in NFPA 70E as an acceptable method for calculating incident energy in an arc-flash hazard analysis. The test data from this paper became part of the IEEE 1584 data set. The distance exponents formulated for the open-air and cubic enclosure tests are almost identical to the distance exponents presented in the IEEE Standard 1584.

2.5.4 IEEE Std. 1584-2002 "Guide for Performing Arc Flash Calculations"

First published in 2002, IEEE 1584, "Guide for Performing Arc Flash Calculations", has become the predominant method in the industry for performing arc flash calculation studies. This guide presented detailed incident energy and arc current calculation methods and included an extensive data set consisting about 300 entries. IEEE 1584-2002 tests covered a wide range of test conditions in both voltage range (208V to 14.3kV) and current conditions (700A to 106kA). In addition, tests were run with grounded, ungrounded or high resistance grounded setups. Low voltage and medium voltage tests were conducted in open air and in metal enclosures. The enclosure sizes were: 12"x14"x7.5" (low voltage test, shallow), 20"x20"x20" (low voltage test, cubic) and 45"x30"x30" (medium voltage test). The scheduled test duration and the calorimeter distance to the arc also varied. Figure 3.3 gives the typical test set up as utilized by IEEE 1584-2002 [7].

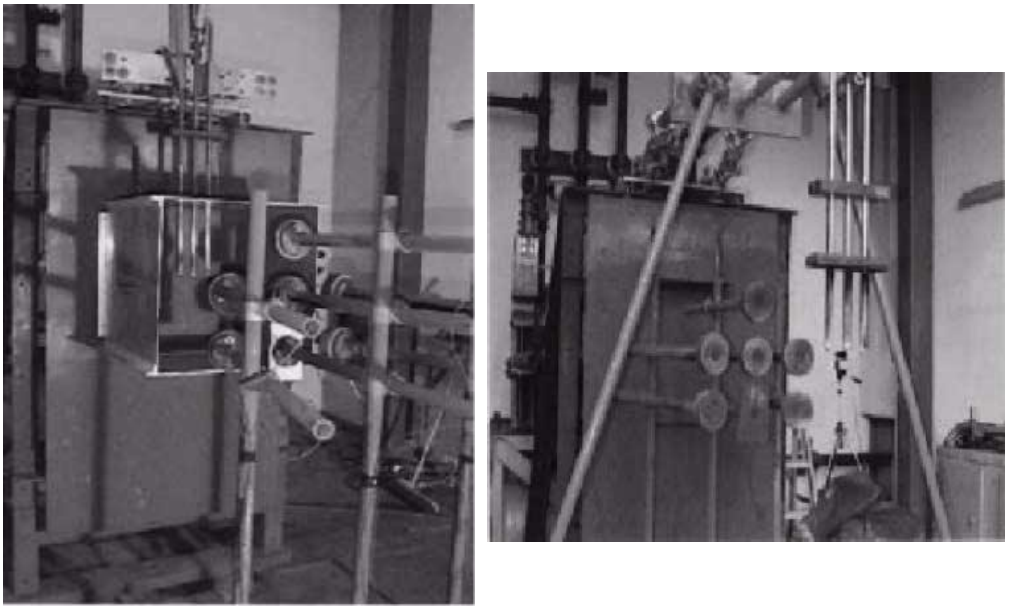

Figure 2- 9 Typical test set up for IEEE 1584-2002 [7]

The analysis method from the standard based on Lee's previous work, all model expression is valid for arcs both in open air and in a box three phase AC systems. The 1584 arc current and incident energy equations were formulated from statistical curve fitting to the test data and is derived using a least square method. The calculation factor was introduced to reach a 95% confidence interval for predicting a PPE category. These thresholds combined the NFPA defined categories of 1 and 2 as a common industry practice.

There are two principal stages presented in IEEE 1584-2002 for arc flash calculation:

1. Calculate RMS arcing current in order to determine the operation time for protection devices.
2. Calculate incident energy from certain distance so that the PPE level can be determined.

Models in IEEE 1584-2004 set the threshold value of voltage at 1kV, which divided the application on 1kV below, and 1 kV above up to 15kV. From their researches, the gap between electrodes affect the magnitude of arcing current and incident energy [7].

IEEE 1584-2002 is the first standard that numerically quantifies the arc flash thermal burn hazard. Industry could use the equation sets to automatically perform the calculations to obtain arcing current, incident energy and the distance for safety boundary.

2.5.5 Researches after IEEE 1584 -2002

After the publication of the IEEE 1584 Standard, R Wilkens's research pointed out the deficiency of the equations provided in IEEE 1584-2002. Stokes and Sweeting also reported the testing design problem when IEEE 1584-2002 performed the incident

energy measurement. In their research, when the calorimeters are placed directly in front of horizontal electrodes in open air, the arc plasma is driven toward the calorimeters, which results in significantly higher calorimeter measurements than IEEE 1584-2002 setups with vertical electrodes. The open air vertical electrodes drive the plasma cloud toward the ground, not directly toward the calorimeters placed in front of the electrodes [33].

Effective from January 1, 2009, the National Electric Safety Code (NESC) requires that all power generating utilities perform arc flash assessments [34]. The employer shall ensure that assessment is performed to determine potential exposure to an electric arc for employees who work on or near energized parts or equipment. If the assessment determines a potential employee's exposure greater than 1.2 cal/cm^2 exists, the employer shall require employees to wear clothing or a clothing system that has an effective arc rating not less than the anticipated level of arc energy.

Currently, there are 3 major arc flash related standards:

1. NFPA 70E, revised in 2015
2. IEEE 1584 Guide, 2002, which undergoing revisions
3. IEEE 1584a, 2004, amendment 1

Chapter 3

Design and perform arc flash testing for model development

3.1 Definitions of testing parameters

For the purpose of this dissertation, the following terms and definitions are applied. These definitions are inclusive and other meanings are also encompassed, as known to persons of ordinary skill in the art. The terms may follow IEEE Standard 1584-2002 and NFPA 70E definitions [7] [22].

- **Arc flash**: An energetic event resulting from formation of an electric arc between energized electrodes of different voltages or phases, or between energized electrodes and the ground, in which sufficient energy is released to pose a risk of injury or harm. Arc flash may result from contact between an energized electrode and a metallic tool, test probe, under-rated instrument or loose parts, or other short circuit or ground fault events. Arc flashes typically generate heat, noise, light, smoke, and explosive shock, positing the risk of physical injury including burns due to thermal energy exposure and ignition of clothing. Cover panels, loose parts, tools, and other components may be ejected, posing additional risks of injury.
- **Arc flash protection boundary**: An approach limit or distance from a prospective arc flash source, within which a person would be exposed to sufficient thermal energy, poses a risk of second degree burns if an electrical arc flash were to occur. The arc flash protection boundary is determined by electrical configuration of the prospective source, including source voltage and current characteristics.
- **Arc flash hazard**: A risk condition is associated with the potential release of energy from an electric arc or arc flash event. Arc flash hazards encompass

thermal energy exposure explosive shock and other forms of energy release, not limited to the risks of direct exposure to electrical current.

- **Arc flash hazard analysis**: The study of potential exposure to arc flash energy, including risk analysis for injury prevention and determination of safe work practices. Arc flash hazard analysis may include, but is not limited to, determination of the arc flash protection boundary for a potential arc flash source configuration, and recommendations for appropriate levels of personal protective equipment and other safe work practices.
- **Arcing fault current**: The arc fault current flowing through an electrical arc plasma, for example, is in an arc flash event.
- **Available fault current**: The electrical current that can be provided to a potential arc flash source or electrode configuration, based on the current and voltage characteristics of the serving utility, the local electrical device configuration, and the impedance of the current path along which the available fault current is defined.
- **Available short circuit current**: The maximum current that can be delivered through a given circuit to a negligible impedance current path, at a given point in the circuit, or at any other point that will cause the highest such current to flow. The available fault current and the available short circuit current may be equivalent for a zero fault impedance.
- **Bolted fault**: A short circuit condition in with substantially zero impedance at the point of the fault, or in which substantially zero impedance is assumed.
- **Circuit**: A conductor or system of conductors through which an electric current flows, or is intended to flow.

- **Electrical hazard**: A condition in which inadvertent or unintentional contact or equipment failure may result in shock, arc flash burn, thermal burn, blast, or a substantial risk thereof.
- **Electrical shock**: A physical effect that occurs when electrical current passes through a body.
- **Electrical utilization equipment**: Equipment that utilizes electric energy for electronics, electromechanics, chemics, heating, lighting, or similar purpose.
- **Energized**: Electrically connected to a voltage, or a source of voltage.
- **Exposed**: Capable of being inadvertently touched or approached nearer than a safe distance, as applied to electrical conductor or circuit parts, including energized electrical conductors and circuit components exposed to inadvertent touch or approach by a person. Exposed parts include electrical conductors or circuit components that are not suitably guarded, isolated, or insulated.
- **Fault current**: A current that flows from one conductor to another conductor, or to the ground, due to an abnormal connection between the two. Fault current may include an arc fault current in an arc flash event.
- **Incident energy**: The amount of energy exposure on a surface at a given distance from an arc source. Incident energy may be defined in units of energy per area, for example in joules per centimeter squared (J/cm^2) or calories per centimeter squared (cal/cm^2).
- **Nominal voltage**: A nominal value assigned to a circuit or system for the purpose of designating its voltage class. Examples of nominal voltage include, but are not limited to, 208V, 480V and 600V. The actual voltage at which a circuit operates may vary from the nominal voltage, within a range that permits satisfactory operation.

- **Working distance**: The distance between a potential arc point or arc flash source and the body of a person positioned with respect to that point, for example, a worker positioned to perform a particular task on or near an electrical circuit associated with the potential arcing point.

3.2 Overview of test set up

In order to improve arc flash modeling and risk analysis, an extensive research has been performed. This research included approximately 2000 different high power arc flash experiments, through those tests to investigate the basic electrical characteristics of arc flash events. Ultimately, these efforts lead to an extensive data resource of arc flash, which could be utilized to develop improved arc flash modeling, which is based not only in regression but also in physics.

Figures 3-1 to 3-6 show the test setups. These include single phase, open air arc flash tests; three phase, open air arc flash tests in both vertical and horizontal electrode orientations; and three phase enclosed arc flash test in both vertical and horizontal electrode orientations.

As shown in Figure 3-1, single phase test was performed in an open air configuration, with in-line metal electrodes spaced apart by variable gap distance along a vertical axis. This configuration is normally described as Faraday Cage or Faraday Shield Structure. In one test example which was perform previously, electrode are formed of 3/4 inch (19.05mm) diameter solid copper rod. Other suitable materials may also be used, for example, steel, aluminum and other conducting metals, in various round, oval, oblong, rectangular, square and other shapes, with various different dimensions.

Figure 3- 1 Single phase arc flash test in Faraday Cage

In three phase, open air configuration of Figure 3-2, in a generally parallel and vertical configuration with individual spacing or gaps G between adjacent pairs of electrodes. Gap distance are equivalent between each pair of electrodes. Calorimeters are arranged on an array, in order to determine incident energy at various distance D from electrodes or arcing points. Copper slug calorimeter were used as thermal energy sensitive device here. Additional sensors are not shown here, such as pressure transducer.

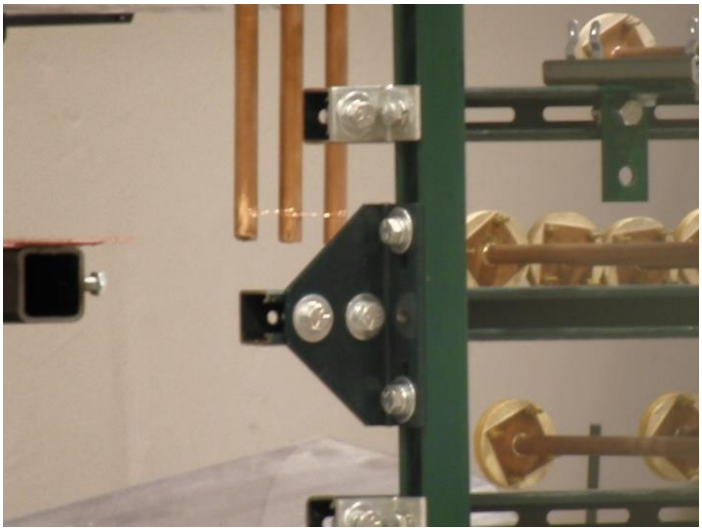

Figure 3- 2 Vertical electrodes in open air arc flash tests

In this particular configuration of Figure 3-2, an array of seven calorimeter sensors are positioned in front of arc source to mimic the chest and face area of personnel. The calorimeters design follows standard of ASTM 1959 recommended slug calorimeter design, which provides schematic design of slug calorimeter on Figure 3-3. From the schematic drawing, thermal couple has been placed on the center of copper plate, and the basement of calorimeter is 1.6 mm thick insulation board.

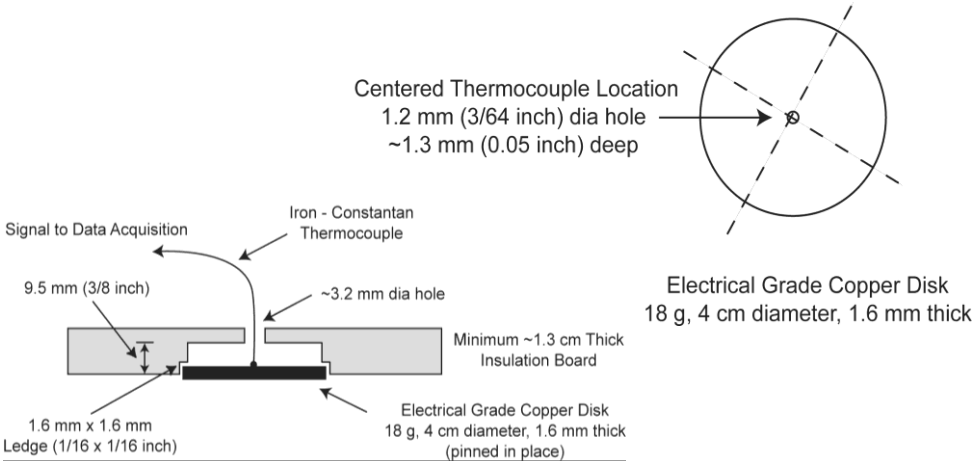

Figure 3- 3 Slug calorimeter design from ASTM 1959

A set of 3 calorimeters is located in the horizontal row at the same height as the tips of electrodes, and another 2 calorimeters in bottom row is positioned about 6 inches below the middle row. These 2 rows, for example, in one previous test, positioned as 24 inches from the arcing point. The top row with 2 calorimeters are positioned in nearer distance from calorimeter to electrode, in phase 1 tests, the distance always set as 18 inches. Figure 3-4 gives an example for calorimeter array layout.

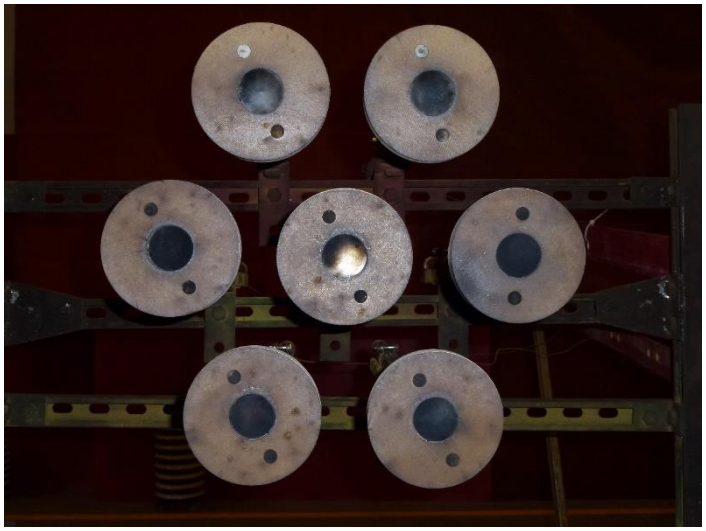

Figure 3- 4 Calorimeter array layout

Figure 3-5 shows an alternate open air configuration, with three phase electrodes in a horizontal orientation. In this configuration, the arrangement of sensors are placed at a same plate, the array of seven copper slug calorimeters, and the middle row is placed in-line with the tip of the center electrode.

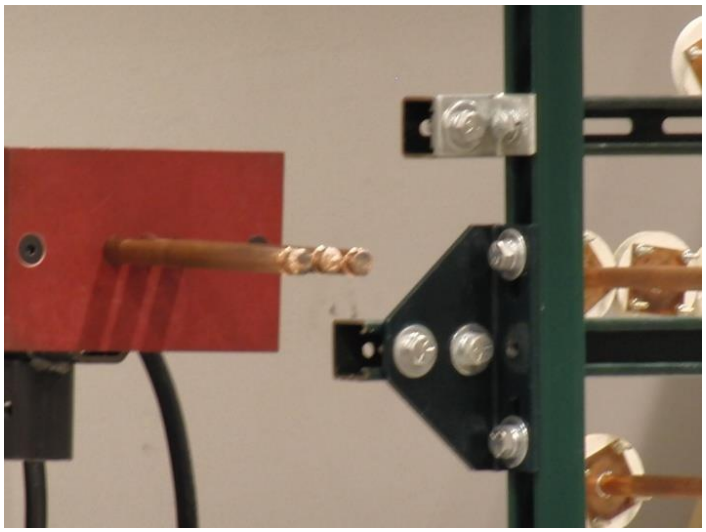

Figure 3- 5 Horizontal electrodes in open air arc flash tests

During an arc flash test, each calorimeter experiences a temperature change, which is converted to incident energy. Although model development for the incident energy estimation is based on the maximum incident energy, the overall and row average incident energies provide additional insight into understanding thermal flow and the resulting heat levels that are experienced. From tests observation, bolted fault current, voltage level, electrode gap distance, electrode orientation, working distance between arcing point to calorimeter array and presence of an enclosure are all strongly impact on incident energy IE level.

Figure 3-6 shows three phase with an enclosed configuration for arc flash test, where three electrodes extended vertically into the panel box or enclosure. In the example provide by this figure, electrodes were formed of 0.75 inch diameter hard drawn copper, gap between each electrode was 1.75 inches. Shaped enclosure has height H between top and bottom panel, width W between two side panels, and depth D is from back panel to the front of enclosure. In general, 20 inches (508mm) box is used in 600V

and below tests, 26 inches cubic box is used in 2.7kV medium voltage test, and 36 inches enclosure is used in 14.3kV arc flash tests.

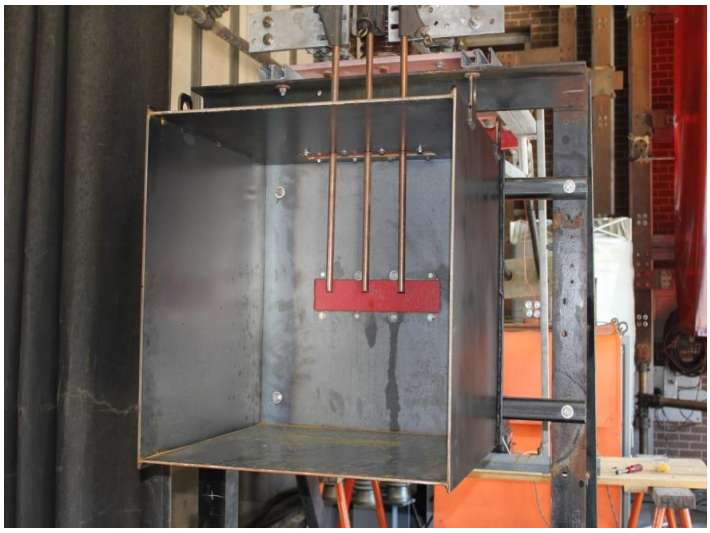

Figure 3- 6 Vertical electrodes in cubic enclosure arc flash tests

Various combination of the different test configurations are also possible, for example, enclosed single phase tests with either horizontal or vertical configuration. Different fusing and circuit breaker configuration are also utilized, in order to determine the corresponding effects on arcing current, arcing duration, and other arc flash event characteristics relevant to arc flash hazards analysis.

During the arc blast, arc energy transfer in the form of heat to surrounding, calorimeter may receive higher incident energy when located in the path of the ejected plasma or hot air. From heat transfer process described before, direct exposure (convective heating) due to contact with the plasma, or high temperature gas, which may results a higher temperature measured. Alternatively, for indirect exposure the incident energy may be less because the radiative performed as the primary energy transport mechanism, rather than the convective.

Figure 3-7 is an illustration of a representative arc flash test, which performed under 480V open circuit voltage with 20kA bolted fault current. From the figure, the test configuration can be described as vertical electrode with cubic enclosure. Sensor array includes seven calorimeters to determine the temperature rise and incident energy from arc, also a set of pressure transducers has been placed on the side of bottom row of sensor array which is next to the calorimeter. High speed cameras, optical light density measurement sensors and sound meters are fixed at the tripod which shown on the figure, in order to further characterize the feature of arc flash beyond the heat hazard.

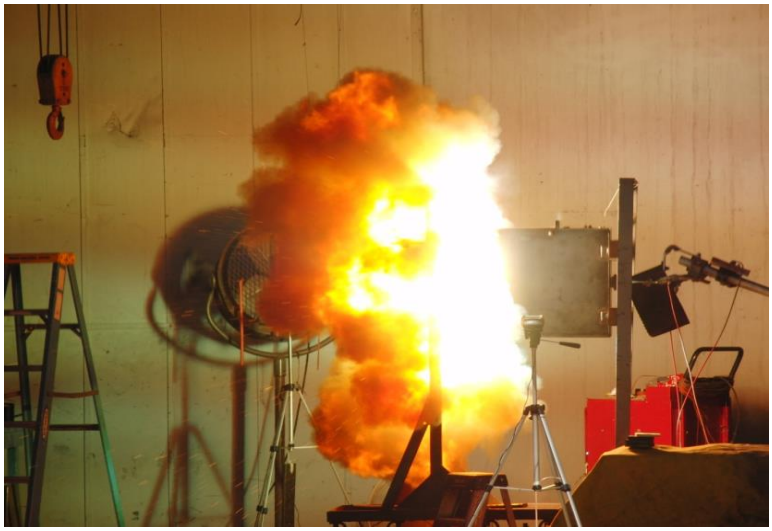

Figure 3- 7 A sample of enclosed arc flash test performed on 480V

As shown in figure above, arc flash events demonstrated its high energy explosion, resulting in substantial of injury to exposed personnel, including both burns and shock effects. These risk factors depend on open circuit voltage, bolted fault current, arcing duration, and other arc flash characteristics, which can be utilized to determine the potential arcing current and incident energy in a workplace to establish proper safety guidelines.

Once formed, arc may be self-sustaining as long as sufficient source current and voltage are available.

Depending on the configuration of arc source, arc column may be driven along electrodes by magnetic field effects. Ejected arc column and plasma generates a cloud of high temperature gas, plasma dust or smoke particles, and molten droplets steam.

3.3 Testing methodology and ranges

A test method widely used for determining the thermal performance of clothing and other materials subject to electrical arc flash energy is described in ASTM 1959, which provided the basic idea to perform thermal measurement and also gave the detailed description for slug calorimeter design.

More generally, the test methodology is defined to enable determination of the incident energy that clothing or other protective material can prevent workers from second degree burn. This test methodology can also be used to determine the incident energy to which a worker would be exposed in case of a corresponding arc flash event.

To determine incident energy level, a calculation based on the temperature rise of one or more calorimeters need to be performed. For example, the temperature rise in each individual calorimeter can be converted from degree Celsius to incident energy by multiplying by an appropriate calibration factor, as defined for the desired system of unit, such as cal/cm^2 or J/cm^2.

Testing from this research covered open circuit voltage from 208V to 15kV. Based on the modeling purpose, extensive test were performed on 600V, 2.7kV and 14.3kV. Selective test on 208V and 480V were performed to validate the estimation results of the model.

In order to simulate electrical equipment, a set of electrode were typically used in both vertically oriented and horizontal oriented in a planar configuration, with side by side

gap spacing. Arc were initiated by using AWG 10 or AWG 20 solid copper wire to connect electrodes at 2” from the electrode tips. Support blocks were also utilized between adjacent electrodes to prevent them from bending due to high magnetic force during the test.

The bolted fault current was measured by shorting the tip of the electrodes. Phase current and voltage were recorded digitally. Arc power was determined by integrating the products of phase current and voltage, then summing to get results. Arc energy was computed by integrating arc power over the arc duration.

The duration of arcing for each test was selected to consider the condition of the test set-up and create measurable temperature rise in the calorimeters. In general, 6-cycle and 12-cycle normally be chosen as the arcing duration, but in some conditions, such as low voltage and low current, longer durations (may reach to 60 cycles) also be considered to ensure the temperature rise can be recognized beyond the ambient background noise. Based on this consideration, the useful incident energy data could be obtained.

Based on engineering practice and real equipment design, a series of enclosure had been appropriately selected based on sizes and shapes. Electrodes position, such as distance between tips and bottom of enclosure and distance between electrodes and back panel, are well designed through the tests. Additionally, electrodes gap width or bus gas also been selected appropriate based on the requirement of Basic Impulse Level (BIL) and related standards. Table 3-1 provides the test design reference for gaps between electrodes and over surface. Table 3-2 lists the typical enclosure dimension for different voltage categories [33].

Table 3- 1 Gap width between electrodes and over surface

Voltage (kV)	BIL (kV)	Minimum Gap (inch)	Maximum Gap (inch)	Over Surface Phase-to-ground (inch)
0.208 – 0.250	UL1558 NEMA MCC	0.25	0.75	0.5
0.251 – 0.600	UL1558	0.5	2.0	4.0
2.5	45	1.5	4.5	4.0
5	60	1.5	4.5	4.0
15	95	3.0	6.0	7.0

Table 3- 2 Typical enclosure dimension for different voltage level

Voltage (kV)	Maximum I_{bf} (kA)	Distance to the Back Panel (inch)	Box Size (inch)
0.208 – 0.250	100	0.5	14x12x8 and 8x6x6
0.251 – 0.600	100	4/10	20x20x20
2.7	65	4 and 4/7	26x26x26 and 36x36x36
4.16	63	4	26x26x26
14.3	42	7	36x36x36

In order to ensure the consistency of the test, multiple tests were performed for selective experimental setup. The arcing duration may vary from test to test, a time duration factor caused accumulated incident energy can be applied in the model development. Incident energy of every calorimeter was recorded.

3.4 Testing summary

From tests plan and design, the five following configuration were adopted to cover most of arc flash occurrence situation in industry:

- **VCB**: vertical oriented electrode in cubic box
- **VCBB**: vertical oriented electrode in cubic box with bottom insulated barrier
- **VOA**: vertical oriented electrode in open air
- **HCB**: horizontal oriented electrode in cubic box
- **HOA**: horizontal oriented electrode in open air

Representative three phase test parameters are provide in Table 3-3, for approximately 2000 individual arc flash tests in alternation current (AC) system for each combination of bolted fault current, electrode gap width and five configurations were performed. For 600V and higher arc flash tests, the incident energy was measured at three different working distances. Also, different enclosure sizes have been adopted, which is corresponding to different voltage level tests.

Table 3- 3 Overview of Test Setup Parameters

Voltage (kV)	Bolted Fault Current (kA)	Gap (in.)	Enclosure Size (in. x in. x in.)	Distance (in.) to back panel
0.208	2.5 – 100	0.25 – 1.0	14 x12 x 8 8 x 6 x 6	0.5
0.208	2.5 – 100	0.25 – 1.0	20 x 20 x 20	4.0
0.48	0.5 – 100	0.4 – 3.0	20 x 20 x 20	4.0/10.0
0.600	0.5 – 100	0.5 – 3.0	20 x 20 x 20	4.0
2.700	0.5 – 63	1.5 – 4.5	26 x 26 x 26	4.0
2.700	20 – 40	1.5 – 4.5	36 x 36 x 36	4.0
14.3	0.5 – 42	3.0 – 6.0	36 x 36 x 36	7.0

As shown in Table 3-3, test data span the voltage range from 208V to 14.3kV, with bolted fault current from 0.5kA to 100kA. Electrodes gap width range from 0.25 inch (6.35 mm) to 6 inches (152.4 mm). Typical enclosure size from 8 x 6 x 6 $inch^3$ (203.2 x

152.4 x 152.4 mm^3) to 36 x 36 x 36 $inch^3$ (914.4 x 914.4 x 914.4 mm^3) cubic box, with back panel distance from 0.5 inch (12.7mm) to 10 inches (254 mm). In modeling process, 600V, 2.7kV and 14.3kV has been selected as reference voltage or “anchor points” in order to estimate the model functions.

Generally, three phase arc events pose a greater overall hazard, and open bus switchgear and open conductor lines where single phase faults are likely to be addressed using the three phase model as a guide. In addition, it is widely recognized that line to line faults quickly escalate into three phase faults. Single-phase-to-ground faults can also escalate into three phase faults for a low voltage solidly grounded system. In general, phase to ground fault in low voltage ungrounded and high resistance ground systems do not create a sustainable arc flash incident. However, three phase fault should still be considered from the worst case scenario point of view.

For each voltage level list in Table 3-3, testing was performed for each combination of bolted fault current and gap width (normally use 3 different gap for each test). For incident energy measurement, three different calorimeter distance from arcing point have been selected.

Both bonded (grounded) and unbonded (ungrounded) test were performed at 480V and 2.7kV. In the bonded configuration, the enclosure boxes were electrically connected to the neutral conductor. In this configuration, neutral current may appear in the first couple of electrical cycles during the low voltage arc flash test (such as 480V) due to the unbalance condition at the initiation stage of the fault. Since part of arcing current flows through the return path, the total arcing energy has been reduced and the incident energy may also decline. This phenomena was observed in the previous tests and was implemented in IEEE Std. 1584-2002. However, the unbalance duration is reduced for medium voltage (such as 2.7kV) and the amount of current in the return path

is small. As the result, incident energy did not appear notable reduction between bonded and unbonded configuration in 2.7kV test. Taking the worst case scenario into consideration, subsequent testing was performed on unbonded configuration, also, modeling process is purely based on unbonded conditions.

3.5 Design of testing equipment

3.5.1 Data acquisition system

Through the tests, laboratories have provided the data recording system for voltage and current. However, the research team has to provide DAQ system to record necessary information such as output of the calorimeters and light sensor in some tests, a special designed DAQ system is developed by the research team to fulfill this requirement. .

In general, the measurement system comprises of four main parts:

1. Sensors for arcing phenomenon measurement;
2. The measured signal transmission pathway;
3. DAQ hardware and their control systems;
4. The host computer.

Figure 3-8 illustrates the structure of the measurement system.

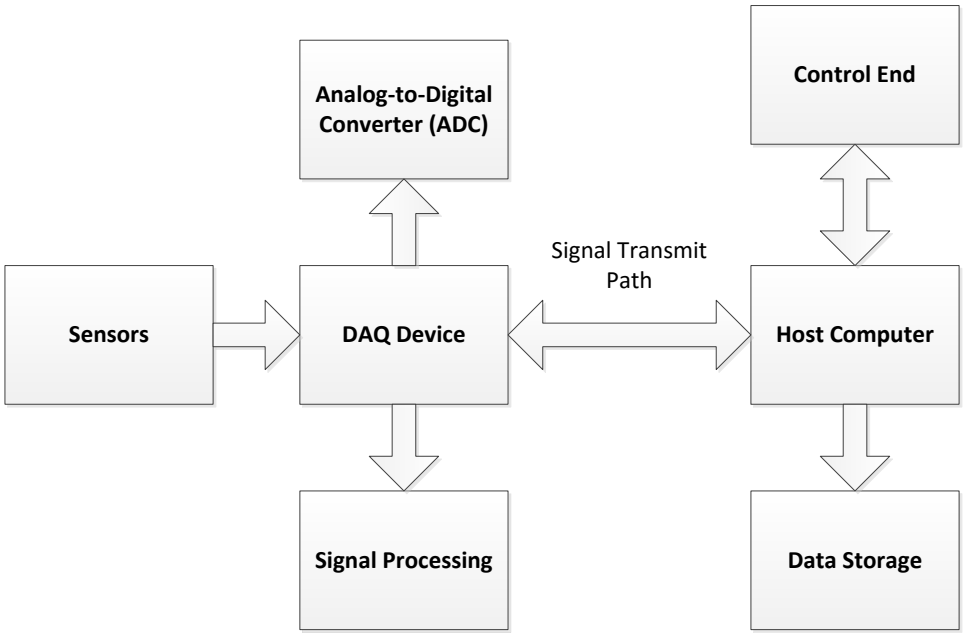

Figure 3- 8 Structure of arc flash measurement system

Sensor, often referred to as a transducer, is the front end of a measurement system, which performs the measurement of physical phenomenon, such as temperature, light intensity, sound level, and pressure. Sensors convert these physical events into a measurable DAQ signal. Depending on the type of sensor, its output can be different types of electrical signals, such as voltage, current, etc [35].

DAQ device plays the role of connecting the control (sensor) end and measurement (receiving) end of the whole system. It executes the commands sent out from the host computer to control the process measurement of sensors. There are two parts for DAQ devices:

1. Data processing module, which contains analog-to-digital converter (ADC). It processes or digitizes incoming analog signals so that the host computer can interpret them.

2. Temporary data storing module, which collects the processed data and then

transfers it to the host computer [35].

Host computer acts as man-machine interface (MMI), which controls the operation of the DAQ device, while performing the data storing and further processing functions [35].

However, compared to other measurement systems, arc flash measurement systems may expose equipment and personnel to more dangerous situations because of the high power involved and explosive nature of the test. Figure 3-9 illustrates this test environment that the measurement system must face.

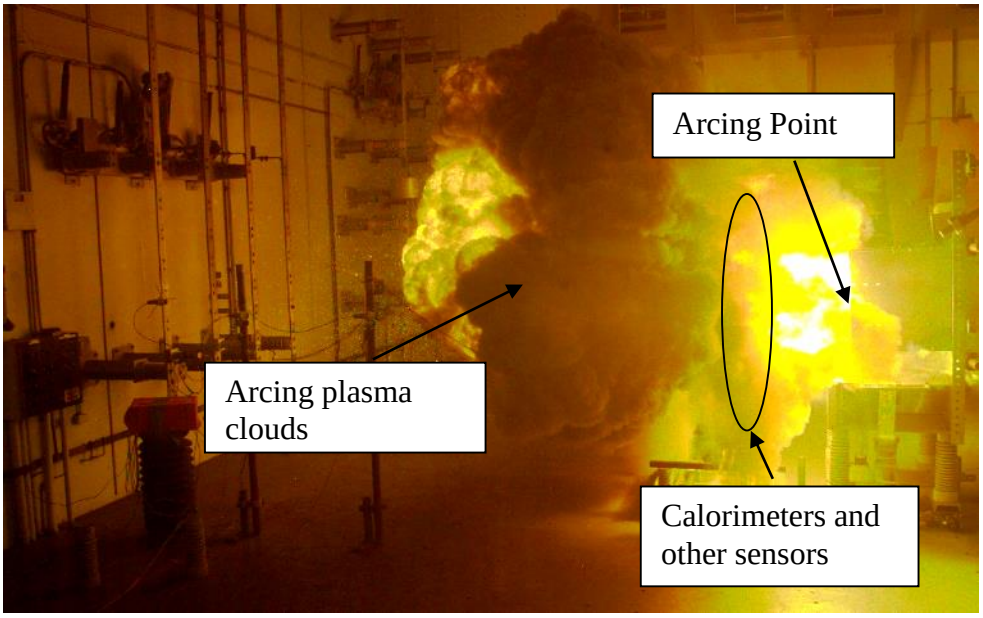

Figure 3- 9 The arc flash test environment

During arc flash testing, the measurement system can come into direct or indirect contact with the high voltage sources. For example, the calorimeters, which measure the incident energy, are always in-contact with high voltage through the plasma cloud. Without a proper grounding and isolation scheme, the millivolts-level signals being measured can be coupled with a kilovolts-level common-mode voltage surge, injecting into the data collection and control end, thus destroying the sensitive electronic device

and/or producing inaccurate measurement results.

There are many issues to consider when performing arc flash tests under high power conditions. When specifying the measurement system, the main concern is the accuracy of the measurement and the safety of the equipment and personnel.

The first generation of DAQ system designed based on two off-the-shelf high speed DAQ modules, with 8 analog inputs per module. The measurement signals through USB cables to transfer the test information to host computer. The units worked well at 480V testing, however, it was destroyed at 600V test. Once aware the destructible surge hazard, sufficient protection and grounding schemes has been added into the second generation design.

3.5.2 Issues of DAQ system isolation and grounding

Unlike arc flash testing, the traditional high power testing of equipment is usually in a non-destructive environment, and thus the protection scheme mostly focuses on avoiding the electromagnetic noise and disturbance from grounding loops. For equipment protection, this typically only requires a transformer or capacitor to achieve electrical isolation. Channel-to-earth ground is a typical topology that is used. Based on this topology, noise and ground loops could be removed by isolated grounding.

Ground loops are the most common source of noise in data acquisition applications. They occur when two connected terminals in a system are at different ground potentials, causing current to flow between two points [36].

Depending on the grounding location, the potential between grounding terminals can be different. Since the temperature measurement signal is normally millivolts-level in arc flash testing, this additional floating voltage can cause significant errors; the contaminated noise can appear as transients or periodic signals in the measurement.

To avoid the impact of ground loops, the device's earth ground and channels

should be electrically isolated. Channel-to-earth isolation is illustrated in Figure 3-10. From the figure, the hash marks indicate the insulation barrier. Isolated measurement systems provide separate ground planes for the signal receiving front end and the DAQ system, which separate the sensor from the rest of the system. Theoretically, a ground loop that exists between the sensor ground and the measurement system ground can be rejected by this grounding method.

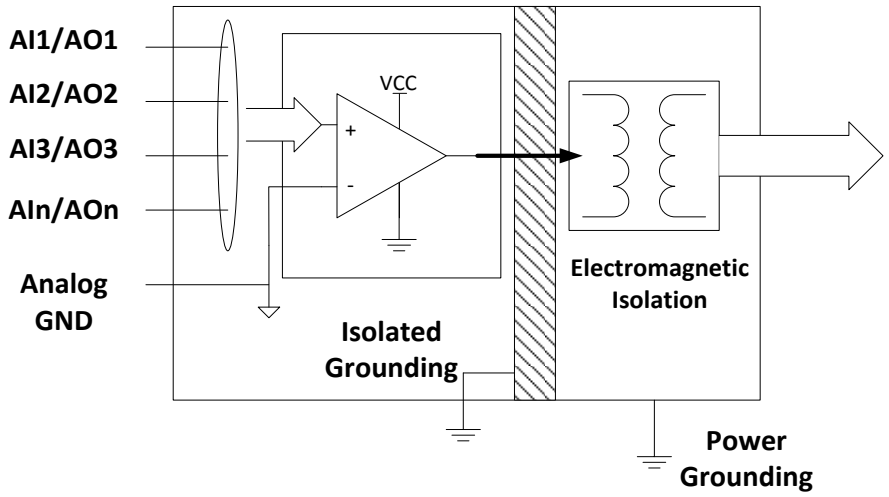

Figure 3- 10 Schematic of Channel-to-Earth Isolation [37]

Based on this channel-to-earth isolated grounding system, the sensors are connected to the isolated grounding system as the signal inputs are then insulated from the laboratory's electrical system grounding to eliminate noise.

However, in arc flash testing, the front end sensor input may involve high common-mode voltages. The calorimeters, which equipped with copper slug disks at the front end, come into contact with very high voltage through the plasma cloud, resulting in several hundreds of volts of transient common-mode voltage- which in turn presents a significant challenge when attempting to measure small (millivolt) changes. Because the ground of each channel is not isolated from those of other channels, the common voltage

will directly add to the original signal amplitude between positive input and their common isolated ground. The noticeable spike in Figure 3-11 demonstrates the size of the error caused by common induced voltage in IE measurement; the actually temperature should be 34.6^{o}C while the contaminated signal reaches 1500^{o}C.

Without common-mode voltage rejection and a sufficiently isolated barrier between each channel, such errors can destroy the measuring instruments.

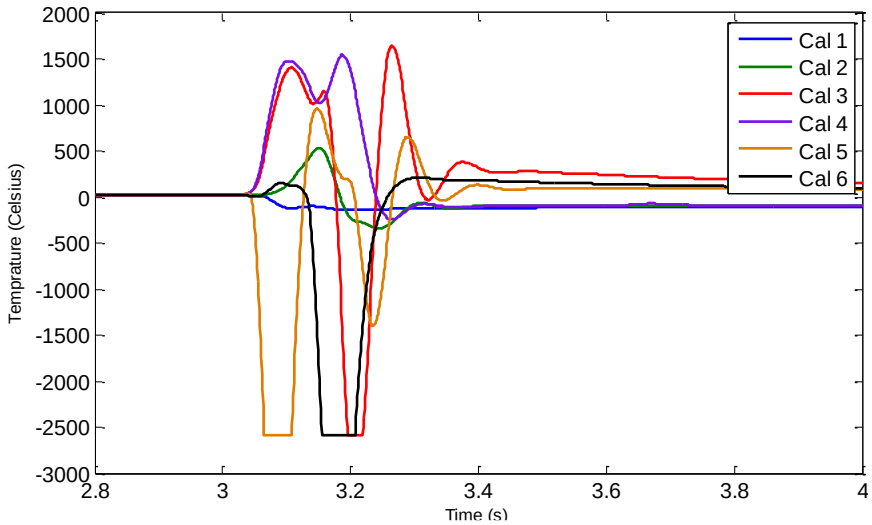

Figure 3- 11 Temperature measurement error caused by common-mode voltage

Due to improper grounding and isolation, a destructive surge in a 600V/40kA arc flash test destroyed the the entire measurement system.

3.5.3 Improved design for arc flash measurement system

The isolation and grounding for equipment must be applied in accordance with the characteristics of each component of the DAQ system, from signal receiving end to the control end, and also for the power supply itself.

The key for the success of this type of test is designing a accurately measurment system with an adequate grounding and isolating system, which has the high common-mode rejection. The design of a robust grounding and isolation scheme from sensor to

power supply must fulfill the following requirements:

1. High common-mode rejection in sensor and signal input;
2. Sufficient channel isolation among input signals;
3. Adequate communication line isolation among each component of the measurement system;
4. A separate isolated power supply for the measurement system;
5. Proper noise reduction and elimination.

Common-mode voltage is an often unwanted offset that is "common" across both the circuit positive and negative input conductors and added into the desired signal [38]. In arc flash testing, common-mode voltage appeared in previous common isolated grounding designs (channel-to-earth) as a surge on a single input with respect to the measurement system ground (see Figure 4.10). This high common-mode voltage not only results in measurement error, but also causes possible damage to components within the equipment.

From the sensor end, consideration must be given to the in-contact situation of an arc flash test, and thus common-mode voltage and unwanted surges need to be eliminated before measurement signal transfer into DAQ devices.

A differential amplifier applied to sensor input is a feasible solution to eliminate common-mode signals. An ideal differential system responds only to the potential difference between its two terminals, the “+” and “-” inputs, which effectively ignores the common-mode voltage [39].

However, practical differential amplifiers have limitations on their common-mode voltage range and common-mode rejection ratio (CMRR), which limits their ability to completely reject the common-mode voltage. CMRR describes the ability of a measurement system to reject common-mode voltages, which defined as the logarithmic

ratio of differential gain to common-mode gain [40].

$$CMRR(dB) = 20\log_{10}(A_d / |A_{cm}|)$$

Where, A_d is the differential gain

A_{cm} is the common-mode gain

In a non-isolated differential measurement system, an electrical path still exists in the circuit between input and output. Therefore, electrical characteristics of the amplifier limit the common-mode signal level that can be applied to the input. Figure 3-12 could clearly state this problem. With the utilization of differential input, a significant amount of common-mode voltage had been removed from the measurement signal. However, in the very beginning of the event when the arcing is initiated, it is very likely to still see some unwanted high amplitude at high frequency common-mode surge voltage still exhibited in the measurement results, which also could mislead the evaluation of the IE level during the test. In low voltage arc flash testing, these kinds of surges may not exhibit sufficient energy to destroy the delicate circuit components, but it may put the system into danger when high voltage testing is involved.

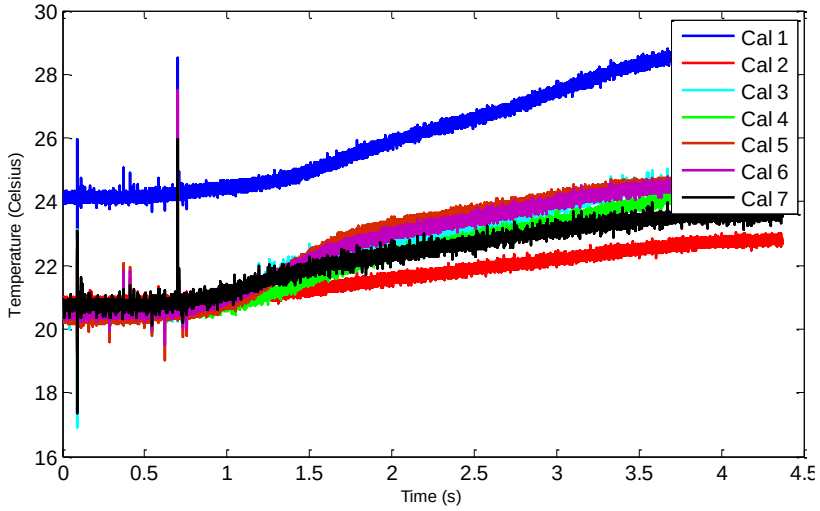

Figure 3- 12 IE measurement on differential input apply only

To bridge the CMRR limitation of differential amplifiers, an isolated differential system should be implemented within the measurement system. Isolated differential inputs provide higher common-mode rejection ratios [41], which allows for accurate measurement of small signals in the presence of a high common-mode voltage. Differential inputs with an isolation barrier allow the front-end of the amplifier to float with respect to common-mode voltage to the limit the barrier's breakdown voltage, which can reach 1,500 volts or more.

In IE measurement practice with copper slug calorimeters, the isolated differential system uses an analog filter preconditioning thermocouple signal prior to differential amplification. After the signal reaches the differential system, an isolation module is used to provide 1500 V RMS input-to-output isolation. With the use of isolation amplifiers, the conductive electrical path is eliminated and the common-mode rejection ratio dramatically increases. This protects the amplifier and the associated instrument while still providing a reasonably accurate measurement. The improved measurement system circuit is shown in Figure 3-13.

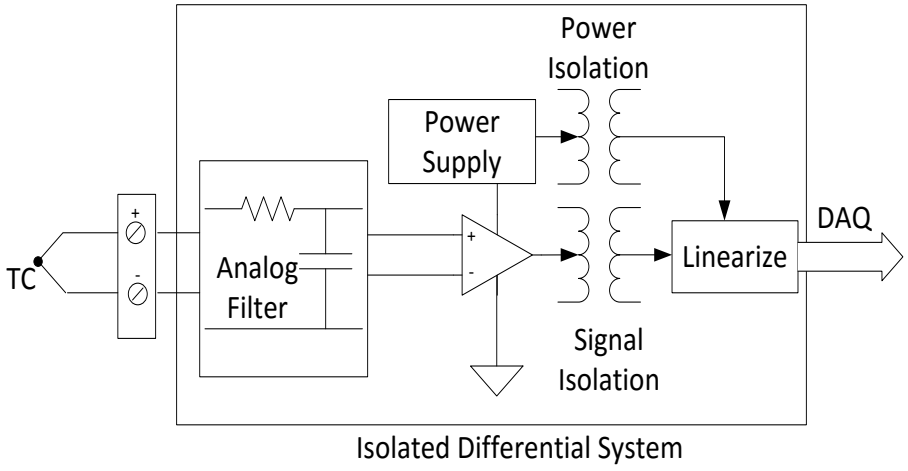

Figure 3- 13 Design of isolated differential system

In addition to providing sufficient common-mode rejection at the front end sensor

(calorimeter), necessary for proper isolation for the whole system in arc flash testing is the separation of one signal from another, in other words, to prevent unintentional interaction between them. For example, the common-mode voltage in each channel input pair is limited by the isolated amplifier, however, the interfernce between the channels or between isolated and non-isolated parts could be large if they share a single isolation system.

The most robust isolation topology is channel-to-channel isolation [42]. Compared to channel-to-earth, this topology allows each channel to be isolated from other isolated and non-isolated system components. Figure 3-14 represents this isolation method. CH1, CH2 are all on separate buses and are isolated from one another.

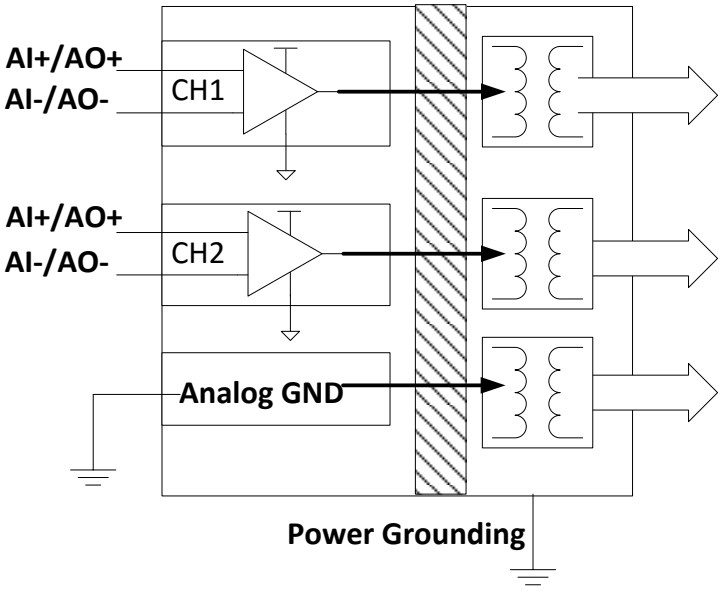

Figure 3- 14 Working principle for channel-to-channel ground

In channel-to-channel ground schemes, each input signal can be assigned to a single isolation amplifier. It provides adeqate protection for each channel, and in the event that a channel is damaged, the other channels will continue to function normally.

Furthermore, channel-to-channel topology with an analog-to-digital converter

(ADC) can perform simultaneous sampling. This is significant because testing frequently requires rapid data acquisition; in the case of arc flash testing, the event being measured lasts only a couple of cycles, and thus the DAQ system needs to pick up signals and transfer them to the control module in a very short period of time. Because its channels can be accessed in parallel, channel-to-channel topology is typically faster than serial transmitted methods, such as channel-to-earth topology. Figure 3-15 illustrates the isolation and grounding design from sensor end to DAQ end.

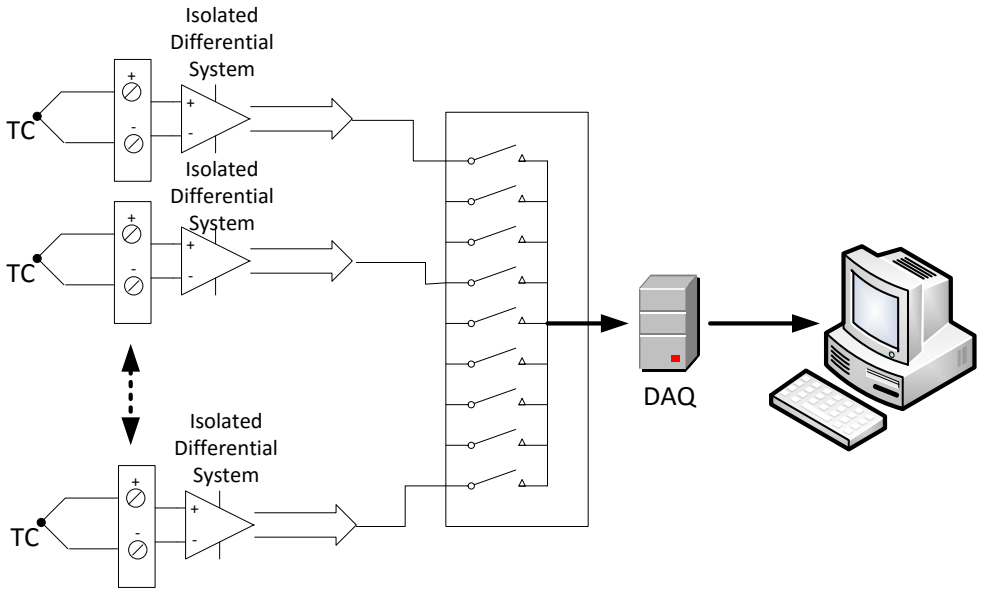

Figure 3- 15 Input isolation with channel-to-channel ground

3.5.4 Design of power supply for measurement equipment

In high power arc flash tests, the lab power system can be affected by the initiation of the 3-phase short circuit fault. Additionally, the local ground level can shift during the test, and the ionized arcing plasma could prorogate a huge surge through the power supply cable to the measurement system. In response to such risks, an isolated power supply can be adopted to avoid the disturbances and any unwanted surges to the measurement equipment.

Two-stages of power isolation, outside power isolation via a UPS power supply and an isolated power supply (switched-mode power supply) for the channel-to-channel system, are implemented in the proposed scheme.

UPS can eliminate the effect of unexpected external power disturbances. With the addition of a surge protection port, it is capable of filtering the surge spike caused by electric phenomenon.

The isolated switched mode power supply, or SMPS, uses a switching regulator to adjust the power output level. The internal isolated DC-DC converter and high frequency transformer can provide an isolation barrier to cut off the input surge. This barrier can withstand disturbances ranging from a few volts to hundreds of volts, which is the range that most power disturbances will fall within, thereby offering an ideal protection scheme for the sensor channel and data processing unit. Figure 3-16 explains how this two-stage power isolation is applied to a DAQ system.

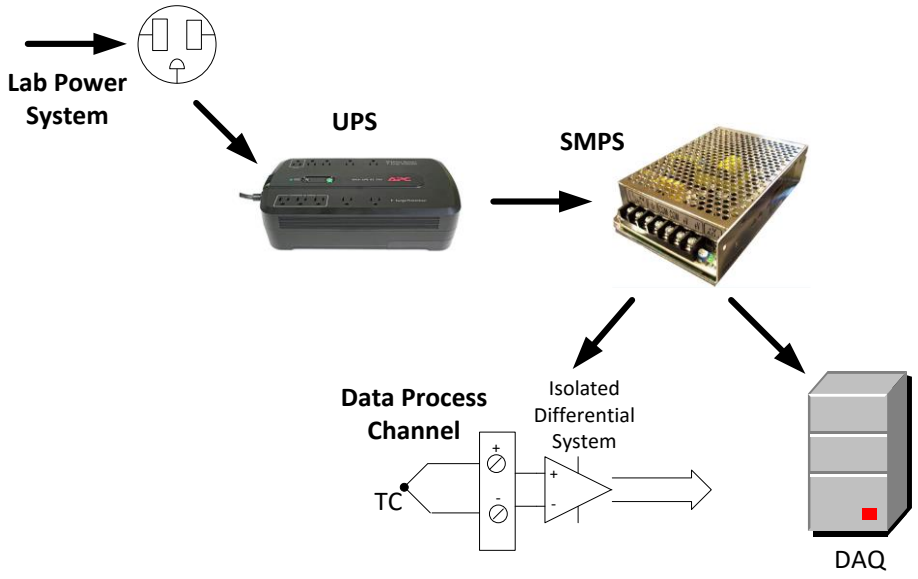

Figure 3- 16 DAQ system applied power supply isolation

3.5.5 Design of signal transferring

1. Control Signal from Control Center to DAQ

During tests, the control side often needs to send a signal to trigger the operation of the DAQ module. In the case of the arc flash test, the control center transmits a signal to the DAQ system to trigger event recording.

An optical isolation scheme is designed to avoid EMI/RFI noise and ground loops between the control center and DAQ module. Figure 3-17 shows the design of the optical isolation circuit. A voltage follower minimizes the power requirement from the trigger signal and provides sufficient power to drive the input of the optical isolation circuit.

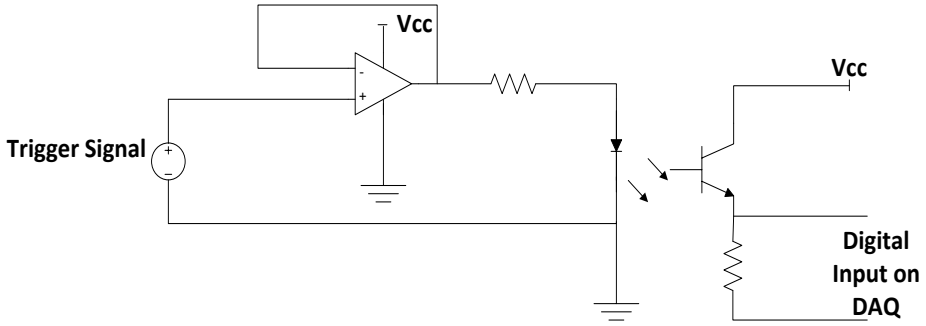

Figure 3- 17 Isolation and signal enhancement circuit for digital trigger input

2. Communication Between DAQ and Host Computer

In arc flash testing, the DAQ always functions as a remote repeater control station near the front end sensors/transducers. Although Ethernet is ideal for taking remote or distributed measurements under normal conditions, it becomes vulnerable when exposed to large amounts of EMI/RFI.

Fiber optics offers an excellent solution to overcome EMI problems: because of its high electrical resistance, it is safe to use near high-voltage equipment [43].

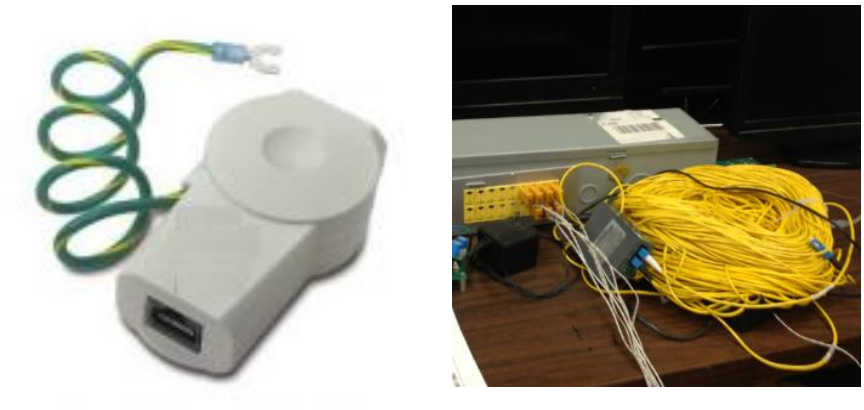

Figure 3- 18 CAT 5 surge arrester (left) and single mode optical fiber cable (right)

To prevent any line disturbances at the converted junction, a CAT 5 surge arrester is applied before the fiber communication cable to ensure instantaneous reaction to line surges or spikes. The optical fiber transmission path is then built between DAQ and host computer. Figure 3-18 shows the surge arrester and a single mode fiber utilized in an arc flash test.

3.5.6 Arc flash measurement system integration

Figure 3-19 displays the topology of the whole system grounding and isolation design. Each component in the measurement system has been well protected from arcing hazards.

For the arc flash tests, isolated inputs with channel-to-channel ground and the DAQ system were assembled within a shielded enclosure. The enclosure has its own floating ground and shielding cover, which was isolated from other test equipment with insulator poles. All of the sensors connect to the measurement system from the connector front panel. The surge arrester, fiber converter, and digital input isolation circuit were also assembled in the shielded enclosure. This all-in-one system provided a portable and easily-installed means of measurement during the test. Figure 3-20 is an image of the actual arc flash measurement system with all of the protection designs.

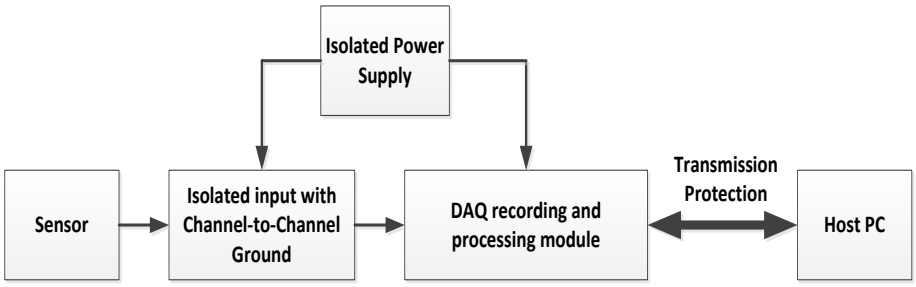

Figure 3- 19 Overview of the whole grounding and isolation system

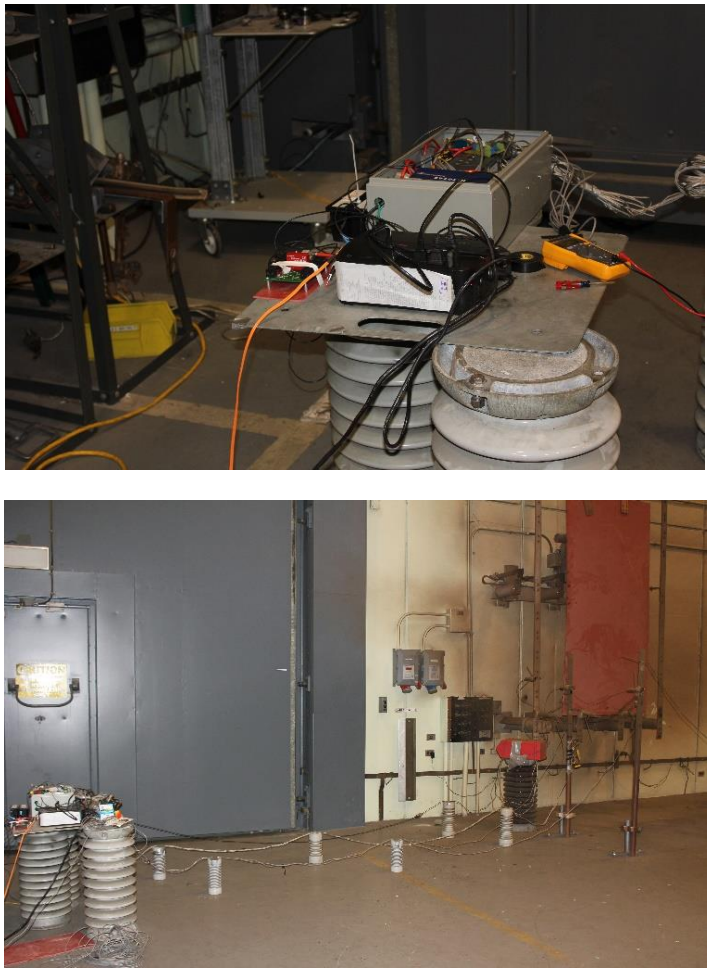

Figure 3- 20 Integrated measurement system with all protections (Top: Whole DAQ system with grounding and isolation design; Bottom: Isolated signal transmission bus)

3.6 Sample test results

Figure 3-21 shows the recorded temperature rise as measured at 33 inches from a recent 4.16kV arc flash test. The x-axis of the figure denotes the time in milliseconds, and the y-axis is the temperature in degrees Celsius. This test operated with a horizontal electrode in a cubic box (HCB) with a 33 kA bolted fault current.

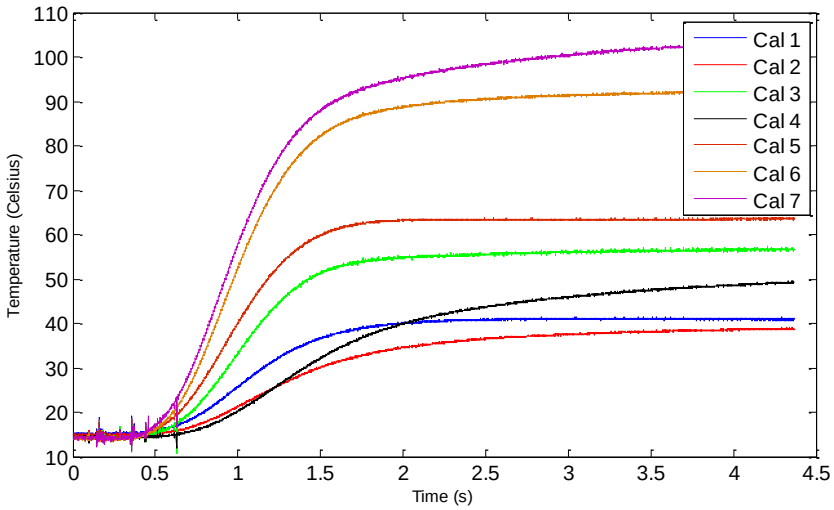

Figure 3- 21 IE measured in 4.16kV HCB with 33kA, under whole grounding and isolation applied

When comparing Figure 16 with Figure 7, one can see that after applying the channel-to-channel ground with isolation differential system, the high frequency spike and the noise caused by common-mode voltage have been completely removed.

Chapter 4

Model development for arcing current and incident energy

4.1 Testing data processing

4.1.1 Arcing current data processing

In order to accurately predict the response time for protective devices to clear a fault current, the arcing current should be precisely estimated. Depending on the fault inception angle and X/R ratio of the combined feeding cable impedance and transformer, the arcing current may contain DC component. As shown in Figure 4- 1, the decaying of DC offset can be seen in a 14.3kV, 20kA arc flash test.

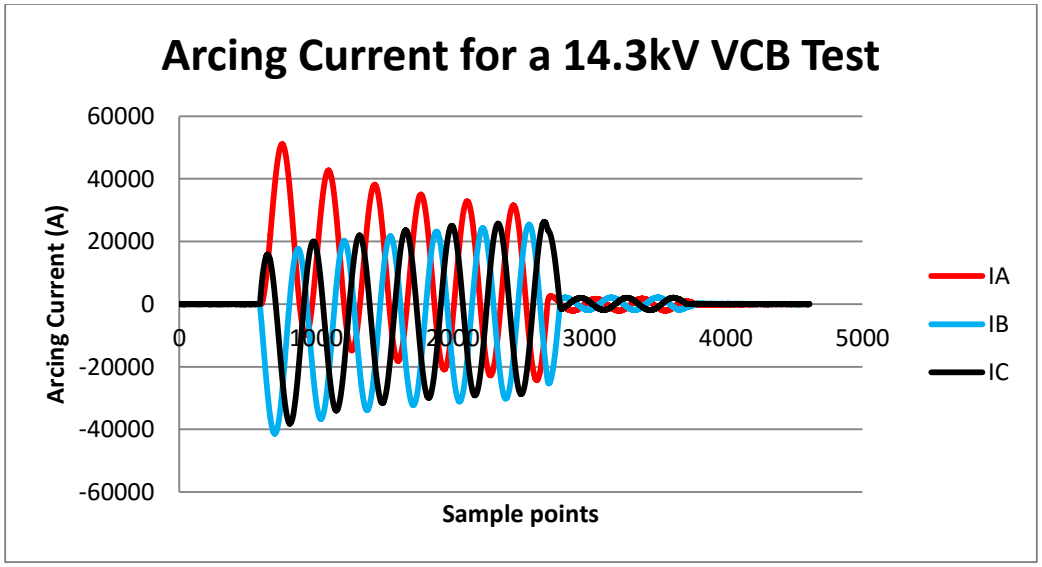

Figure 4- 1 Arcing current recording from 14.3kV arc flash test

In normal conditions, electrical system follows relatively symmetrical sine wave. When a fault is suddenly applied to the system, addition of the dc component to the symmetrical short circuit current gives the asymmetrical fault current. As qualitatively illustrated in the above figure, a DC component is introduced at the initiation of the fault due to the system's inductance preventing instantaneous changes in current. Figure 4-2

shows the DC offset and decay trend in asymmetrical AC current. Table 4-1 provides the typical decay rate of DC offset based on system X/R ratio.

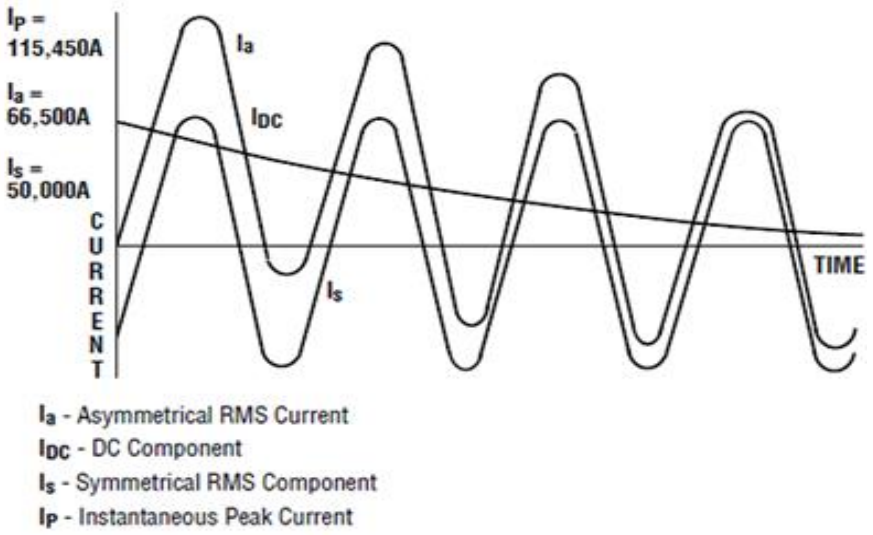

Figure 4- 2 DC offset and decay trend in asymmetrical AC current

Table 4- 1 Typical DC offset decay rate in power system

Short Circuit Power Factor (%)	Short Circuit X/R Ratio	Maximum 1-phase Instantaneous Peak	Maximum 1-phase RMS at ½ Cycle	Average 3-phase RMS at ½ Cycle
10	9.9301	2.455	1.437	1.229
20	4.8990	2.183	1.247	1.127
30	3.1798	1.978	1.130	1.064
40	2.2913	1.819	1.062	1.031
50	1.7321	1.694	1.026	1.013
100	0.000	1.414	1.000	1.000

The decay time of DC component depends on X/R ratio of the circuits, and it may affect fuse clearing time. However, in most of microprocessor relay system operation, DC offset has been excluded, the RMS current value is the only component to determine the operation time. Microprocessor relays execute mathematical procedures then produce analytic characteristics when fault occurs. The key to the behavior of microprocessor relays is the output of the digital filter.

Since we cannot order a fault and normally don't know the X/R ratio of the system, based on the worst case scenario, it is better to remove the DC offset and harmonic components when perform the conservative estimation of the arcing current.

A filtering algorithm has embedded into the mathematical procedures for arcing current data processing, in order to operate the modeling data based on RMS of fundamental AC component. A commonly used digital filter in protective relay industry manufacture is cosine filter. The algorithm of cosine filter is, for example, if number of samples per cycle is 16, the filter equations used in the arcing current modeling process are shown below [44]:

The filter coefficients: $$CFC_n = \cos(\frac{2\pi}{16} n)$$

The cosine filter: $$IX_{sample+spc} = \frac{2}{N+1} \sum_{n=0}^{N} I_{sample+spc-n} \cdot CFC_n$$

The phasor magnitude: $$|I_o|_{sample+spc} = \sqrt{(IX_{sample+spc})^2 + (IX_{sample+spc-\frac{spc}{4}})^2}$$

The phasor output: $$I_{o_{sample+spc}} = IX_{sample+spc} + j \cdot IX_{sample+spc-\frac{spc}{4}}$$

Where, N = 16

n = 0, 1, 2 … N

sample = sequence of samples 0, 1, 2, 3, …

spc = number of samples per cycle

$I_{sample+spc-n}$ = current samples

$IX_{sample+spc}$ = filter output

Filtering process determines the components' change in magnitude when the sampling interval remains fixed and the input frequency is varied. While extracting the fundamental component, the filter rejects all exponentially decayed DC part and harmonics.

The DC offset of the arcing current is thus filtered before performing I_{arc} estimation in the current model; however, in incident energy estimation, from a conservative hazard protection point of view, the original unfiltered current data will be utilized in arc energy calculation.

The measured arcing current data are processed by a cycle-by-cycle cosine filter applied to the raw data based on recording sampling rate (typical is 20k samples/second). A sliding window is employed for each cycle of data to determine the fundamental 60 Hz RMS current, while removing DC offset and all other higher order harmonics. Figure 4-3 shows the filtered RMS value of arcing current compared to the un-filtered RMS value of arcing current.

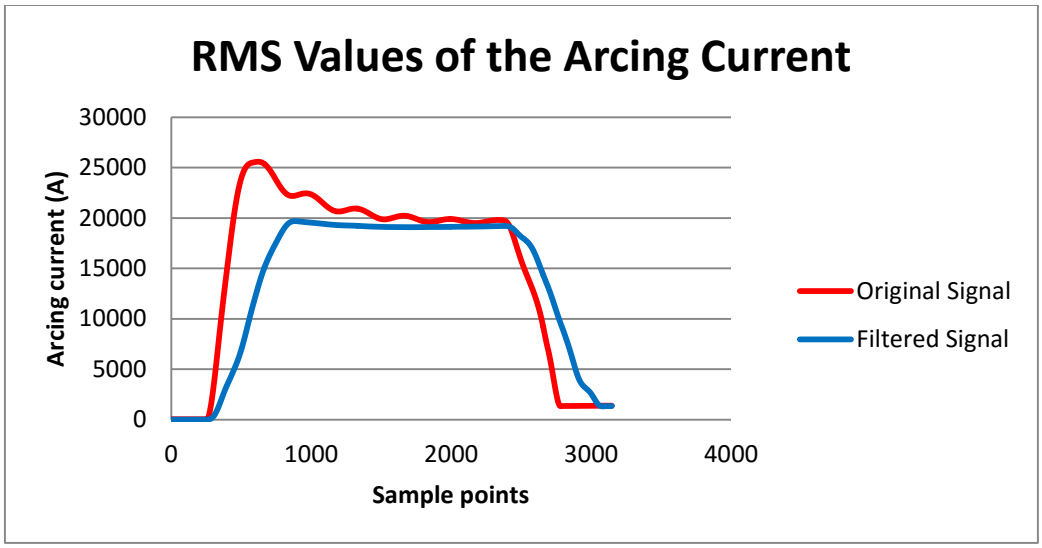

Figure 4- 3 Filtered and un-filtered RMS arcing current comparison

To create a stable arcing, it takes some time to establish arcing path in the beginning of arc initiated. Thus, to guarantee the accuracy of arcing current data, there are 2 cycles of data may need to be excluded because of the non-arcing data mixing. The first one is the pre-arc cycle which system turn from normal condition to fault condition, and another one is post-arc cycle, which system from fault condition to arc extinguish condition. Based on the this condition, last 2 cycles of data after descending order will exclude the time to burning the starter wire or arc trigger delays. An average current will be taken from Ns*(N-2) current data points, which in order not to overestimate arc flash energetics.

As observed from the test, the arcing current is relatively stable when the open circuit voltage is higher than 600V. However, arcing current becomes dynamic and unstable at lower voltage (480V and below) which makes it difficult to model I_{arc} based on laboratory test data.

Figure 4-4 is a six cycle arcing current plot on three phase 480V test, with 17.2kA bolted fault current. Compared to the 14.3kV arcing current recording shown in Figure 4-

1, a 480V arcing current may have a complex time structure during the arc event. There is no consistent trend during the whole single test.

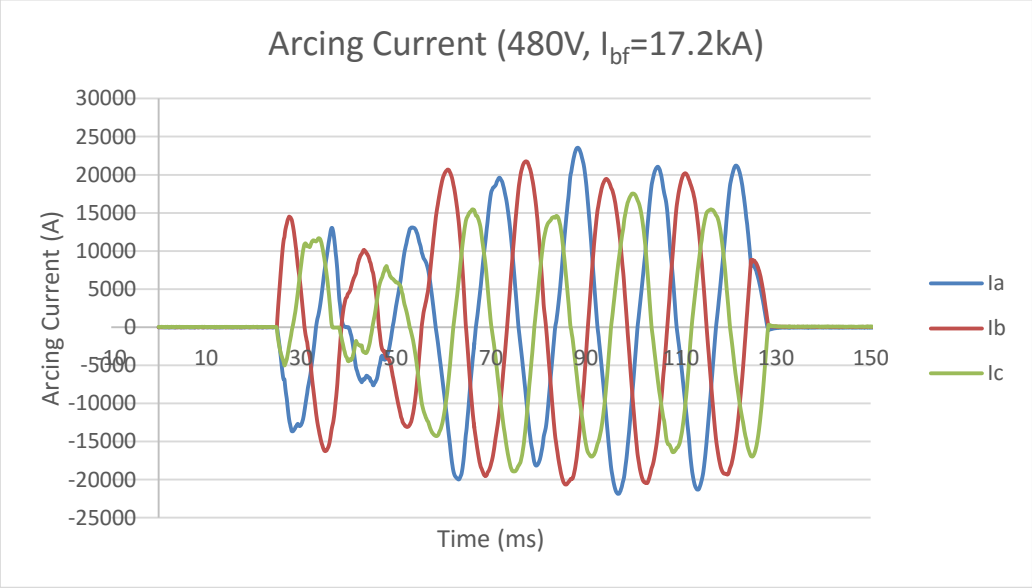

Figure 4- 4 Arcing current recording for 480V arc flash test

Based on this, a more accurate arcing current below 600V may be derived from well-modeled 600V estimation results. From previous observations and research, in low voltage tests, when bolted fault current is fixed, lower voltage tests created a decreasing trend for arcing current. More specifically, in low voltage range, the speed of system resistance in per centimeters increasing are higher than voltage decreasing. On the other hand, in the context of arcing energy, electrical force decreased in the lower energy test. Based on this phenomenon, the length of arc column shrinks as arc energy decreases. Then, the arcing resistance also decreased because of decreased voltage drop from the arc column.

Thus, it is reasonable to assume the total resistance from the testing circuit remains the same level within low voltage level (600V and below) arc flash tests, because the increased arcing resistance and the decreased system resistance canceled

each other out. Thus it can be assumed that the total resistance remains the same from 208V to 600V. Table 4-2 provide some sample arcing resistance recording for 600V and below tests.

Table 4- 2 600V and below arcing current, voltage and resistance

Configuration	V_{oc} (kV)	I_{bf} (kA)	Gap (mm)	I_{arc} (kA)	V_{arc} (V)	R_{arc} (Ohm)
VCBB	0.300	20.000	25.4	13.734	108.66	7.91
VCBB	0.480	20.000	25.4	16.539	114.07	6.90
VCBB	0.300	20.000	25.4	15.736	103.66	6.59
VCBB	0.480	20.000	25.4	16.872	101.96	6.04

From the table 4-2 above, those data basically proved the resistance within the range, and arcing resistance in the same test configuration shows their similarity under the same bolted fault current and system voltage.

4.1.2 Incident energy data processing

Arc energy depends on many electrical factor characteristics. Under the same bolted fault current, higher voltage typically implies higher arc energy. A greater gap width could also result in increased arc energy as well. From the observation on arc flash tests, the arc column increases with gap width which could cause an increased arc energy by wider gap distance, or. Sample energy results for horizontal electrode in open air and vertical electrode in open air are provided in Table 4-3 and 4-4.

As shown in Table 4-3 and 4-4, in the same configuration, arc energy tends to increase with correspondingly larger gap spacing under same bolted fault current level. Although the arc energy may be different at different voltage levels, the ratio of incident energy to arc energy (IE/E_{arc}) tends to be similar when the bolted fault currents are identical. Table 4-5 and 4-6 shows the sample result for horizontal electrode in open air and vertical electrode in open air test, respectively.

Table 4- 3 Arc energy comparison on different gap width

(Horizontal electrodes in open air tests)

600V, 20kA (HOA)			2.7kV, 20kA (HOA)		
G (inch)	Arc Energy (MJ)		G (inch)	Arc Energy (MJ)	
	6 cycles	6 cycles		6 cycles	12 cycles
1.25	0.9196	1.8652	3.0	2.0908	4.1432
1.25	0.8796	1.8959	3.0	2.0469	4.0150
1.25	0.8946	1.7772	3.0	2.0409	3.9868
2.0	0.9890	1.9584	4.5	2.1033	4.1882
2.0	0.9859	1.9154	4.5	2.1568	4.1318
2.0	1.0236	1.9285	4.5	2.1527	4.1430

Table 4- 4 Arc energy comparison on different gap width

(Vertical electrodes in open air tests)

600V, 20kA (VOA)			2.7kV, 20kA (VOA)		
G (inch)	Arc Energy (MJ)		G (inch)	Arc Energy (MJ)	
	6 cycles	6 cycles		6 cycles	12 cycles
0.5	0.9507	1.8779	3.0	1.9977	4.0263
0.5	0.9954	1.8752	3.0	2.0207	3.8896
0.5	0.9972	1.8529	3.0	1.9754	3.9059
1.25	1.0072	1.9741	4.5	2.4400	4.7643
1.25	1.0027	1.9352	4.5	2.4020	4.6293
1.25	0.9984	1.8876	4.5	2.4225	4.5813

Table 4- 5 IE/E_{arc} comparison

(Horizontal electrodes in open air arc flash tests)

600V, 20kA (HOA)			2.7kV, 20kA (HOA)		
D (inch)	IE/E_{arc} (cal/cm$_2$/MJ)		D (inch)	IE/E_{arc} (cal/cm$_2$/MJ)	
	Average	Peak		Average	Peak
36	1.2482	1.3116	36	1.2355	1.3097
27	1.9224	2.1035	27	1.8883	2.0972
18	3.6633	4.5528	18	3.7651	4.8112

For HOA configurations on Table 4-5, the IE to arc energy (IE/E_{arc}) is similar between 600V and 2.7kV. The slight difference may be caused by the loss along a longer arc column at higher voltages, or plasma flow partially blocked by calorimeter in a nearer

distance. From the standpoint of model development, the differences or errors are within tolerance.

4.2 Modeling parameters sensitivity analysis

For the model development process, parameter identification is the first step to understand the correlation between dependent and independent variables and between dependent variables. A simple observation from test data can provide some basic hints to tease out that relationship. Representative 600V energy analysis is provided in Figure 4-5 to 4-7, which are a vertical electrode in open air test configuration, horizontal electrode in open air test configuration and vertical electrode in cubic box test configuration, respectively. These data were obtained with a 2 inch electrode gap width over a 12-cycle arc duration, and the incident energy measurement distance is 18 inch from arcing point to calorimeters. As shown on these figures, incident energy tends to rise with increasing bolted fault current, in which the arcing energy is increasing. In open air tests, there is substantially less incident energy in VOA compared to enclosed tests because the enclosure may direct the plasma toward to calorimeter array. Similarly, lower incident energy is detected in vertical electrode configurations compared to horizontal setups.

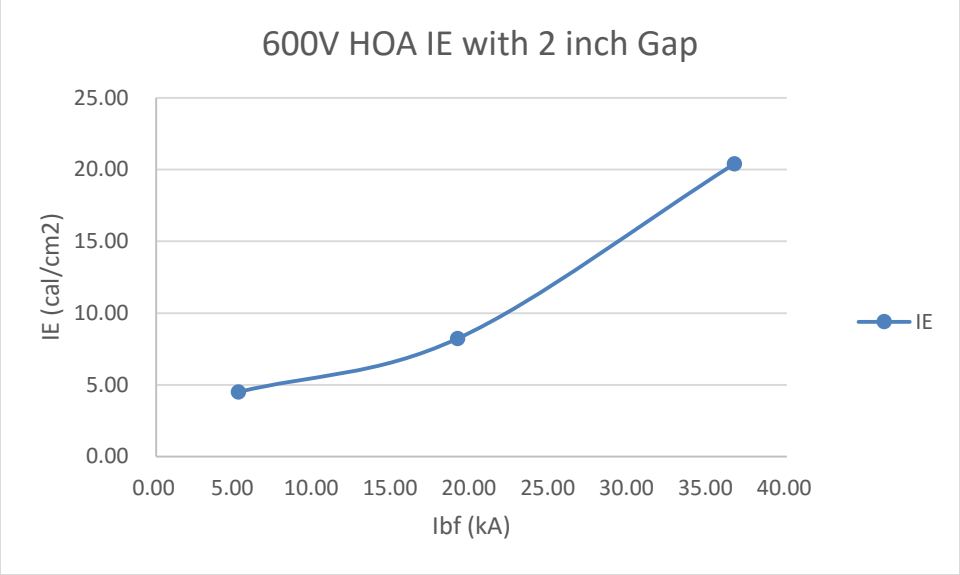

Figure 4- 5 600V HOA IE with 2 inch gap

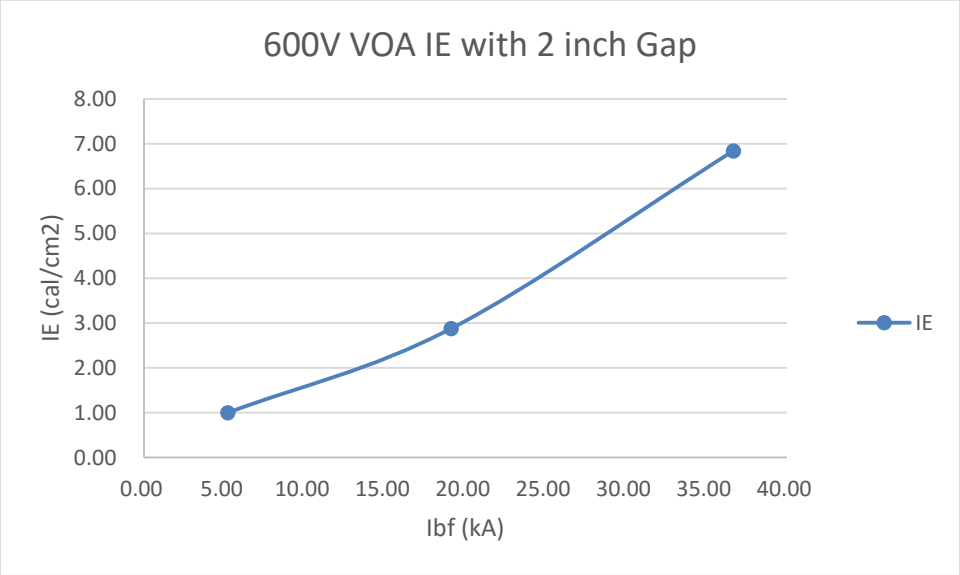

Figure 4- 6 600V VOA IE with 2 inch gap

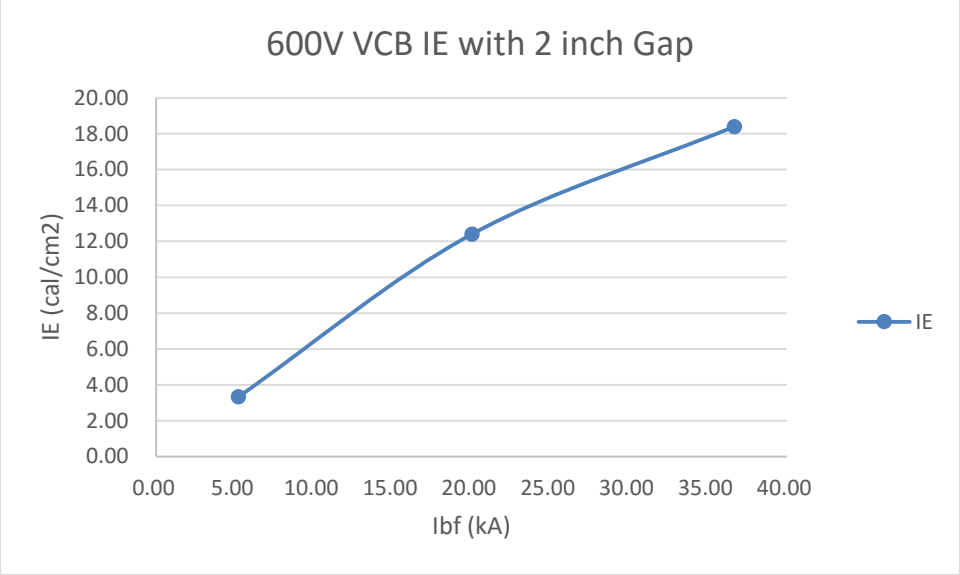

Figure 4- 7 600V VCB IE with 2 inch gap

Figure 4-8 and 4-9 are representative incident energy plots for a 2.7kV test in an enclosed horizontal electrode configuration. Figure 4-8 plots the incident energy of a 3-inch electrode gap setup, and Figure 4-9 illustrates the incident energy in a 4.5-inch electrode gap configuration. In both cases, the calorimeter was placed 24 inches from the arcing point. . As shown in figures, the correlation between incident energy level and gap distance is relatively strong. In other words, arc energy over wider electrode gap distance has highly increased.

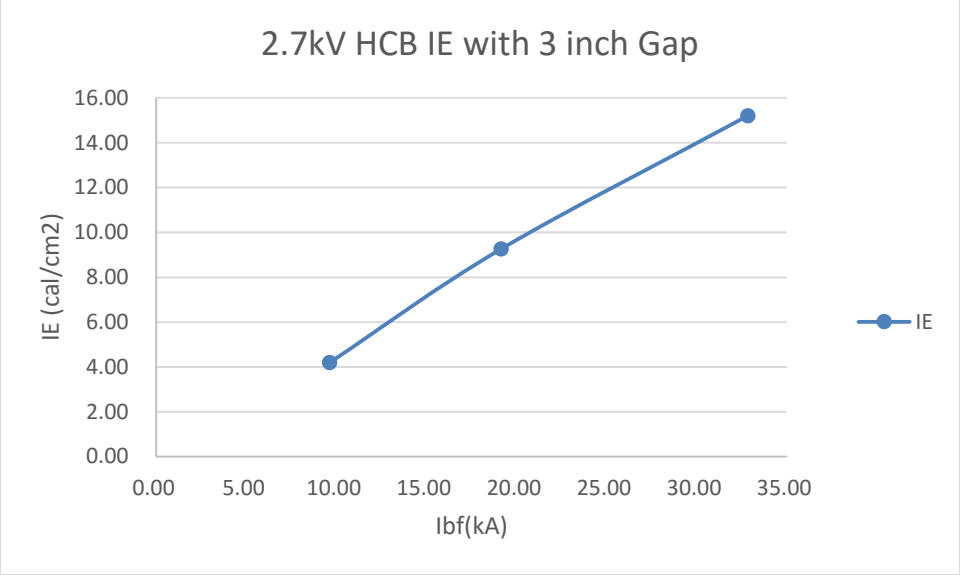

Figure 4- 8 2.7kV HCB IE with 3 inch gap

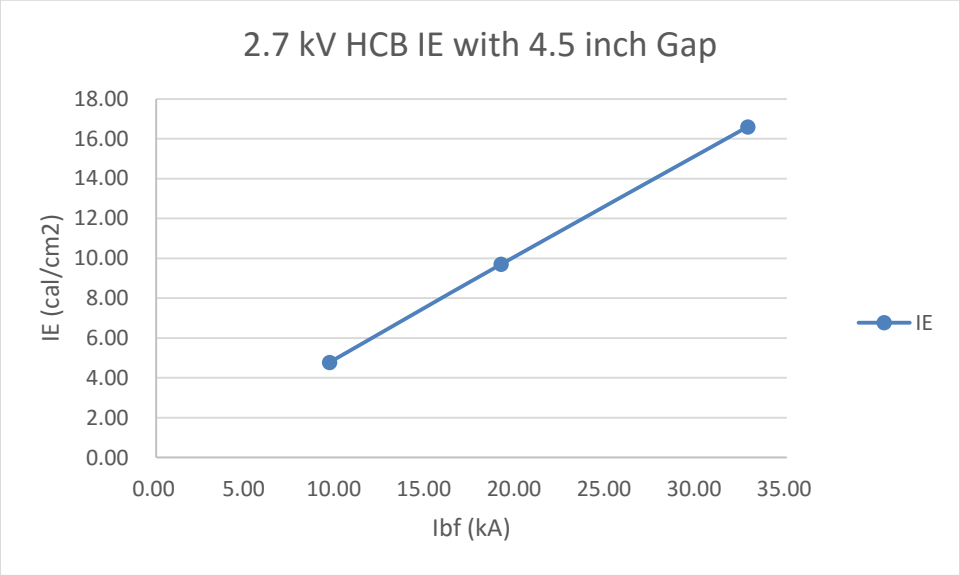

Figure 4- 9 2.7kV HCB IE with 4.5 inch gap

Figure 4-10 and 4-11 are representative incident energy plots for a 14.3kV test for horizontal electrode in open air test configuration and vertical electrode in open air configuration, with 20kA bolted fault current and 3.75 gap width between electrodes.

From these two figures, the incident energy level falls off with distance, and there is more incident energy exposure in horizontal electrode configuration, as compared to the vertical one. Thus it can be seen that the test configuration has a substantial impact on incident energy level.

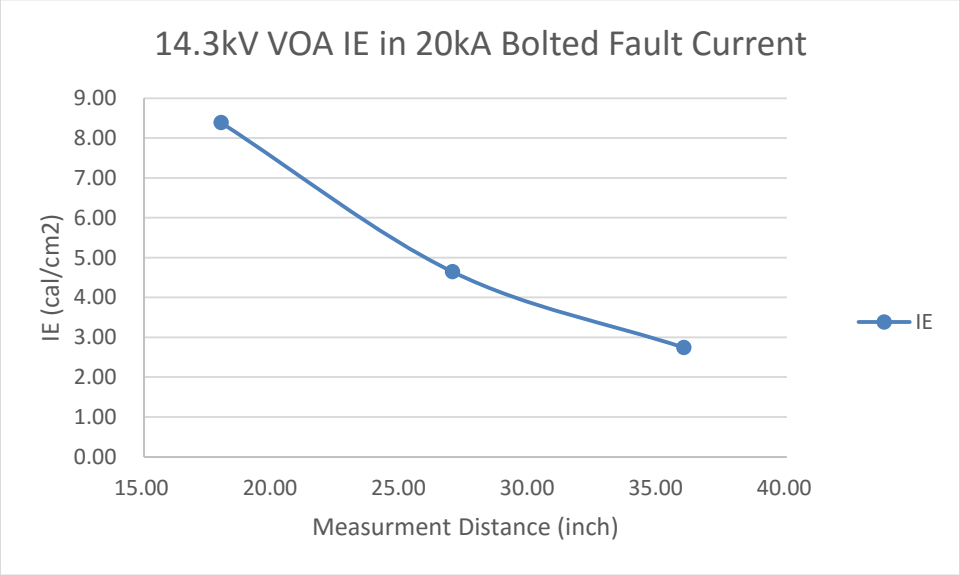

Figure 4- 10 14.3kV VOA IE in 20kA bolted fault current

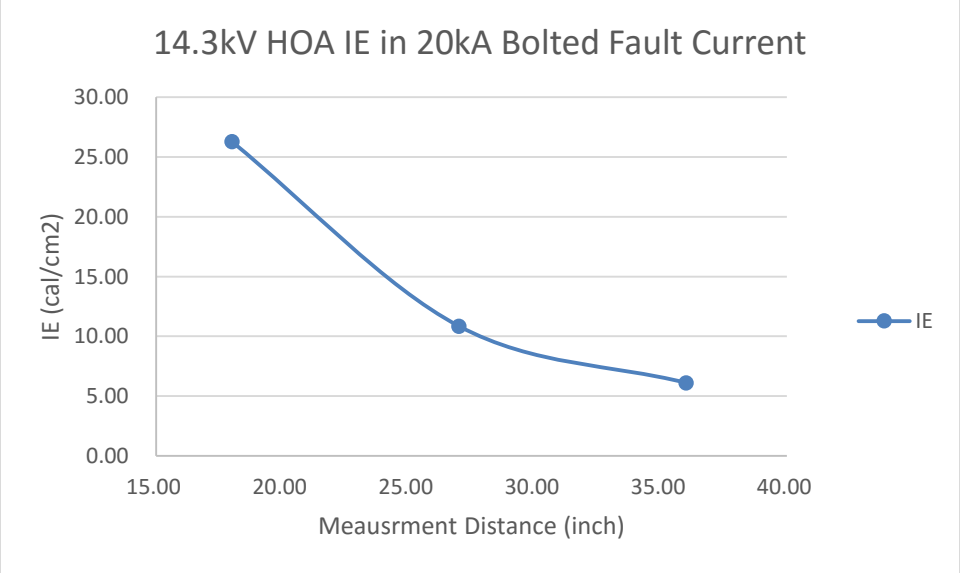

Figure 4- 11 14.3kV VOA IE in 20kA bolted fault current

Additionally, high speed video also shows the configuration impact to incident energy exposure. Figure 4-12 to 4-14 are the snap shots of high speed video, which illustrate the direction of plasma trajectories.

Figure 4- 12 Ejected arc plasma on horizontal electrodes in open air

Figure 4- 13 Ejected arc plasma on vertical electrodes in open air

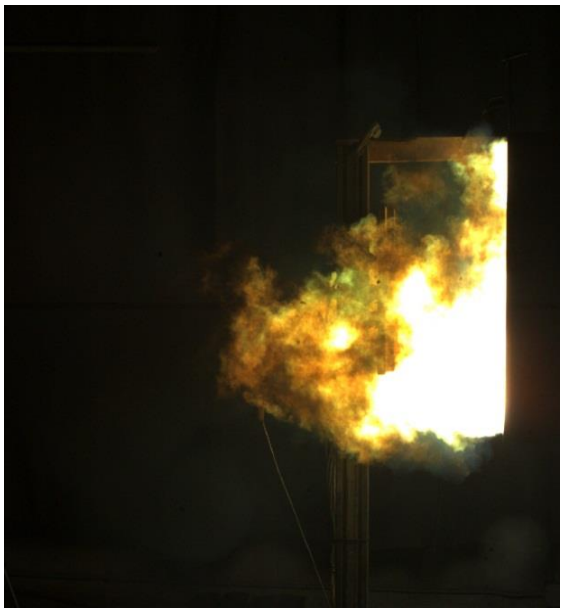

Figure 4- 14 Ejected arc plasma on vertical electrodes with enclosure

To provide the theoretical basis, some applied statistic approaches may be utilized to analyze parameter sensitivity to incident energy and arcing current.

Although, single variable linear regression provides a response indication of the nature of the relationship for the independent variable against the dependent variable, multiple independent variables can interact with each other to affect the dependent variable and complicate the analysis. Partial regression analysis is an approach to show the effect of adding a variable to a model already having one or more independent variables; also, it may take into account the effect among the other independent variables in the model [45].

- Partial regression is formed by [45]:
    1. Computing the residuals of regressing the response variable against the independent variables but omitting Xi

2. Computing the residuals from regressing Xi against the remaining independent variables
3. Plotting the residuals from (1) against the residuals from (2)

For example, Figure 4-15 shows one partial regression plots on arcing current modeling process. This example plot indicates the dependence between bolted fault current and arcing current.

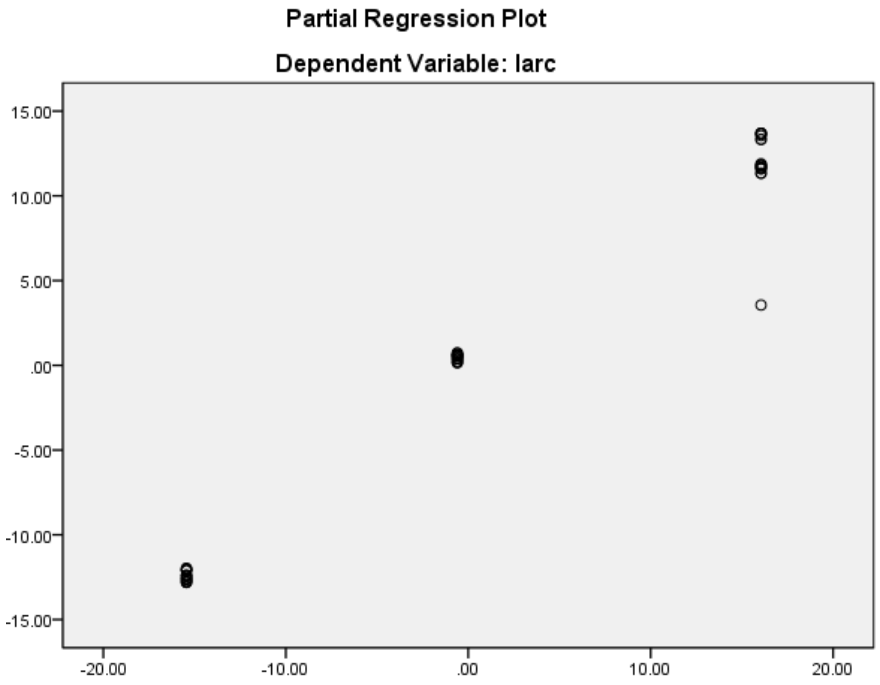

Figure 4- 15 Sample result for partial regression plotting

From the figure, the plot shows a very good linearization performance between arcing current and bolted fault current, which means partial regression coefficients are affecting dependent variable significantly. Additionally, the increasing trend from the figure indicates the positive correlation between independent variable and dependent variables.

4.2.1 Arcing current parameter sensitivity analysis

When performing a linear regression with a single independent variable, a scatter plot of the response variable against the independent variable provides a good indication of the nature of the relationship. Here is one detailed example to show the sensitivity analysis for 14.3kV arcing current analysis steps.

1) Take logarithm on all variables before regression process.

2) Convert I_{arc} to log(I_{arc}), I_{bf} to log(I_{bf}), Gap to logG for model development purpose.

3) Put all 14.3kV converted data into commercial available statistic software. (Figure 4-16)

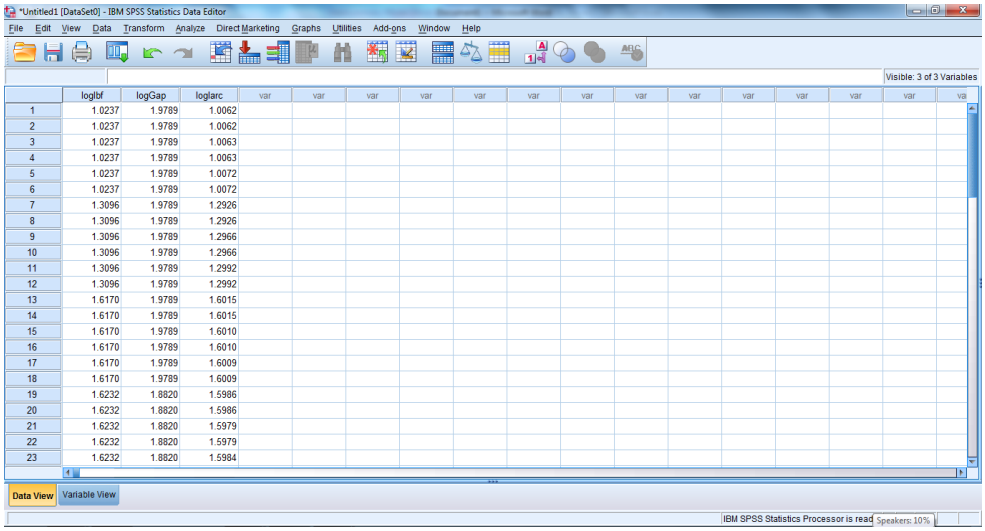

Figure 4- 16 Data input interface

4) Choose logIarc as dependent variable Y, logIbf and logGap as independent X1 and X2, respectively. (Figure 4-17)

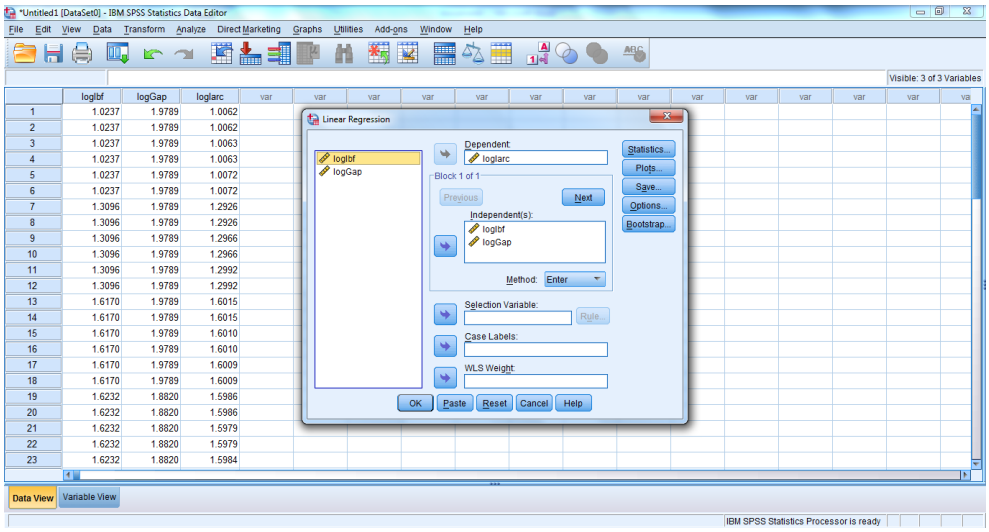

Figure 4- 17 Parameter selection

5) Compute the residuals of regressing the response variable against the dependent variables Y but omitting X1, then X2.

6) Compute the residuals from regressing X1, then X2 against the remaining dependent variables Y.

7) Plot the residuals from step 5 against the residuals from step 6. (Figure 4-18)

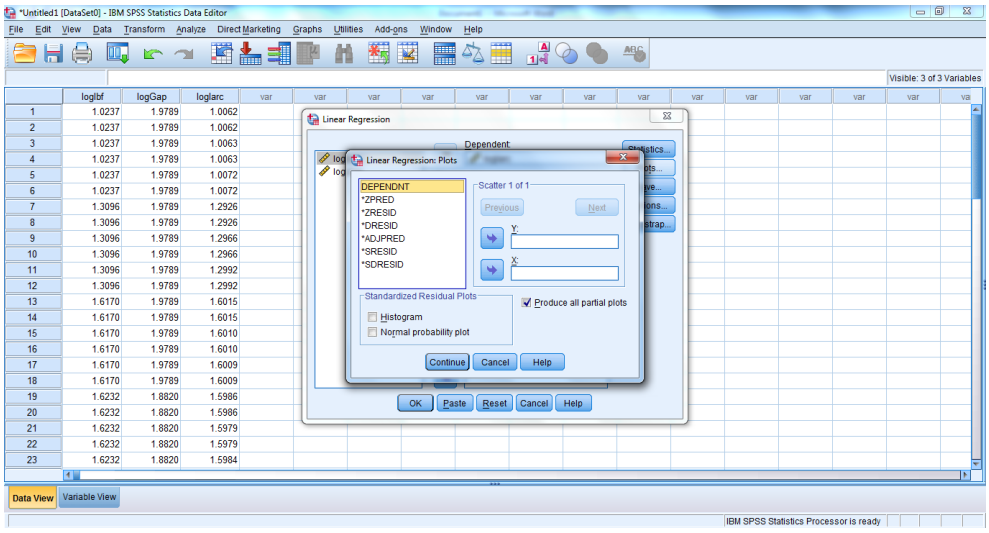

Figure 4- 18 Partial regression calculation

8) The software will generate the regression results and plot the partial regression figures, which is provided in Figure 4-19 and 4-20.

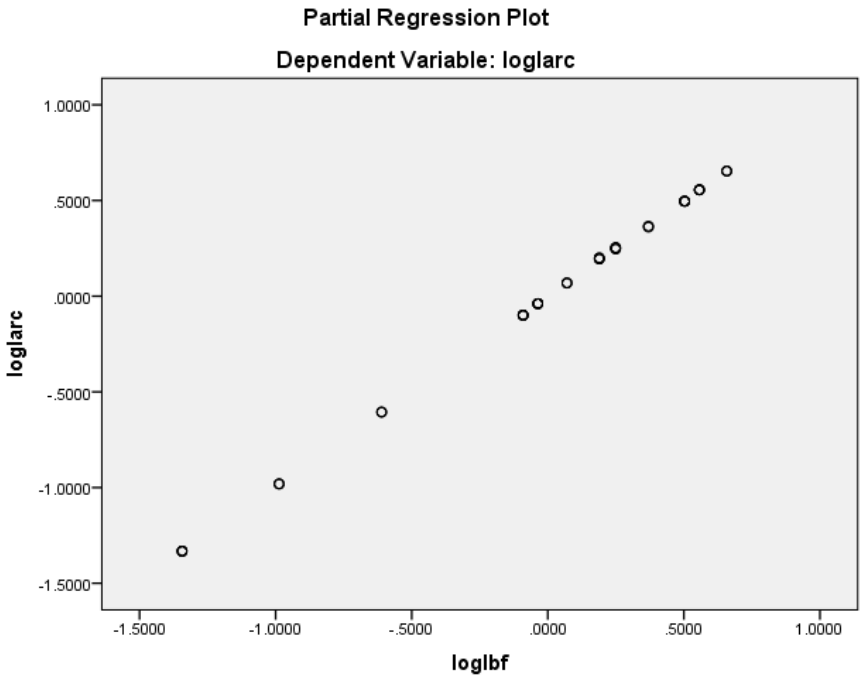

Figure 4- 19 Sensitivity analysis for Ibf against to Iarc

From the partial regression plots Figure 4-19 shown above ($log I_{arc}$ vs $log I_{bf}$), it has strong positive linear correlation between $log I_{arc}$ and $log I_{bf}$.

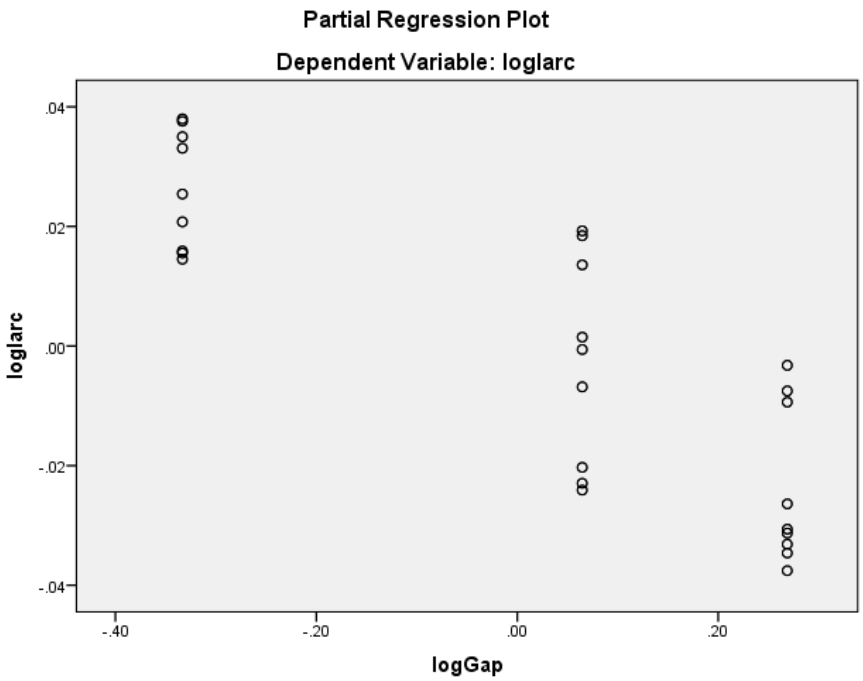

Figure 4- 20 Sensitivity analysis for Gap against to I_{arc}

From the partial regression plots Figure 4-20 shown above (*log*I_{arc} vs *log*Gap), there is good linearization performance between *log*I_{arc} and *log*Gap. With the same I_{bf}, I_{arc} decreases with increasing of gap width. Additionally, at the same gap level, I_{ratio} (I_{arc}/I_{bf}) will decrease when I_{bf} increases.

4.2.2 Incident energy parameter sensitivity analysis

The process of IE model development involves approximately 150 possible correlations among five variables. A partial regression had been performed to find the correlation between IE to other parameters. The partial regression result for IE lists as figures below from Figure 4-21 to 4-23.

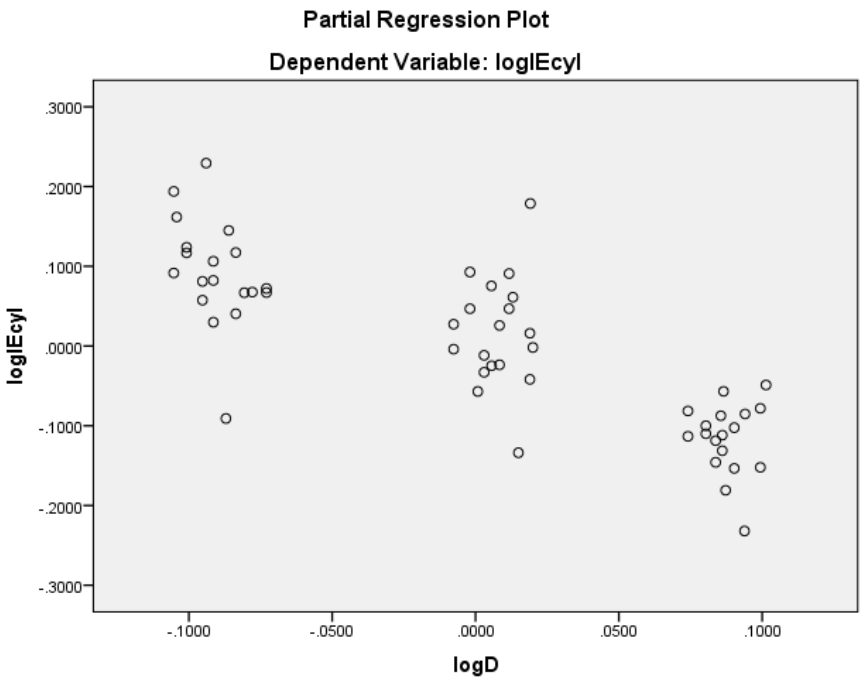

Figure 4- 21 Sensitivity analysis for Distance against to IE

From the figure above, the partial regression results clearly show the relationship between distance and IE. Shorter distance will result in a greater reception of energy during the arc flash.

Also, I_{arc} and IE are positively correlated, as shown in Figure 4-22.

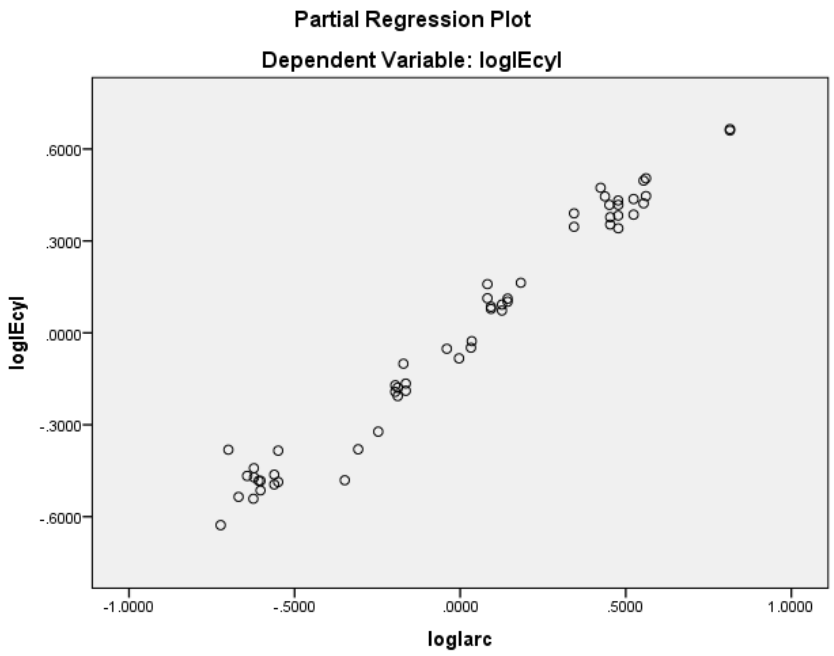

Figure 4- 22 Sensitivity analysis for Iarc against to IE

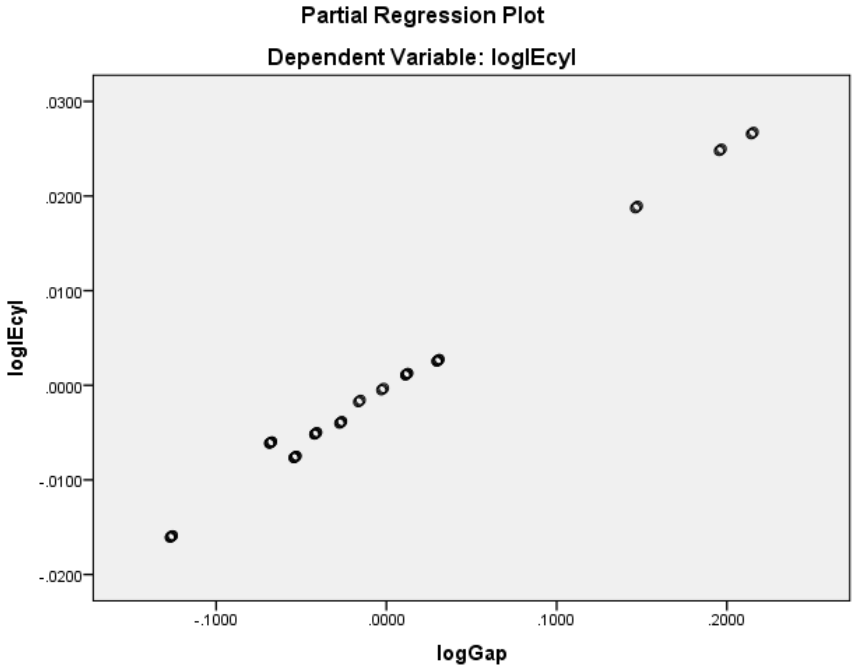

Figure 4- 23 Sensitivity analysis for Gap against to IE

The gap width is also the vital factor for IE level. From Figure 4-23 shown above, the larger gap between electrodes will cause more severe IE conditions.

4.3 Arcing current and Incident energy modeling procedure

Based on test results and parameter sensitivity results, the following factors are known to affect the level of arcing current and incident energy:

- Bolted fault current level
- Open circuit voltage level
- Gap width between electrodes
- Distance from arcing point to calorimeters
- Arc duration
- Electrode orientation
- Enclosure configuration

For incident energy model development several assumptions need to be utilized to drive the modeling process. Representative assumptions include, but are not limited to:

1. Arc flash energy will create same the temperature rise in the calorimeter, during the same arc flash event. This assumption allows for generating multiple data points from a single event.
2. If test configurations and major rating, such as bolted fault current, are identical, regardless of voltage level, 1 MJ arc energy will create a similar temperature rise in a calorimeter during the arc flash.
3. From first and second assumptions and the sample IE to energy ratio result listed before, it is assumed that the IE to arc energy ratio is not only substantially identical for vertical electrodes, or horizontal electrodes in open are arc flash test, but also identical for vertical electrode, or horizontal electrodes with enclosure

arc flash test. The same assumption may also applied to vertical electrodes with bottom insulated barrier in box configuration.

With the above assumptions and observations, data analysis and model development procedure will be carried out through the following procedure. Also, these assumptions provide for box size correction factors calculation when different enclosures are utilized. The brief step descriptions are provided below:

Step 1: Select a configuration, representative configuration include VCB, VCBB, VOA, HCB and HOA, for a specific anchor voltage class (600V, 2.7kV and 14.3kV).

Step 2: Select test case from performed tests with typical parameter selections such as bolted fault current, electrodes gap and measurement distance.

Step 3: Arcing current modeling data processing. RMS arcing current will be calculated from the filtered signal for the corresponding period. Average value of N-2 cycles descending order data will be utilized as arcing current modeling data.

Step 4: Calculate the total arc energy during the arc event.

Step 5: Obtain maximum IE recording. The maximum incident energy IE_{max} is obtained from recorded data, using the highest temperature rise from any single calorimeters.

Step 6: Calculate ΔIE per MJ based upon the previous assumption. The ratio is defined in units of cal/cm^2/MJ. As mentioned before, depending on model, it may be assumed that the IE/MJ is identical for each configuration.

Step 7: Convert MJ/Cyl to IE/Cyl. To develop a unified data processing procedure, the recording data is analyzed sample-by-sample. The arc energy for a complete cycle will be calculated by adding energy from one cycle N_s consecutive sampling points (MJ/Cyl).

Step 8: Using sliding window to move forward one data point and repeat the procedure over N_s data point representing a cycle. For example, if the sampling rate is 20k samples/s, and the AC frequency is 60 Hz, this procedure will enable to generate 333 (N_s) data points per cycle.

Step 9: Sort IE/Cyl in descending sequence, and keep top Ns*(N-2) data points. N is the number of cycles the arc flash duration and N_s is the number of samples per cycle. Based on cycle-by-cycle analysis, a higher incident energy per cycle is extracting while the initial time for burning the starter wire is excluding. Ns*(N-2) will exclude the time to burning the starter wire or arc trigger delays, which in order not to underestimate arc flash energetics.

Step 10: Combine data points for tests with the same configuration and sort them in descendent order. Top 50% data points will be used for IE estimation. Statistical analysis will be performed to obtain average (IE/Cyl) and its standard deviation. These procedures can be utilized to set the boundary range for arcing current estimation, for example, calculate the 95% confidence [IE/Cyl] value (upper bound) for estimated arcing current (Iarc).

Step 11: Repeat the procedure until all cases within the configuration for a specific voltage class are completed. The incident energy models are obtained as the function of bolted fault current, open circuit voltage, gap spacing of the electrodes, and distance to arcing point. The function could be listed in Table 4-6 below for each single test.

Step 12: Configuration correction. Use the relationships of (cal/cm^2)/MJ at different voltage levels to establish the correction factor for different enclosures. Specifically, the ratio of average incident energy to arc energy is different in different enclosure dimension. Table 4-7 shows the sample of (cal/cm^2)/MJ for 2700V

(26”x26”x26”) and 2700V (36”x36”x36”) at VCB. Curve fitting process will be performed to estimate the correction factor at specified distance (D). Similar procedures for other configurations (VCBB and HCB) and voltages will be carried out to establish the correction factor. The normalized incident energy on particular enclosure size at first, then it will be corrected to actual size using the correction factor based on correction equation for each test configuration. Note that for open air configuration, there is no need to perform this step.

Table 4- 6 Summary of each test set-up

Gap	Bolted Fault	Distance	[IE/Cyl]	Arcing Current
G_1	I_{bf1}	D_1	--.--	--.--
G_1	I_{bf1}	D_2	--.--	--.--
G_1	I_{bf1}	D_3	--.--	--.--
G_1	I_{bf2}	D_1	--.--	--.--
G_1	I_{bf2}	D_2	--.--	--.--
G_1	I_{bf2}	D_3	--.--	--.--
G_1	I_{bf3}	D_1	--.--	--.--
G_1	I_{bf3}	D_2	--.--	--.--
G_1	I_{bf3}	D_3	--.--	--.--
G_2	I_{bf1}	D_1	--.--	--.--
G_2	I_{bf1}	D_2	--.--	--.--
G_2	I_{bf1}	D_3	--.--	--.--
G_2	I_{bf2}	D_1	--.--	--.--
G_2	I_{bf2}	D_2	--.--	--.--
G_2	I_{bf2}	D_3	--.--	--.--
G_2	I_{bf3}	D_1	--.--	--.--
G_2	I_{bf3}	D_2	--.--	--.--
G_2	I_{bf3}	D_3	--.--	--.--
G_3	I_{bf1}	D_1	--.--	--.--
G_3	I_{bf1}	D_2	--.--	--.--
G_3	I_{bf1}	D_3	--.--	--.--
G_3	I_{bf2}	D_1	--.--	--.--
G_3	I_{bf2}	D_2	--.--	--.--
G_3	I_{bf2}	D_3	--.--	--.--
G_3	I_{bf3}	D_1	--.--	--.--
G_3	I_{bf3}	D_2	--.--	--.--
G_3	I_{bf3}	D_3	--.--	--.--

Table 4- 7 (cal/cm^2)/MJ for different enclosure dimension 2700V tests at VCB

2700V (26”x26”x26”)		2700V (36”x36”x36”)	
Configuration	(cal/cm^2)/MJ	Configuration	(cal/cm^2)/MJ
VCB-20-24	2.4335	VCB-20-31	1.9009
VCB-20-33	1.6088	VCB-20-34	1.2567
VCB-20-42	0.9645	VCB-20-43	0.7534

Step 13: Obtain I_{arc} and IE/Cyl models as function of bolted fault current, open circuit voltage, gaps of electrodes, and distance to the arcing point for this configuration at specified voltage through regression process.

Step 14: Repeat procedure for all configurations and tested voltages. Depending on application in practice, with the enclosure correction factor, the results for enclosed configurations, such as HCB, VCB, and VCBB, are able to be normalized to 20”x20”x20” enclosure.

Step 15: I_{arc} and IE estimation models for each configuration at two other tested voltages can be created through the above mentioned process (Tables 4-8 and 4-9). Also, these models may be utilized to determine the arc flash safety protection boundary.

Table 4- 8 I_{arc} Estimation Models

Voltage	VCB	VCBB	HCB	HOA	VOA
0.60 kV	$I_{arcVCB-0.6}$	$I_{arcVCBB-0.6}$	$I_{arcHCB-0.6}$	$I_{arcHOA-0.6}$	$I_{arcVOA-0.6}$
2.7kV	$I_{arcVCB-2.7}$	$I_{arcVCBB-2.7}$	$I_{arcHCB-2.7}$	$I_{arcHOA-2.7}$	$I_{arcVOA-2.7}$
14.3 kV	$I_{arcVCB-14.3}$	$I_{arcVCBB-14.3}$	$I_{arcHCB-14.3}$	$I_{arcHOA-14.3}$	$I_{arcVOA-14.3}$

Table 4- 9 [IE/Cyl] Estimation Models

Voltage	VCB	VCBB	HCB	HOA	VOA
0.60kV	$[IE/Cyl]_{VCB-0.6}$	$[IE/Cyl]_{VCBB-0.6}$	$[IE/Cyl]_{HCB-0.6}$	$[IE/Cyl]_{HOA-0.6}$	$[IE/Cyl]_{VOA-0.6}$
2.7kV	$[IE/Cyl]_{VCB-2.7}$	$[IE/Cyl]_{VCBB-2.7}$	$[IE/Cyl]_{HCB-2.7}$	$[IE/Cyl]_{HOA-2.7}$	$[IE/Cyl]_{VOA-2.7}$
14.3kV	$[IE/Cyl]_{VCB-14.3}$	$[IE/Cyl]_{VCBB-14.3}$	$[IE/Cyl]_{HCB-14.3}$	$[IE/Cyl]_{HOA-14.3}$	$[IE/Cyl]_{VOA-14.3}$

Step 16: Use interpolation to estimate the system voltage between 2700V and 14.3kV. Use interpolation and extrapolation to estimate system voltage between 600V and 2700V.

Step 17: Since the arc flash behavior becomes more dynamic at low voltage, below 600V models will direct derive from 600V models.

4.4 Model Implementation

The purpose of the model development could be simply described as

- Cover whole test data range
- Continuous nonlinear model generation
- Minimize the relative and absolute errors respect to test results

To develop the model from data, linear regression was utilized. In statistics, regression analysis focuses on the relationship between a dependent variable and one or more independent variables. It is widely used for prediction and forecasting in the aid of data analysis.

In this whole modeling analysis process, linear regression is used to develop the initial statistical model that is then adjusted based on testing observation and physics.

Figure 4-24 is the flow chart to illustrate a method for implementing the thermal component of the arc flash phenomenon modeling process. This process could be divided into two phases: arcing current modeling and incident energy modeling. In particular, the method of incident energy modeling could be also applied to arc flash protection boundary estimation.

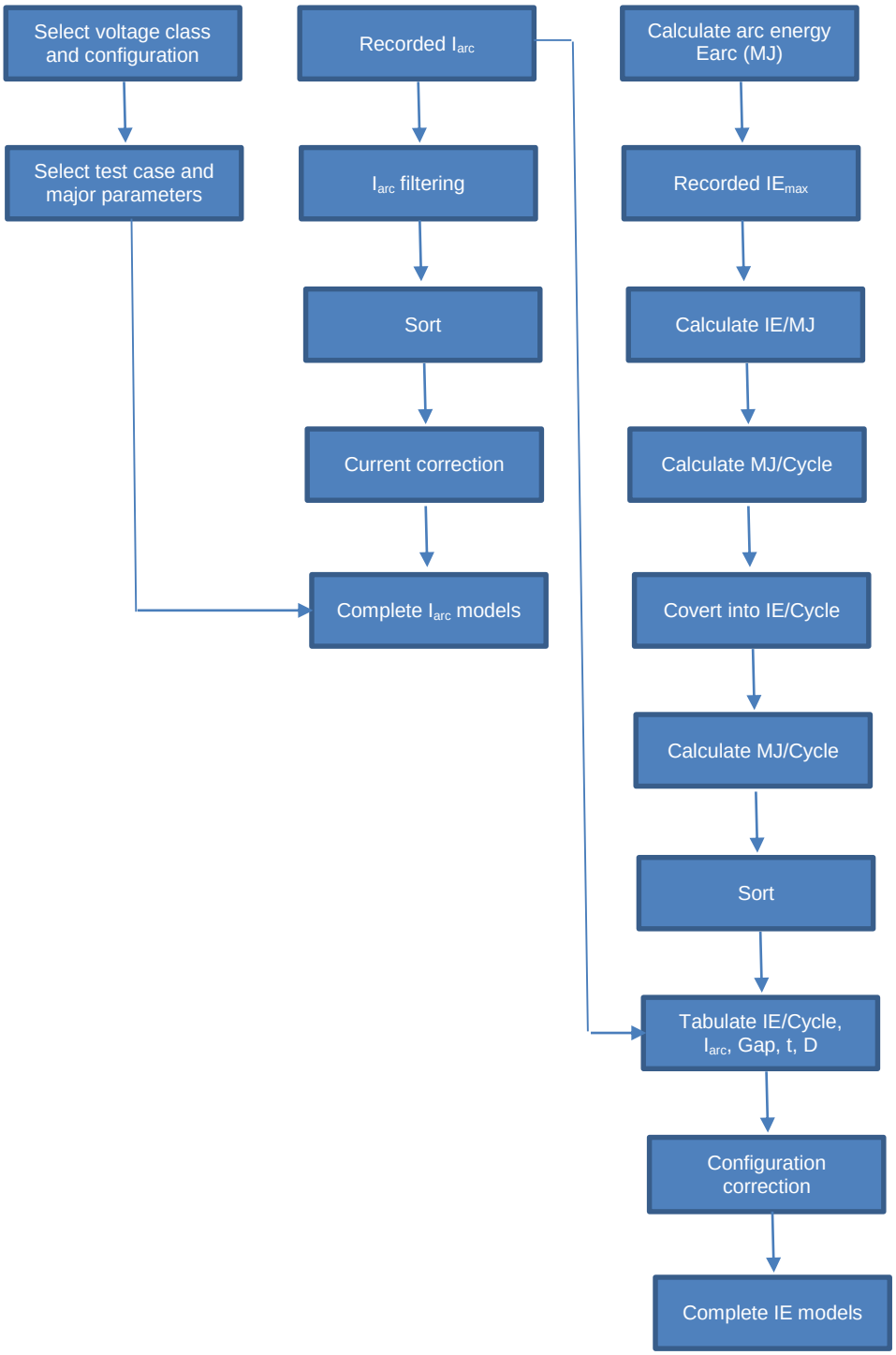

Figure 4- 24 Flow chart of modeling process

As the flow chart shows above, the whole modeling process could be executed in several phases.

Original test data input may include system operating voltage or open circuit voltage, symmetrical bolted fault current, electrodes gap width, measurement distance and test configurations. In test configuration identification, VCB, VCBB and HCB need to be included with/in/alongside/to determine the enclosure dimensions. All original test data are collected by a DAQ system.

During process arcing current estimation, arc current modeling is performed to estimate arcing current. Based on original arcing current information, some data processing methods can be applied to generate the modeling data sets. As mentioned before, a filtering process need to be adopted first to the original arcing current data, which in order to remove DC offset and harmonics. Then, based on those processed arcing current data at three reference voltage points, 600V, 2.7kV and 14.3kV, a multiple regression can be applied based on non-linearized independent parameters to perform curve fitting. Also, a combination of interpolation and extrapolation techniques can be used to expand the modeling range from three reference voltages to the voltage range spanning 208V to 15kV. Additionally, to convert these statistic current models to physical practice, a correction curve based on system X/R ratios and the ratio of arcing current to bolted fault current has to be added into the arcing current model to reflect the true correlation between arcing current and different system voltage level corresponding to source impedance change. From arcing current estimation, expected system protection operation time or protection response can be calculated. The protection response includes, for example, a clearing time on the breaker or fuse, relay operation time, and any other desired safety margins. Depending on the application, a user-provided fault

current for arc flash can also be considered. This user-defined current value could be verified and adjusted from arcing current model estimation results.

The estimated arcing current from the last step can be utilized as an internal variable for the incident energy modeling process. Input data from estimated arcing current, arc duration time T, working distance or measurement distance D should be used in this modeling process. From the part of parameter sensitivity analysis described above, the incident energy may be calculated from arcing current, bolted fault current, system voltage level, gap width, arc duration, working distance and enclosure size. Typically, the incident energy from the modeling process can be calculated on a per-cycle basis, where the total incident energy exposure depends on the arc duration, or the number of cycles that arcing fault lasts. Similar to arcing current modeling approach, three voltage reference points can be used. Once modeling from the reference points is completed, a combined extrapolation and interpolation technique is utilized for curve fitting in order to estimate incident energy at a particular operation voltage or user defined voltage.

In lower voltage range, specifically, under 600V, arcing performance is relatively dynamic and unstable. Between 600V and 2.7kV, the incident energy and arc current may be estimated through a combination of interpolation and extrapolation. A linear interpolation can be performed between 600V and 2.7kV first; then a linear extrapolation can be performed on model results for 2.7kV and 14.3kV. Based on various reference voltages, the estimated incident energy and arcing current can be then determined by adding proportional contributions of the interpolated and extrapolated terms, and combines the interpolated and extrapolated values in other ranges,.

With the increasing of voltage level, variance of arcing current and incident energy became small, the relation between this ranges can be assumed as linear. In

practice, when voltage up to the range between 2.7kV and 14.3kV, a linear extrapolation could be used to estimate the incident energy and arcing current. Since the modeling process limited to the voltage range between 208V to 14.3kV, voltages greater than 15kV are not considered in this dissertation.

Simply, linear interpolation can be defined between 2.7kV and 14.3kV arcing event, and a combination of interpolation and extrapolation can be used between 600V and 2.7kV. In interpolation, the value of a desired function, such as IE, between two reference points is estimated based on weighting defined. For example, according to interpolation approximation, incident energy can be estimated for specific voltage V between two reference points $V_n < V < V_{n+1}$:

$$IE(V) = IE(V_N) + \frac{IE(V_{N+1}) - IE(V_N)}{V_{N+1} - V_N}(V - V_N)$$

In this expression, V_n and V_{n+1} are two adjacent reference points, and the value of incident energy at voltage V could be estimated by the interpolation equation above. Similarly, the arcing current at any voltage V could be expressed as:

$$I_{arc}(V) = I_{arc}(V_N) + \frac{I_{arc}(V_{N+1}) - I_{arc}(V_N)}{V_{N+1} - V_N}(V - V_N)$$

On the other hand, linear extrapolation can also be utilized for voltage V between reference point V_n and V_{n-1}. In an extrapolation process, the range is different with interpolation, where $V_n > V > V_{n-1}$.

A combined approach which uses both interpolation and extrapolation to solve the curve fitting problem on a weighted voltage range could also be employed. This method could be applied to estimating arcing current and incident energy between 600V and 2.7kV. In this combined approach, the interpolation between adjacent reference voltages is combined in a weighted sum with extrapolation based on those voltage

reference points, where the weight factor depends on the fractional distance from lower voltage range. For example,

$$IE(V) = IE_{\text{int}}(V_{N-1}, V_N)\frac{V_N - V}{V_N - V_{N-1}} + \frac{V - V_{N-1}}{V_N - V_{N-1}} IE_{ext}(V_N, V_{N+1})$$

In this expression, $IE_{int}(V_{n-1},V_n)$ is the interpolated value of incident energy at voltage V between V_{n-1} and V_n voltage reference points, and $IE_{ext}(V_n, V_{n+1})$ is extrapolated value at voltage V from range V_n to V_{n+1}. The weighting considered between the interpolated and extrapolated can be different. The weighting factor on combined interpolated and extrapolated process is non-zero in one reference interval, specifically at a lower reference voltage interval. But in higher voltage intervals, the weighting of extrapolated may be set to zero to guarantee pure interpolation. Additionally, based on the incident energy and arcing current models in reference voltage, the value estimated from this extrapolation/interpolation process may be formed as the combination with other essential parameters such as gap width, working distance, bolted fault current and so on.

The incident energy estimated results related to arc flash assessment, typically, indicated the arc flash protection boundary which identified the safety working distance to incident energy exposure less than 1.2 cal/cm^2. Also, based on this incident energy results, a hazard level could be estimated, which indicated the category of personal protective equipment for individuals working within the arc flash protection boundary.

4.5 Model validation and example

For more detailed explanation for the modeling process, an arc flash test case is provided here with the completed procedure of both arcing current and incident energy modeling process as one example. A detailed results comparison between test recording and model estimation is provided in Appendix A.

4.5.1 Arcing current data processing

1) Original real time arcing current plotting and RMS plotting. (Figure 4-25 and 4-26)

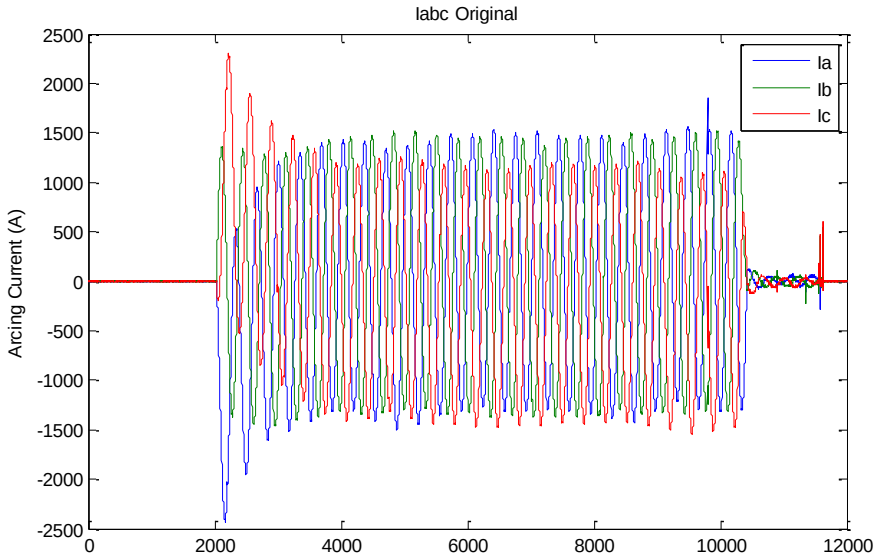

Figure 4- 25 Original real time arcing current plotting

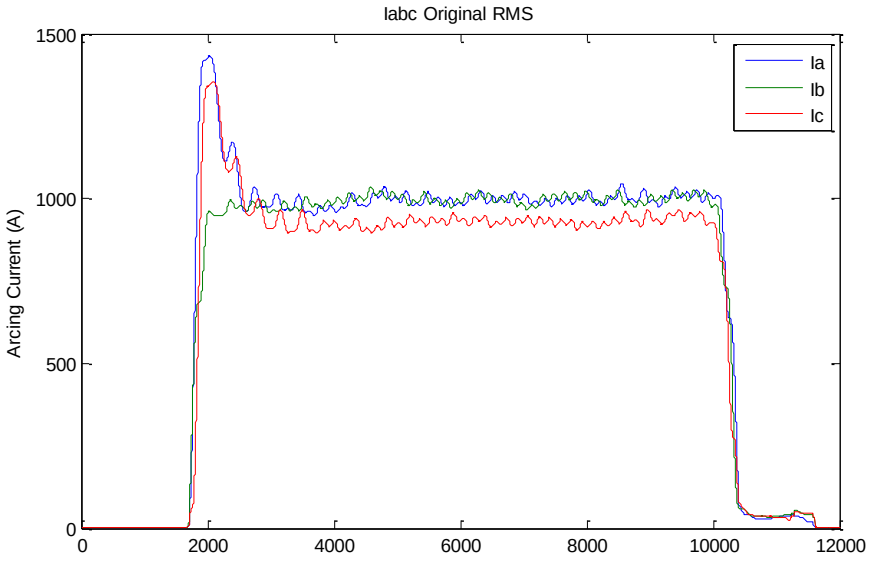

Figure 4- 26 RMS value of original arcing current plotting

2) Arcing current filtered by a cosine filter. (Figure 4-27 to 4-29)

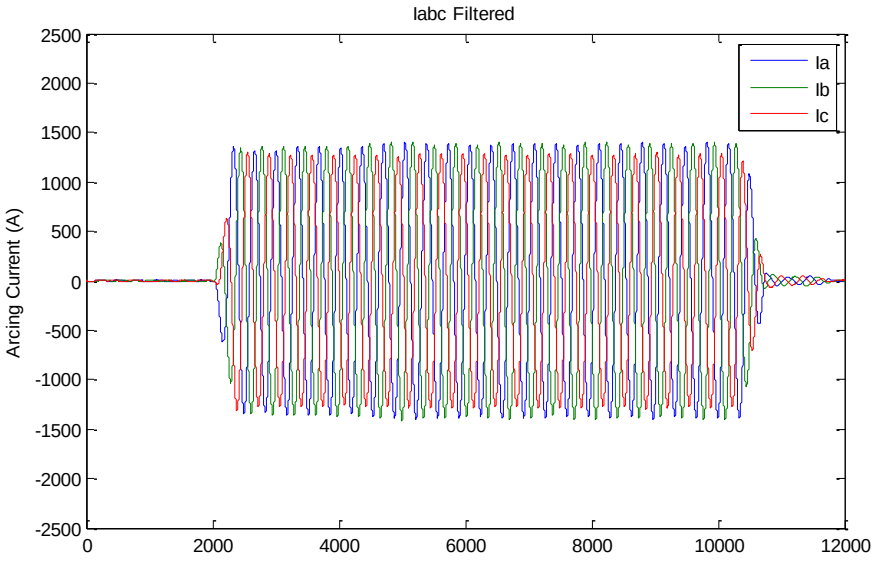

Figure 4- 27 Filtered real time arcing current plotting

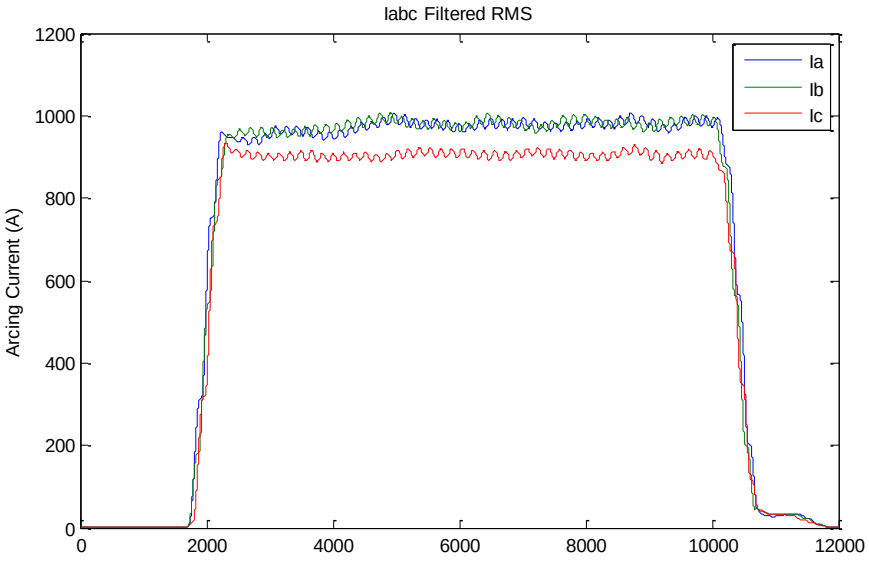

Figure 4- 28 Filtered RMS arcing current plotting

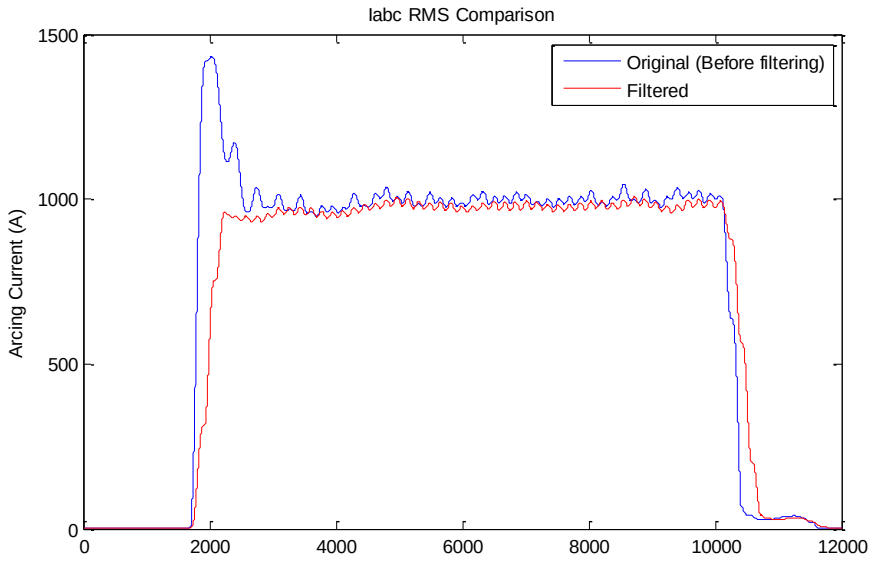

Figure 4- 29 Comparison between original RMS data and filtered RMS arcing current

4.5.2. Model development procedure

4.5.3.1 Arcing current model

Step 1: Take the logarithm of all variables prior to regression.

Step 2: Convert I_{arc} to *log*I_{arc}, I_{bf} to *log*I_{bf}, Gap to *log*Gap for model development purpose.

Step 3: Put all 14.3kV converted data into multiple linear regression process. (Table 4-10)

Table 4- 10 14.3kV VCB arcing current modeling data

Config.	V_{oc}	I_{bf}	Gap	I_{arc}
VCB	14.32	10.56	95.25	10.14263
VCB	14.32	10.56	95.25	10.14263
VCB	14.32	10.56	95.25	10.14611
•••	•••	•••	•••	•••
•••	•••	•••	•••	•••
•••	•••	•••	•••	•••
VCB	14.16	2.703	101.6	2.656683
VCB	14.16	2.703	101.6	2.648847
VCB	14.16	1.136	101.6	1.116515

Step 4: Based on the selected parameter and arcing current recording, linear regression can be performed. The linear regression results will be:

$$\log I_{arc}=0.005124+0.99*\log I_{bf}-0.016*\log G$$

From the Table 4-11, it clearly shows the dependent and independent variables in 14.3kV I_{arc} model.

Table 4- 11 Variables Entered/Removed

Model	Variables Entered	Variables Removed	Method
1	*log*Gap, *log*I_{bf}	No	Enter

Note:

a. Dependent Variable: *log*I_{arc}

b. All requested variables entered.

In statistics, R Square is called coefficient of determination, which provides a measure of how well future outcomes are likely to be predicted by the model and ranges from 0 to 1. The most general definition of R square is:

$$R^2 = 1 - \frac{SS_{err}}{SS_{tot}}$$

$$SS_{tot} = \sum_i (x_i - \bar{x})^2$$

$$SSerr = \sum_i (x_i - f_i)^2$$

$$\bar{x} = \frac{1}{n}\sum_i^n x_i$$

Where x_i is sample value, f_i is modeled value.

From Table 4-12 Model Summary, R square equals to 1. Based on the definition of R square, it indicates independent variables ($logI_{bf}$ and logGap) selection could reflect the way of dependent variable ($logI_{arc}$) changing very precisely.

Table 4- 12 Model Summary

Model	R	R Square	Adjusted R Square	Std. Error of the Estimate
1	1.000a	1.000	1.000	.0050226

a. Predictors: (Constant), *log*Gap, $logI_{bf}$

b. Dependent Variable: $logI_{arc}$

Step 5: However, based on the changes of system resistance according to different bolted fault current, the arcing current curve cannot always in a linear condition. In order to represent the actual characteristics of arcing current with the increasing system voltage and current, a pattern curve has been imposed on original regression curve. Table 4-13 gives the ratio trend corresponding to current level

Table 4- 13 Ratio of arcing current and bolted fault current

Bolted Fault Current (kA)	Ratio of Arcing Current and Bolted Fault Current (I_{arc}/I_{bf})
42	0.943200952
20.08	0.963315239
10.076	0.978900854
2.703	0.979965594
1.136	0.983667254
0.5	0.997106

Step 6: Based on the trend of I_{ratio} in different level of I_{bf} (from lab test recording), we'll follow the trend to extend the ratio value to 65kA. Then 5-th degree polynomial curve fitting will be generated. Figure 4-30 illustrate the curve of current correction factors.

Icf = -1.557*10^-12*I_{bf}^6+4.556*10^-10*I_{bf}^5-4.186*10^-8*I_{bf}^4-8.346*10^-7*I_{bf} ^3+5.482*10^-5*I_{bf} ^2-0.003191*I_{bf} +0.9729

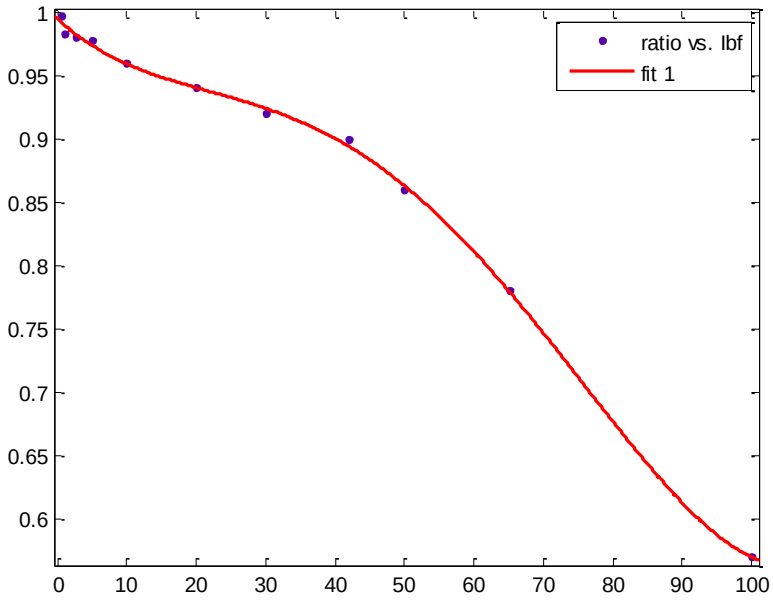

Figure 4- 30 Curve of current correction factor

Step 7: Impose the curve into the original linear regression result. Figure 4-31 provides the comparison between the adjusted curve and original curve.

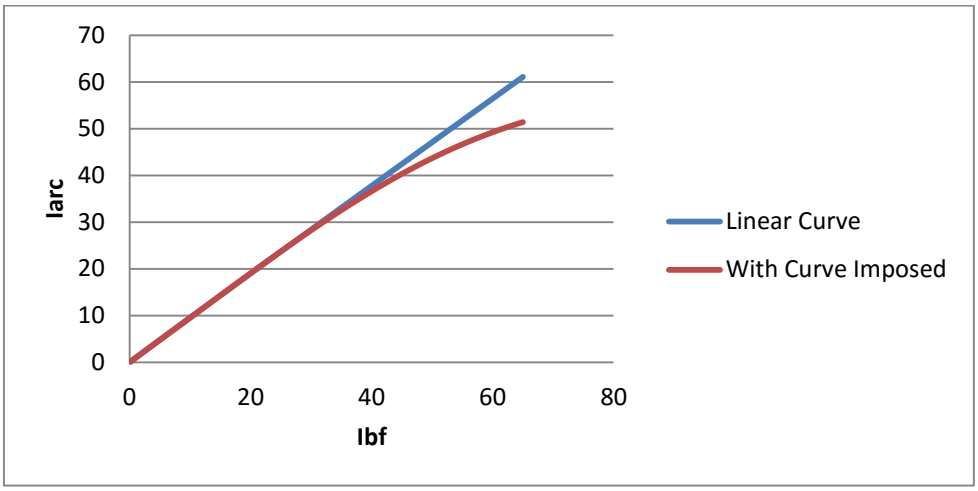

Figure 4- 31 Comparison between corrected current and un-corrected current

Step 8: The final I_{arc} equation for 14.3kV VCB is:

Iarc=10^(-0.007042+1.105**log*(I_{bf})-0.011**log*(Gap)*(-1.557*10^-12*I_{bf}^6+4.556*10^-10*I_{bf}^5-4.186*10^-8*I_{bf}^4-8.346*10^-7*I_{bf} ^3+5.482*10^-5*I_{bf} ^2-0.003191*I_{bf} +0.9729))

4.5.3 Incident energy data processing

Step 1: Obtain maximum IE from the recording data.

Step 2: Calculate the power and times 0.00005 (20K sample per second) to convert them into Joules.

Step 3: Calculate the total arc energy during the event

Step 4: Calculate ΔIE per MJ, and MJ/Cyl

Step 5: Move forward one data point and repeat the procedure. This procedure will generate 333 data points per cycle.

Step 6: Convert MJ/Cyl to IE/Cyl.

Step 7: Sort IE/Cyl in descendent order and keep top 50% data points, in other words, based on 20k sample rate, 333*(N-2)/2 data points. N is the arc flash duration. In this example case, the N=24, 3663 data points can be extracted from a 24-cycle arc flash test.

Step 8: Statistical analysis will be performed to obtain average IE/Cyl and its standard deviation. Calculate the 95% confidence IE/Cyl value (upper bound).

4.5.4 Incident energy model

The essential parameters (arcing current, gap width, working distance, ratio of bolted fault current and arcing current) for incident energy modeling could be obtained from sensitivity analysis, then the model development steps can be processed:

Step 1: Take the logarithm on all variables prior to regression.

Step 2: Use I_{ratio}, *log*I_{arc}, I_{bf}, *log*Gap, *log*D as independent variables for model development.

Step 3: Use IE/cycle from data processing part as the dependent variable.

Step 4: Put all 14.3kV VCB data into multiple linear regression process. (Table 4-14)

Table 4- 14 14.3kV VCB incident energy modeling data

Config.	Voc	I_{bf}	Gap	D	Duration	I_{arc}	IEmax
VCB	14.32	10.56	95.25	1193.8	104.11	10.14263	0.675
VCB	14.32	10.56	95.25	1193.8	206.14	10.14263	1.2555
VCB	14.32	10.56	95.25	990.6	104.03	10.14611	0.864
•••	•••	•••	•••	•••	•••	•••	•••
•••	•••	•••	•••	•••	•••	•••	•••
•••	•••	•••	•••	•••	•••	•••	•••
VCB	14.07	0.5	101.6	1193.8	418.42	0.497526	0.2835
VCB	14.07	0.5	101.6	990.6	429.73	0.497335	0.324
VCB	14.07	0.5	101.6	787.4	414.87	0.49668	0.3645

Step 5: Use Iarc equation (from Iarc model development) to replace the Iarc

Step 6: The final IE equation will be:

IE=t*60/1000x10^(3.993925-0.999749*I_{arc}/(-1.557*10^-12*I_{bf}^6+4.556*10^-10*I_{bf}^5-4.186*10^-8*I_{bf}^4-8.346*10^-7*I_{bf}^3+5.482*10^-5*I_{bf}^2-0.003191*I_{bf}+0.9729)/Ibf+0.11**log*(Gap)-1.677**log*(D)+1.06**log*(I_{arc}))

From Table 4-15, R square equals to 0.984, which indicates independent variables selection could reflect the way of dependent variable IE changing very precisely.

Table 4- 15 Model Summary

Model	R	R Square	Adjusted R Square	Std. Error of the Estimate
1	.992a	.984	.982	.0649722

a. Predictors: (Constant), *log*I_{arc}, *log*D, *log*Gap, I_{ratio}

b. Dependent Variable: *log*IEcyl

4.6 Arc flash thermal hazards assessment model

Based on the discussion above, a group of derived model is provided to enable arc flash thermal hazard assessment, including the calculation of arcing current, incident energy and arc flash protection boundary.

The applicable parameter ranges for these arc flash hazard models are listed below:

- System open circuit voltage in the range of 208V to 15kV.
- Bolted fault current from the range of 0.5kA to 100kA and 0.2kA to 65kA, for 208V to 600V and 601V to 15kV, respectively.
- AC cycle frequency in the range of 50Hz or 60Hz.

- Electrodes gap width between 0.25 inch to 10 inch, where 0.25 inch to 3 inch for 600V and below, 0.75 inch to 10 inch above 600V.
- Minimum working distance from arcing point is 12 inches.

Equipment enclosure of commonly available sizes is in Table 4-16:

Table 4- 16 Enclosure available size utilized in modeling process

Open Circuit Voltage (kV)	Box Size (WxHxD)
0.6	20"x20"x20"
2.7	26"x26"x26"
14.3	36"x36"x36"

Noted that, the maximum enclosure size should be less than 50 inches for each side dimension, and the width of the enclosure must be larger than four times the gap width.

Based on the modeling process, arcing current can be modeled and estimated at each reference voltage point V_{ref}. Each model in reference voltage corresponding to different electrode gap width, different bolted fault current and configurations. For example, an arcing current model can be expressed as:

$$Iarc(Vref) = 10\,\wedge\,(K_1 + K_2 \cdot log(I_{bf}) + k3 \cdot log(G)) \bullet (I_{cf})$$

In this expression, $I_{arc}(V_{ref})$ is the model estimation for arcing current in kA for a given reference voltage V_{ref}, I_{bf} is bolted fault current in kA and G is the gap width in mm. I_{cf} is the current correction curve which is utilized in order to adjust the curve fitting results under a physical realization. The I_{cf} may have the form as a high order polynomial equation on bolted fault current, for example:

$$I_{cf} = x_1 \cdot {I_{bf}}^{n} + x_2 \cdot {I_{bf}}^{n-1} + ... + x_{n-1} \cdot I_{bf} + x_n$$

Representative parameters and corresponding coefficient values of k and x provided in Table 4-17, for 14.3kV VCB configurations as one example. Note that, one or

more coefficients may be placed as zero, which indicates the corresponding parameters may have no functionality dependent on arcing current estimation.

Arcing current estimation results can be used to determine the protection devices operation time, also a current limiting fuse can be applied to estimation results.

Incident energy estimation equation sets can be more complex than arcing current equation. To increase the accuracy of the modeling process and to minimize regression errors, all independent parameters need to use a non-linearized approach. In practice, a logarithm based non-linearized transformation may apply to the step. Based on logarithmic scaling, with incident energy expressed in terms of incident energy per cycle, the model equation could be expressed as:

$$IE(V_{ref})_{cycle} = 10\,\hat{}\,(K_1 + K_2 \cdot logG + k3 \cdot I_{arc} \cdot I_{cf} / I_{bf} + k_4 \cdot log(I_{bf}) + k_5 \cdot logD + k_6 \cdot log(I_{arc}) + log(1/Box_{cf}))$$

In this incident energy equation, as mentioned in arcing current modeling part, all logarithms have a base of 10. IE_{cycle} is in units of cal/cm2 for a given reference voltage V_{ref}. Bolted fault current and arcing current are expressed in units of kA as I_{bf} and I_{arc}, respectively. Gap width is given in mm, with the expression of G. D represents the measurement distance or working distance, which is in units of mm. Enclosure size correction factors are added into equation as Box_{cf}. In open air arc flash tests, the Box_{cf} will be automatically set to 1.

To complete the incident energy calculation, total incident energy is determined by the total arc duration, which can be expressed as T, in unit of seconds.

$$IE_{total} = IE_{cycle} \cdot t \cdot 60/1000$$

The length of arc duration gives the time required for a relay or other protective devices to operate based on corresponding arcing current and configurations. Table 4-18 lists the coefficients of 14.3kV VCB incident energy models.

The arc flash protection boundary can be used to estimate a personnel safety distance. The safety distance could be determined by finding the distance D at which the incident energy falls below 1.2 cal/cm2.The arc flash protection boundary equation sets can be modeled as the same format as incident energy equations, which are based on a series of reference voltage. In this modeling process, the arc flash protection boundary may also be represented as a logarithmic expression:

$$Boundary = 10\,\text{^}\,(K_1 + K_2 \cdot \log G + k3 \cdot I_{arc} \cdot I_{cf} / I_{bf} + k_4 \cdot log(I_{bf}) + k_6 \cdot log(I_{arc}) + log(1/Box_{cf}) - \log(1.2/(t \cdot 60/1000)/(-K_5))$$

In this equation, the boundary is the estimated arc flash protection boundary distance for given a voltage reference in units of mm. Definition of other parameters is the same as incident energy equations. Table 4-19 lists the coefficients of protection boundary models for 14.3kV VCB as one example.

Similarly procedures applied on the other configurations and voltage levels, the coefficient table for arcing current, incident energy and protection boundary models generated as the same format as the example of 14.3kV VCB configuration. Those tables will not be detailed listed in here.

Table 4- 17 Coefficients for arcing current models

		k1	k2	k3	x1	x2	x3	x4	x5	x6	x7
VCB	14300V	-0.007042	1.015	-0.011	-1.557E-12	4.556E-10	-4.186E-08	8.346E-07	5.482E-05	-0.003191	0.9729

Table 4- 18 Coefficient for 14.3kV IE model

14300V	**k1**	**k2**	**k3**	**x1**	**x2**	**x3**	**x4**	**x5**	**x6**	**x7**	**k4**	**k5**	**k6**
VCB	3.993925	0.11	-0.999749	-1.557E-12	4.556E-10	-4.186E-08	8.346E-07	5.482E-05	-0.003191	0.9729	0	-1.568	0.99

Table 4- 19 Coefficient for 14.3kV protection boundary model

14300V	**k1**	**k2**	**k3**	**x1**	**x2**	**x3**	**x4**	**x5**	**x6**	**x7**	**k4**	**k5**	**k6**
VCB	3.993925	0.11	-0.999749	-1.557E-12	4.556E-10	-4.186E-08	8.346E-07	5.482E-05	-0.003191	0.9729	0	-1.568	0.99

Figure 4-32 to 4-35 provide the results comparison for incident energy between lab recording and model estimation.

From the comparison, the model estimation results show well-fitted with lab recording data, and because of the conservative estimation point of view, the incident energy model estimation results may shows the higher value but within the error tolerance range.

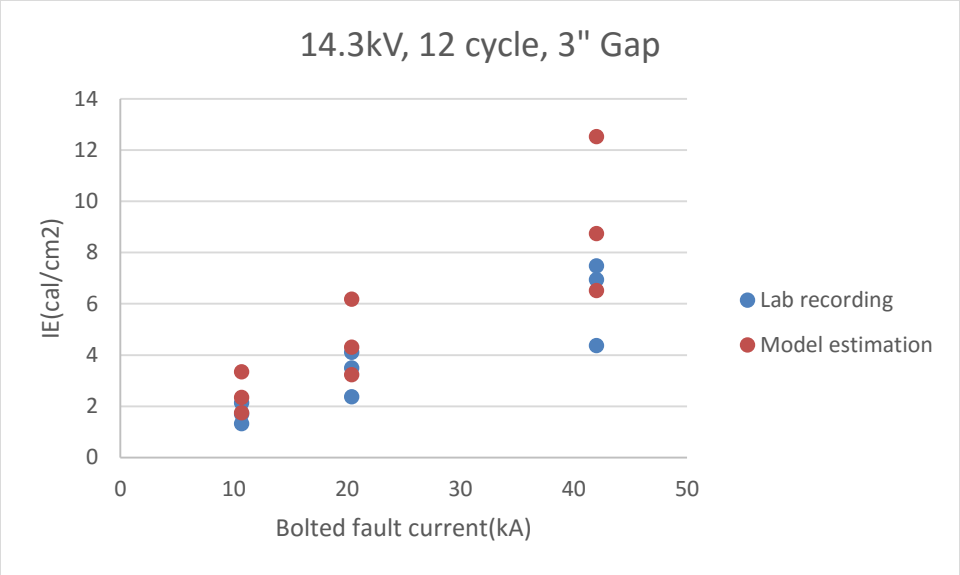

Figure 4- 32 12 cycle 14.3kV VCB test in 3” gap

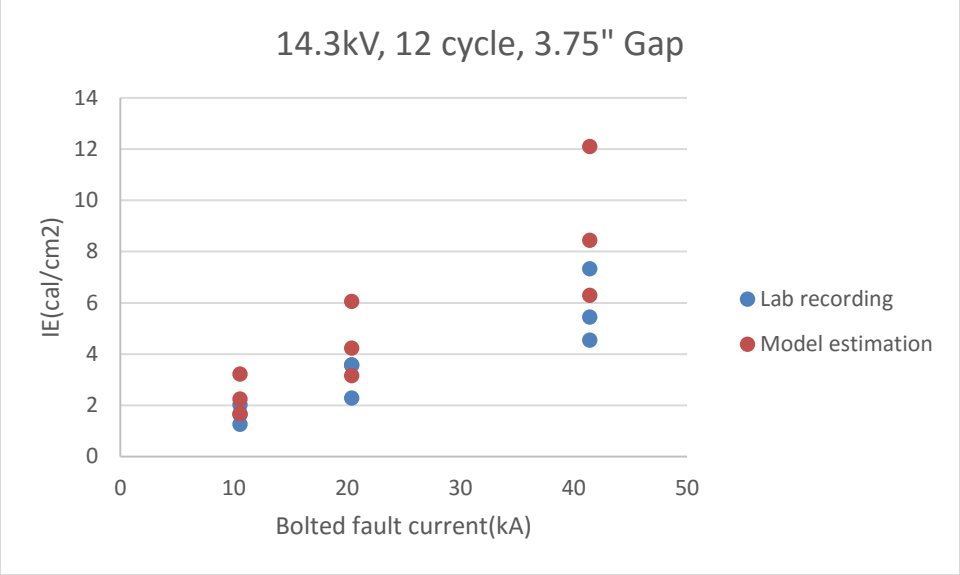

Figure 4- 33 12 cycle 14.3kV VCB test in 3.75” gap

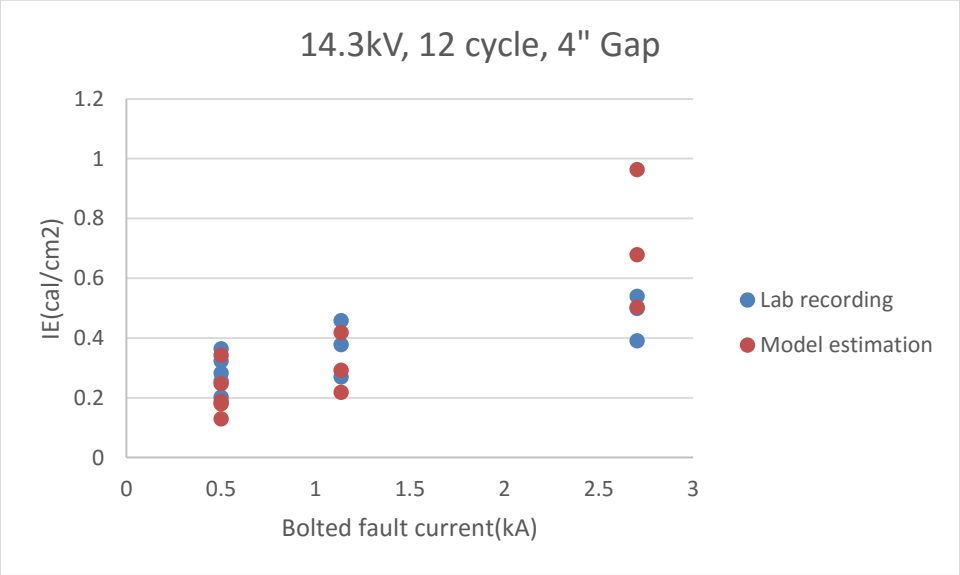

Figure 4- 34 12 cycle 14.3kV VCB test in 4” gap

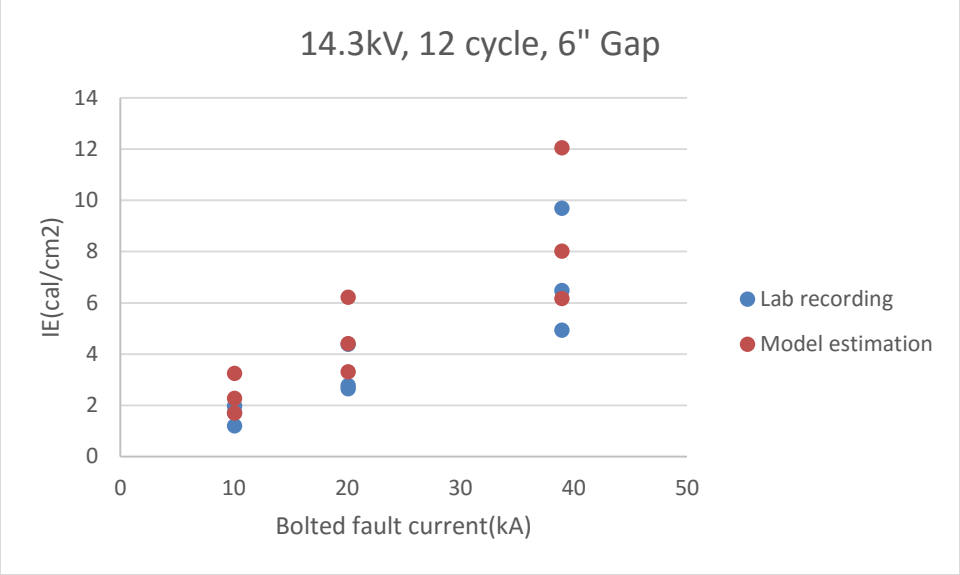

Figure 4- 35 12 cycle 14.3kV VCB test in 6” gap

A detailed results comparison between test recording and model estimation for other configurations and voltage levels are provided in Appendix A.

4.7 Model applications

From the three equations describing arcing current, incident energy and arc flash protection boundary, a representative model of arc flash thermal hazard assessment has been provided. In practice, the coefficient values may vary based on test data and modeling procedures; parameters applied within the modeling may differ from application to application. Similar models also could be generated from other reference voltage, which also depends on particular applications.

Incident energy estimation may be accomplished using the arcing current model with other essential parameters. Incident energy is the total value for exposure over an arc fault time and defined by a particular measurement distance. For any given configuration and system voltage, the incident energy value can be estimated by extrapolation and interpolation approach as discussed before.

The results of incident energy estimation may be used to define a risk category for hazards, such as 0 to 4, which is required by NFPA 70E. This category can be utilized to define minimum personal protective equipment for personnel working on the electrical equipment or within an arc flash protection boundary.

In practice, field test data could be acquired in many ways. For example, operating voltage and current rating are typically defined on equipment, and electrode gap width may be specifically required by a particular voltage class and equipment configuration. For example, in 5kV and 15kV switchgear applications, the typical bus gaps and working distance could be much larger than in low voltage system switchgears. A typical application is provided in Table 4-20. Some real equipment test can also be included in the work for arc flash hazards assessment research.

Table 4- 20 Representative filed parameters for different equipment class [7]

Equipment Class	Typical Gap Width	Typical Working Distance
15kV switchgear	6 inch / 153 mm	36 inch / 910 mm
5kV switchgear	4 inch / 104 mm	36 inch / 910 mm
Low voltage switchgear	1.25 inch / 32 mm	24 inch / 610 mm
Low voltage MCC Low voltage panelboard	1 inch / 25 mm	18 inch / 455 mm
Cable	0.5 inch / 13 mm	18 inch / 455 mm

In actual power systems, the arcing current could be separately passed through a number of different protective devices. The duration time or clearing time may be determined by each individual protective device. Different type of protective devices need to be considers for arc duration time calculation, such as fuse, breaker, and relay operated protection systems.

Enclosure dimensions are determined by equipment enclosure geometry, and configuration depends on arcing fault locations. Even inside the same equipment, the fault location may change the plasma direction and the arcing path. In general, electrode orientation defined as the direction of the terminals towards the arc column to personnel, floor or other working surfaces. Table 4-21 provides a simple reference to determine the configurations. Some real equipment tests provide the examples for the way to determine configuration chosen for arc flash event.

Table 4- 21 Typical equipment configuration and electrodes orientation

Configuration	Electrode Orientation	Enclosure	Electrode Termination
VCB	Vertical	Enclosed	None, or a tap in a bus, arcing will initiated at end of bus
VCBB	Vertical	Enclosed	Terminated in a barrier, arcing is remaining at barrier
HCB	Horizontal	Enclosed	None, conductors extend toward in front locations
VOA	Vertical	Open air	Same with VCB
HOA	Horizontal	Open air	Same with HCB

Figure 4-36 to 4-40 provide the typical equipment configuration and relevant electrode characteristics.

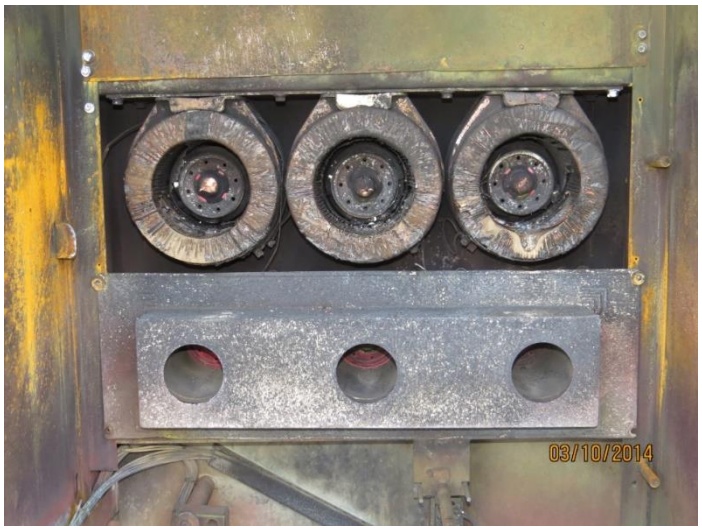

Figure 4- 36 HCB/HOA configuration in switchgear

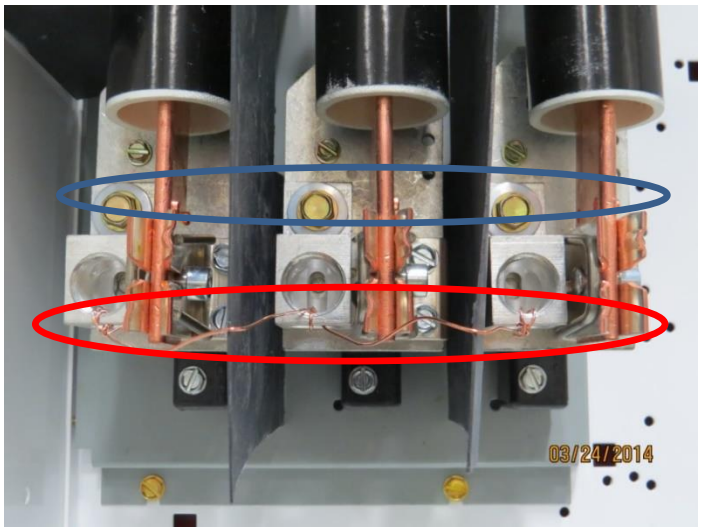

Figure 4- 37 VCB (upper circle) and HCB/HOA (lower circle) configuration on current limiting fuse

Figure 4- 38 VCBB configuration on switchgear

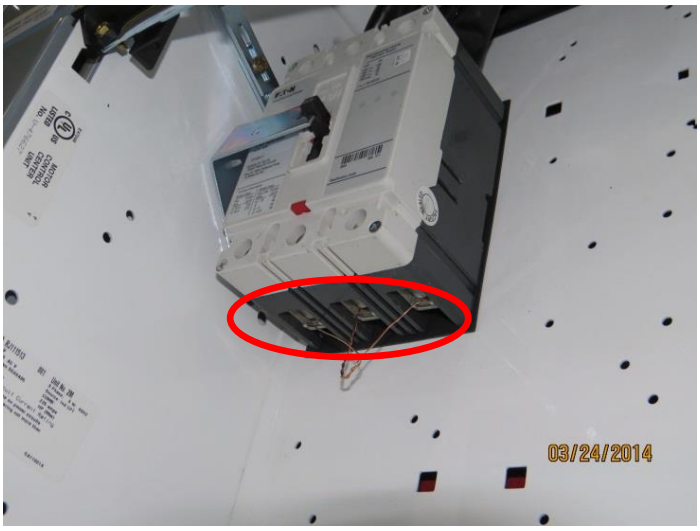

Figure 4- 39 VCB configuration on switchgear

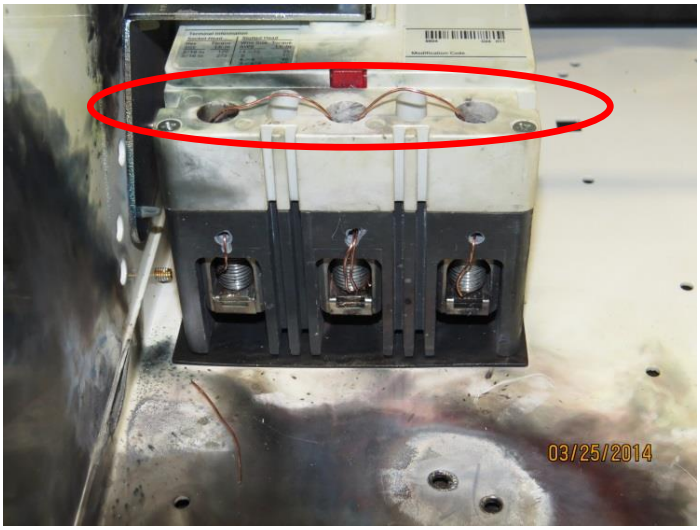

Figure 4- 40 HCB configuration on switchgear

Chapter 5

Arc flash non-thermal hazards measurement

5.1 Arc flash light hazard measurement

5.1.1 Basis of arc flash light hazards

The most obvious arc flash hazard is excessive heat exposure and serious burn injuries. In addition to burn injuries, the blast pressure can cause permanent hearing loss and intense light can cause blindness [46].

The intense light generated by an arc flash can be dangerous; eye injuries account for about 4.2 percent of all arc flash related injuries [5] [47]. Temporary blindness due to sudden bright light, known as flash blindness, is a common occurrence. High-intensity light in the visible, infrared (IR), and ultraviolet (UV) spectrums can damage important structures such as the cornea or retina.

Due to these potentially harsh conditions, work is being conducted to establish industry standards for the appropriate personal protective equipment when arc flash light hazards are present [22]. Personal protective equipment (PPE) is required by OSHA and NFPA standards to protect workers from hazards in the workplace. Those standards include headgear requirements, which involve a non-conductive helmet, a UV-blocking shield and safety glasses. Though eye shields or glasses can block UV radiation, high intensity visible light during the arc flash incident can still damage the eyes.

Proper selection and use of eye protection is the best way to mitigate the hazard posed by the bright light generated during an arc flash. Accurate measurement of light intensity is the first step in understanding the level of eye protection needed. However, due to the dynamic nature of an arc flash blast, it is difficult to provide a precise description and reliable measurement of light intensity during the arc flash event.

5.1.2 Background for light intensity measurement

A number of research projects were conducted by the U.S. Armed Forces on flash blindness in 1960s. The research was fueled by the need to know how well service personnel, especially pilots, could perform after a nuclear blast. The recovery time of flash blindness depends on the light intensity, direction, duration, and size of the flash; pupil size; age of the subject; individual variation; and the spectrum of light radiated by the flash. Flash blindness is the temporary loss of vision when the retina is subject to high-intensity light. A reduction in visual acuity can last a few minutes to a few days. Contributing factors are the glare, the afterimage, and the bleaching of the photochemical substances within the rods and cones of the retina. Scotomatic glare occurs when extremely bright light fatigues the retina. The retina's sensitivity is reduced, and therefore, so is its ability to respond normally to light [48] [49].

5.1.2.1 Light with spectrum

The electromagnetic spectrum is the frequency range of all types of electromagnetic radiation. Radiation over the range of wavelengths between 380 nm and 760 nm is detected by the human eye and perceived as visible light. From previous tests, in an arc flash explosion, the radiated light falls in the visible, UV, and IR spectrums, and is predominately in the range between 400 to 600 nm [50]. Figure 5-1 shows the spectrum band of visible light, as well as the entire electromagnetic spectrum.

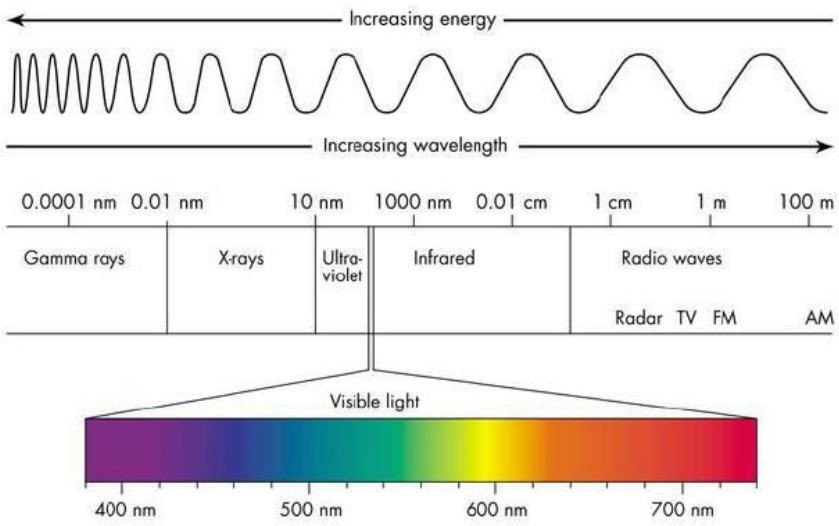

Figure 5- 1 Light spectrum [51]

5.1.2.2 Spectral sensitivity to human eyes

The Commission Internationale de l'Éclairage (CIE) luminosity function curve (also known as $V(\lambda)$ curve) is a very precise representation of visual sensitivity of the human eyes to light of different wavelengths [52].

There are two curves in common use. First is the photopic curve, which approximates the response of the human eye under well-lit conditions. For low-light conditions, the response of the eye is governed by the “scotopic” curve [53]. Figure 5-2 shows these response curves.

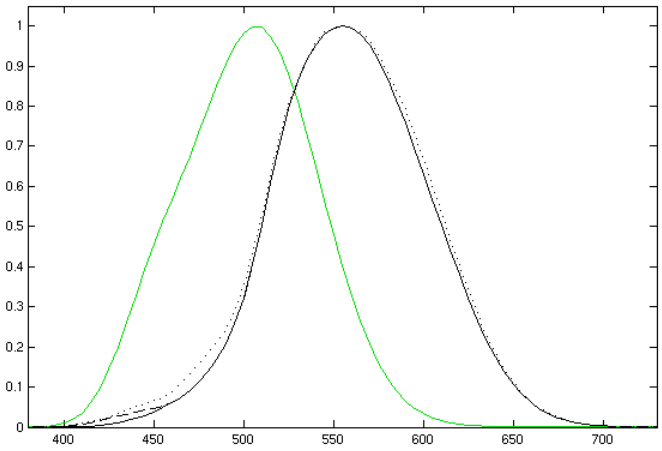

Figure 5- 2 Photopic (black) and scotopic (green) luminosity curves (x-axis is wavelength in nanometer, y-axis is normalized intensity) (Curve data from Wyszecki & Stiles (1982), Table I(4.3.2)) [54]

In a typical working environment, the visual level is much better than “well-lit”. Therefore, the response of the eye follows photopic response curve during arc flash blast. [55]

Based on the photopic $V(\lambda)$ curve and practical measurement processes, there are three basic requirements for light measurement devices:

1) The response of the light sensor should match luminosity curve, which means the sensor should mimic the human eye in terms of spectral sensitivity.

2) The detection speed of sensor should at least match the response of human eyes to suddenly changed light intensity; in other words, the sensor needs to be fast enough to catch the peak light.

3) The brightness measurable range should encompass the peak brightness of the arcing light.

5.1.3 Light measurement sensors

Light sensors are more commonly known as “photoelectric devices” or “photosensors” and convert light energy directly into electrical signals [56].

The traditional light sensor is commonly known as a Light Dependent Resistor (LDR). Generally, this kind of sensor is made by a piece of exposed optically sensitive material such as cadmium sulfide (CdS) or standard silicon (Si) that changes its resistance according to the intensity of the light.

Typically, CdS has a peak sensitivity wavelength of about 560nm to 600nm [56], and Si has a peak sensitivity in the 800nm to 900nm spectral range [57].

Spectral sensitivity is a critical parameter to define a light sensor. It determines in which spectrum band the sensor is most effective.

Generally speaking, light sources emit visible, IR, and UV radiation. Figure 5-3 compares traditional LDR (Si) sensitivity with human eyes. Standard Si-based light sensors cover a wavelength range from 350nm to 1100nm, with the peak around 880nm. However, the spectral responses of human eyes concentrate on visible light from 400nm to 700 nm and exhibit peak sensitivity at 560nm. Si sensors could give people a false reading if they are used to evaluate visible light intensity.

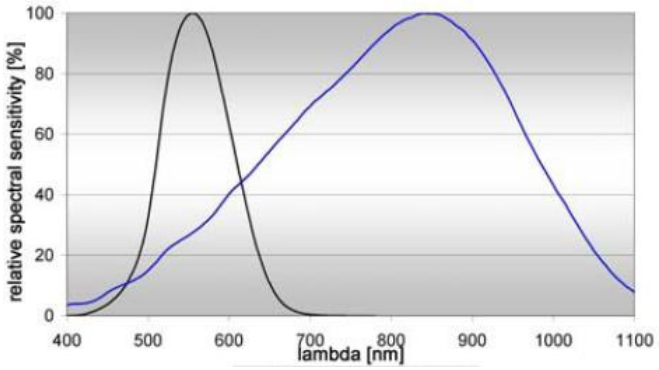

Figure 5- 3 Comparison of Si light sensor sensitivity (blue) and human eye sensitivity (black) [57].

Another disadvantage to traditional LDRs is the response time. They are relatively slow to respond to the changes of light levels. LDR cells have a certain time delay in responding to incident light. In the worst-case scenario, they can take several seconds to change to a new value. It is not unusual that a LDR needs almost 1/5 cycle to respond to sudden changes in light [58].

A new generation of light sensors can be characterized as “photodiode devices”, which are made from silicon semiconductor hybrid with an opto-device [57]. Photodiodes can switch their operation condition between ON and OFF in less than one millisecond, which matches the arcing light capture speed requirement very well.

Based on a specialized photodiode with an amplifier, ambient light sensors can be designed to perceive brightness in the same way as human eyes do. Figure 5-4 compares the spectral sensitivity of a Si photo sensor and the selected ambient light sensor with the human eye. From the comparison results, it is obvious that the selected ambient light sensor can mimic the spectral sensitivity response of the human eye.

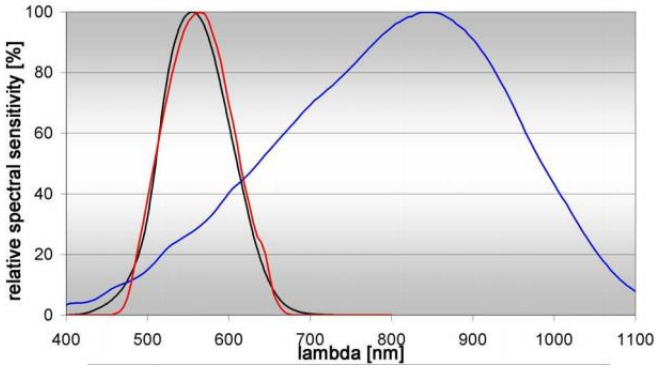

Figure 5- 4 Spectral response of Si (blue), ambient light sensor (red) and human eye sensitivity (black) [59]

In addition, the selected ambient light sensor has a fast response to sudden changes in brightness. If intensity increases from a low brightness (100 lux and below) to

a higher level (1000 lux and above), the time delay is 0.03ms. Conversely, if light intensity decreases by a similar amount, the response time is 1ms. From previously documented arc flash test files, the light capture speed of the selected sensor is able to follow the arc brightness change and catch the peak (6~20ms) [60]. Figure 5-5 shows the typical response of the selected sensor.

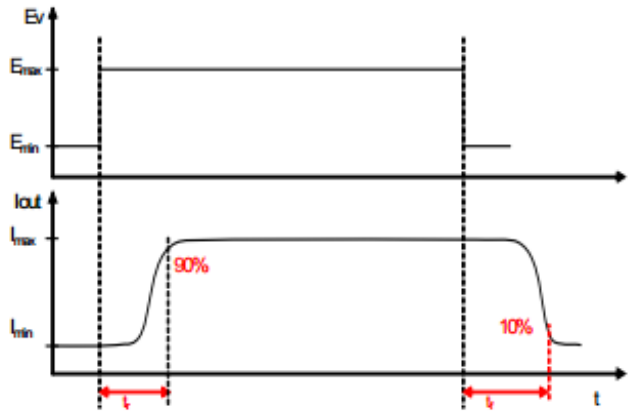

Figure 5- 5 Response time of ambient light sensor

Ambient light sensors are photodetectors. The photocurrent of the selected sensor is proportional to the luminance level. The current output of the sensor follows an analog logarithmic function as shown below [61].

$$I_{out} = S * \log(E_v / E_o)$$

where E_v is luminance in Lux

$E_o = 1Lux$

S is sensitivity, and $S = 10\mu A$

Logarithmic output is advantageous in measuring light. Linear output detectors such as phototransistors cannot detect the small variations in intensity at low levels of illumination. With a logarithmic response, the small changes in light levels can induce a

detectable response in the sensor, whereas at higher light intensities, only relatively large variations need to be considered.

5.1.4 Arc light measurement system design

5.1.4.1 Measurable ranges identification

Since the intensity of light can be higher than 1 million lux during arc event [60], the neutral density filters were applied to extend the measurable range of sensor beyond 100k lux.

Neutral density (ND) filters reduce the intensity of all visible light equally, giving no changes in hue of color rendition. For a ND filter, the amount of optical power transmitted through the filter can be calculated from the logarithmic equation below [62]:

$$d = -\log_{10}\frac{I}{I_0}$$

where d is optical density

I is measurable intensity

I_0 is after the filter to the incident intensity

Table 5-1 lists theoretical attenuation rating of ND filters.

Table 5- 1 Typical rating for ND filter [63]

ND number Notation	Optical density	% Transmittance
ND2	0.3	50%
ND4	0.6	25 %
ND8	0.9	12.5%
ND16	1.2	6.25 %
ND32	1.5	3.125%
ND64	1.8	1.563 %
ND128	2.1	0.781%

Figures 5-6 and 5-7 show the sample frequency response of two ND4 filters, respectively. The measured results were calibrated to their actual values.

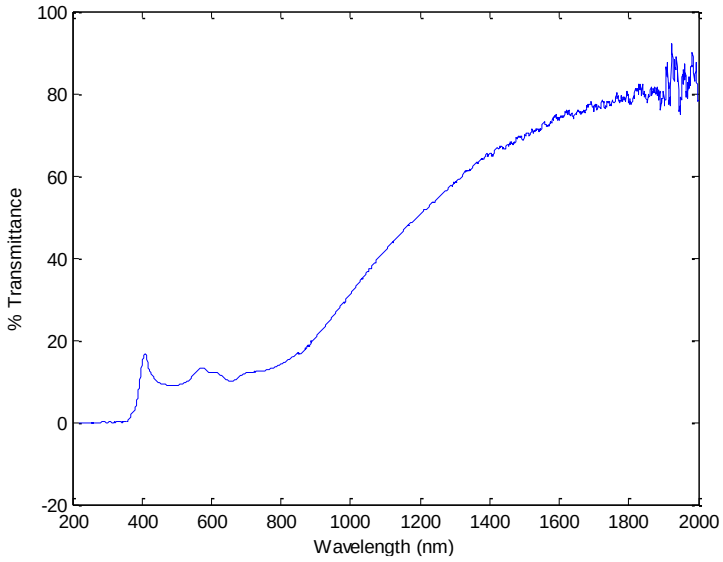

Figure 5- 6 ND4 (1) transmittance corresponding to wavelength

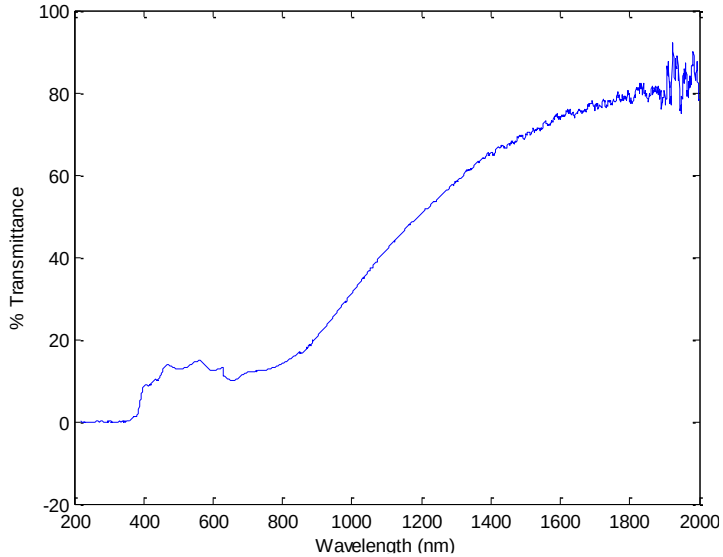

Figure 5- 7 ND4 (2) transmittance corresponding to wavelength

The response curves illustrate that bothND4 (1) and ND4 (2) have relatively uniform attenuation in the visible light spectrum. However, each ND filter has unique transmittance characteristics. For example, the two tested ND4 filters have the same

spectral response, but have different transmittance rates in the same spectrum range. In the range of visible light, ND4 (1) and ND4 (2) have attenuation factors of 7.257 and 6.452, respectively. To ensure the accuracy of the ND filter utilized in light measurement tests, the frequency response of every neutral density filter was characterized in the laboratory. Before adopting a light measurement system, each filter was characterized to identify the transmittance rate. The final measured light intensity also needed to be calibrated to actual values.

Based on the published light intensity measurements (higher than 1 million lux), two ND8 and one ND128 were used to extend the brightness measurement range of the sensor up to 1 billion lux.

5.1.4.2 Circuit design

Since the selected sensor uses current I_{out} as output, it can be directly transformed into voltage by employing a load resistor R_L , which is convenient for data collection through a data acquisition system (DAQ). Figure 5-8 provides the manufacturer-suggested operating circuit. A 100 $k\Omega$ resistor is adopted as the load resistance in the circuit.

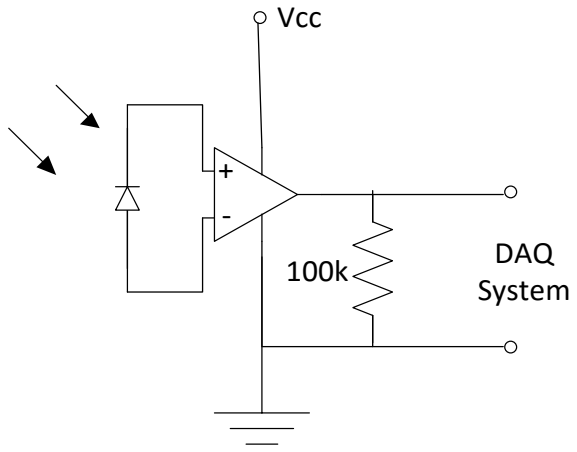

Figure 5- 8 Operating circuit for ambient light sensor [57]

Since the input resistance of the DAQ is less than infinite, the output voltage of the sensor will be altered due to the loading effect. For example, the reported input resistance of the DAQ system was 6680Ω in one of the laboratories. Consequently as shown in Figure 5-9, the output voltage of the sensor circuit is much lower than the open circuit value. Though one can recover the actual number if the input resistance of the DAQ is given, additional complexity was introduced when performing data analysis.

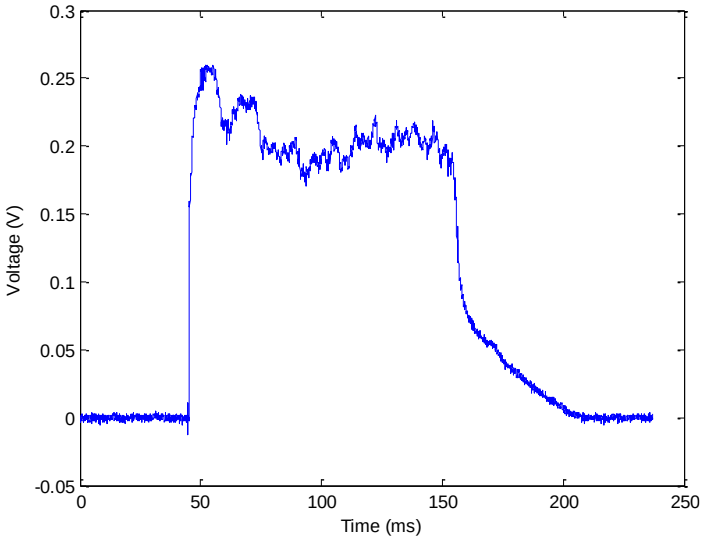

Figure 5- 9 Sensor measurement with manufacturer-suggested circuit (actual light intensity is 16.57 million lux)

To eliminate the loading effect, a buffer amplifier was designed to transfer the circuit from high output impedance to low output impedance.

In order to have a good performance, the buffer circuit should have high input impedance and low output impedance. In the improved design, a high input impedance operational amplifier (OP Amp) was used to perform the core function of the buffer circuit. The improved light measurement system circuit is shown in Figure 5-10.

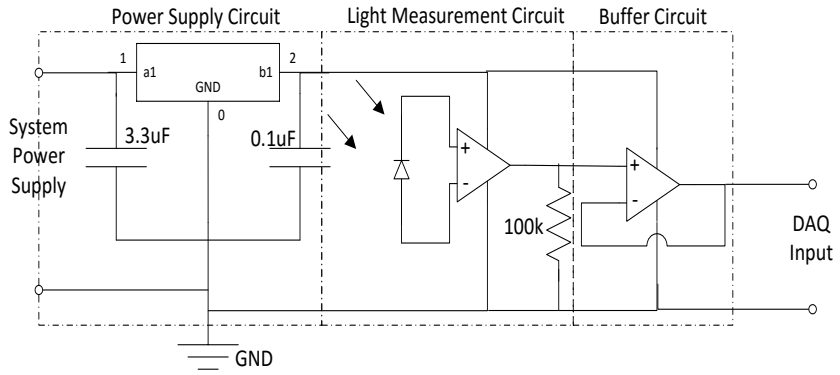

Figure 5- 10 Circuit of the whole light measurement system

This design can effectively eliminate the loading effect and also maximize the power transfer capability between two stage circuits. Figure 5-11 shows light intensity measurement results during an arc flash test. The light information was recorded at a distance of 3 meter from a 3-phase, 2.7kV horizontal open-air arc at a bolted-fault current level of 32kA. The recorded sensor voltage was converted into a peak intensity of 13.1 million lux, approximately 130 times brighter than direct sunlight.

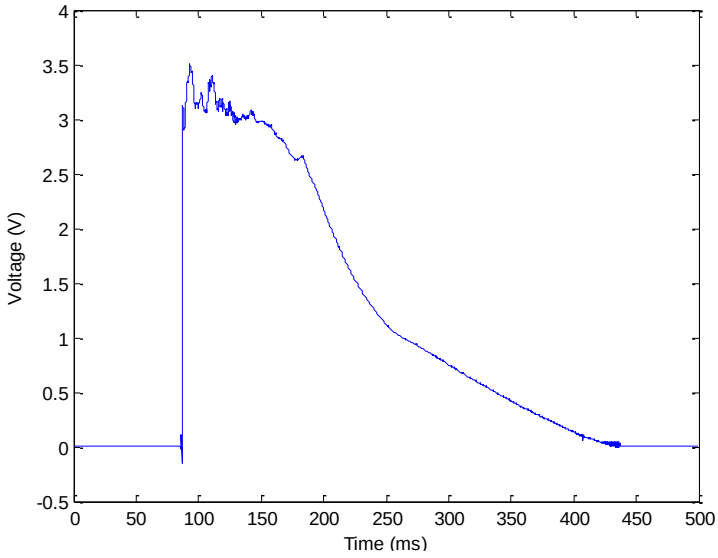

Figure 5- 11 Sensor measurement with improved circuit

Figures 5-12 and 5-13 show the improved light measurement system utilized in arc flash testing, with or without ND filters, respectively.

Figure 5- 12 Light measurement device with ND filter

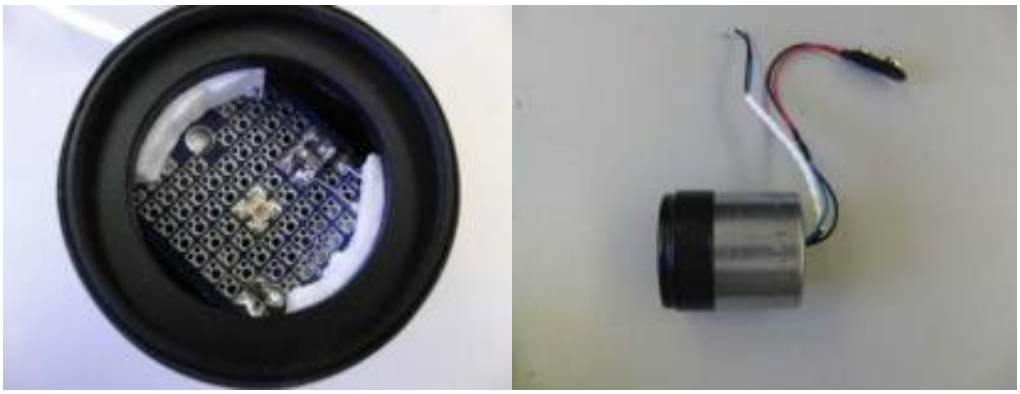

Figure 5- 13 Light measurement device without ND filter

5.1.5 Layout of light measurement device in field testing

Since light intensity depends on the distance between the arcing point (light source) and the sensors, the light intensity was measured at 3 meters, 4.5 meters and 6 meters from the arcing point. This established the foundation to develop a light intensity estimation model in the future. The layout scheme is shown in Figure 5-14.

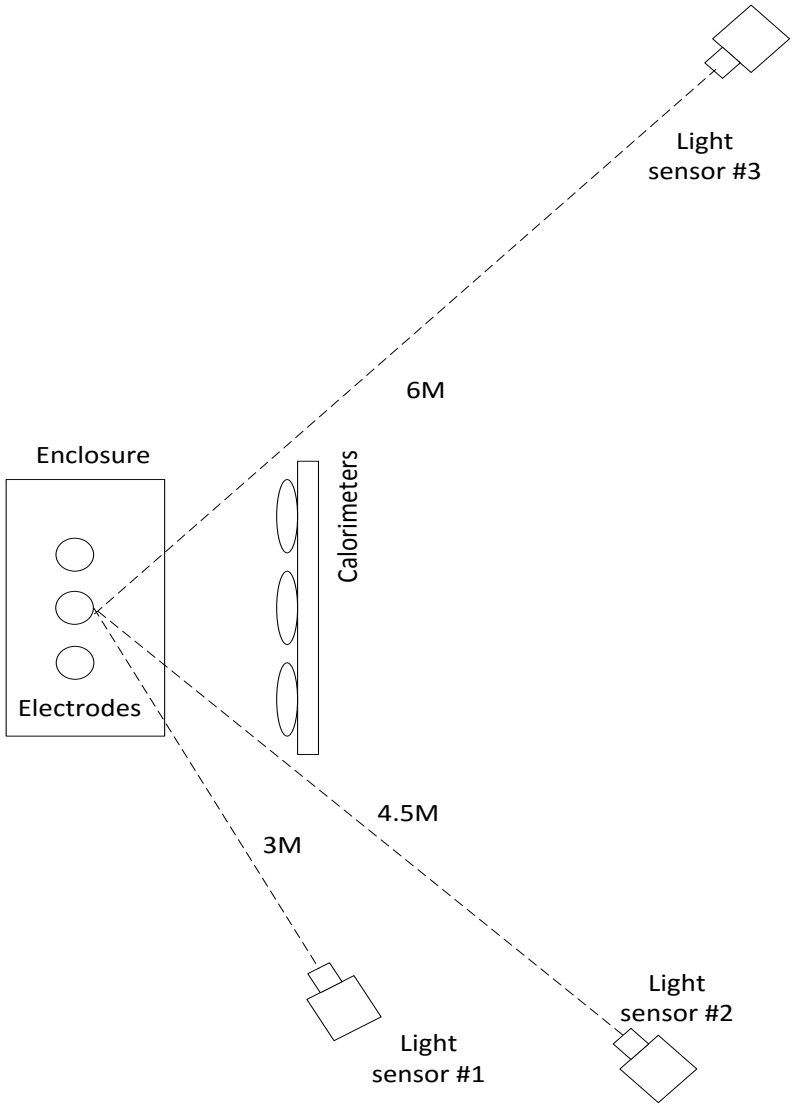

Figure 5- 14 Light measurement device layout scheme in field testing

However, many factors including enclosure, placement of other sensors such as calorimeters, and smoke can affect the visibility of the light visible from the arcing point. Moreover, according to the directional characteristics of photodiodes, the sensor must

aim at the center of the arcing point to measure the peak light intensity. Figure 5-15 displays the viewing angle information from the photodiode manufacturer.

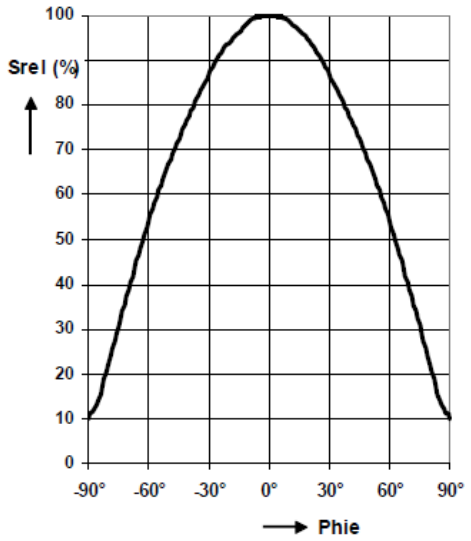

Figure 5- 15 Directional characteristics of the selected ambient light sensor (x-axis is degree, y-axis is % of measurement) [57]

Simply stated, improper alignment can introduce light measurement errors which occur during the arc test. The sensor might miss the peak light, and an unsynchronized response among three light sensors at the same time stamp might occur. Figure 5-16 illustrates this potential problem.

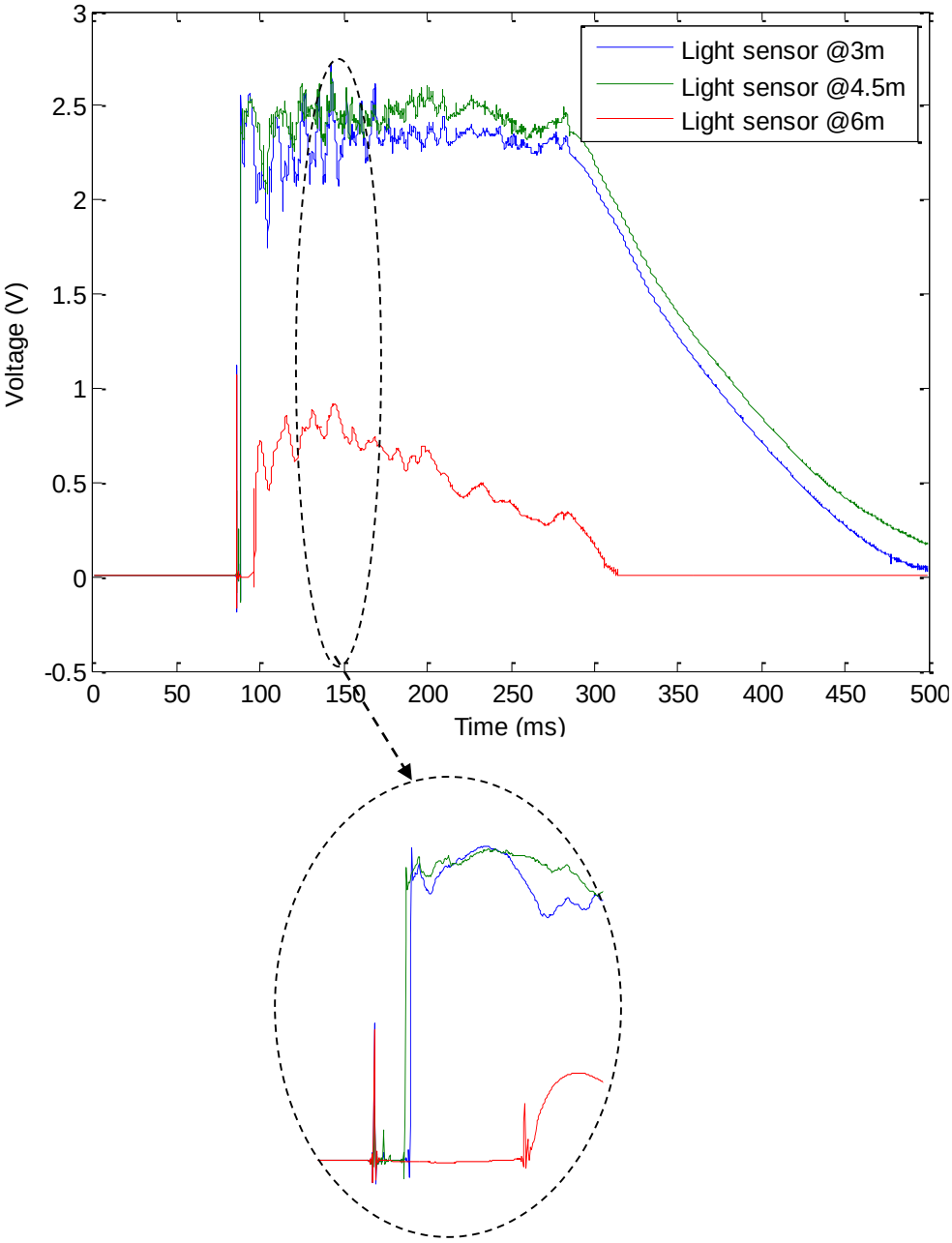

Figure 5- 16 Misalignment of light measurement

To eliminate any misalignment errors, a laser pointer, serving as a precision aiming tool, was installed on the top of each light sensor. Figure 5-17 shows the results of one test using the improved aiming method; Figure 5-18 shows the actual circuit.

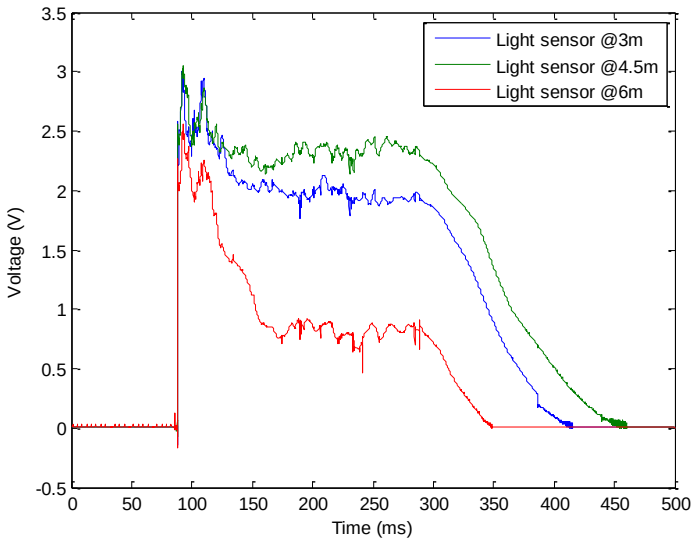

Figure 5- 17 Light measurement results after the aiming direction was adjusted

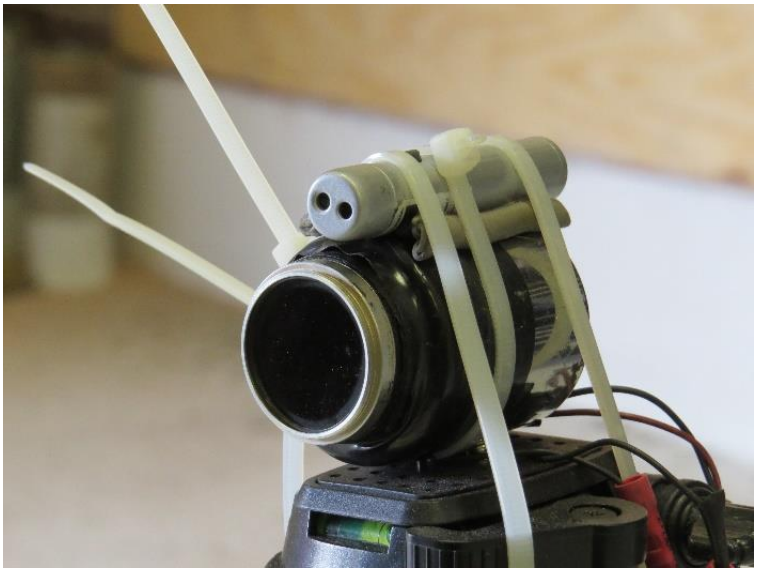

Figure 5- 18 Using laser pointer to align light measurement system

5.1.6 Sample results of light intensity measurement

Figure 5-19 displays a frame taken from a high speed video during an open air horizontal electrode arc flash test. It can be seen in the figure that the arc column moved strictly in the horizontal direction and concentrated at the center of the electrodes. Heavy smoke can be observed around the arcing point, which demonstrates the necessity of precise light sensor direction adjustment.

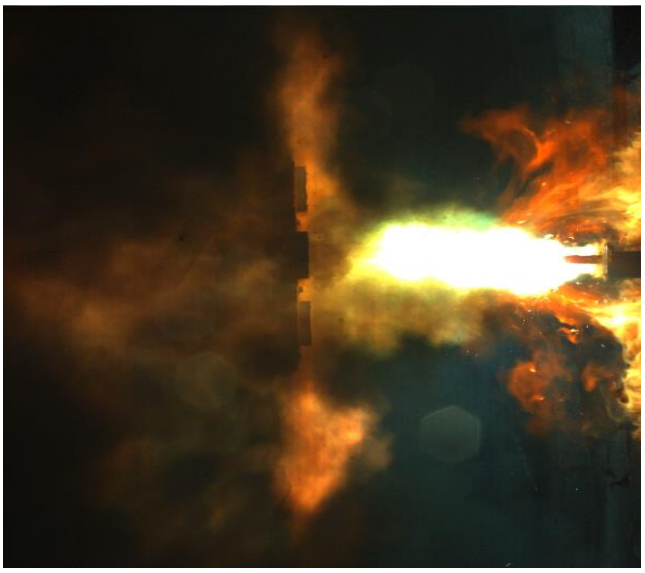

Figure 5- 19 Snap shot of arc flash from high speed video

Figure 5.20 shows the recorded light intensity level in lux at 3m, 4.5m and 6m from the arcing point. Those tests results were taken from recent 2.7kV arc test. The x-axis of the figure indicates the configuration of each test. All tests operated with horizontal electrodes in open air (HOA) with 10kA, 20kA and 30kA short circuit current from right to left on the plot. A calorimeter was installed 27 inches from arc flash point.

As expected, the figure shows that light intensity increases when the measurement distance is reduced. In addition, the value of the bolted fault current also

significantly affected the arcing light intensity. According to test records, the light intensity at 3m exceeded 200 million lux when the bolted fault current reached 40kA at 14.3kV.

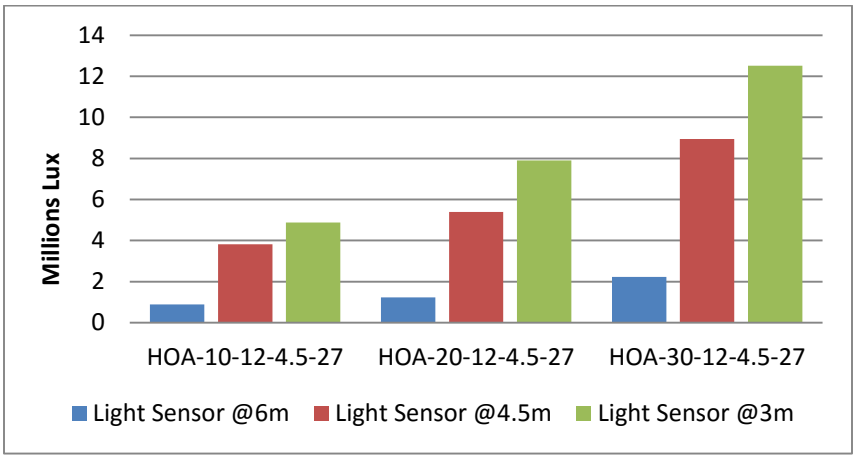

Figure 5- 20 Light intensity measured in 2.7kV HOA test with 10kA, 20kA and 30kA short circuit current, and calorimeters installed on 27 inches

5.2 Pressure blast hazards measurement

5.2.1 Basis of arc flash pressure hazards

In addition to burn and light injuries, when an arcing fault is initiated, the gases expand rapidly in the vicinity of the arc, the blast pressure can also cause severe injure for human [46]. The intense blast pressure generated by an arc flash can be dangerous. Severely air pressure wave with propel force in the surrounding area that blown off worker's feet or knocked them off ladders, even wounded the human body with projectile parts.

To mitigate the arc flash pressure hazards, it is imperative to develop industry safety standards regarding the pressure intensity of electric arc. Proper selection and use of Personal protective equipment (PPE) and designate safety working distance is the best way to mitigate the hazard posed by the generated pressure during an arc flash [5]. PPE is required by the Occupational Safety and Health Administration and National Fire

Protection Association standards to protect workers from hazards in the workplace. Those standards include headgear requirements, and heat retard cloths fabric requirements. Although the cloths can resist heat and fire, the pressure during the blast can still threaten the safety of people.

Accurate measurement of pressure level is the first step in understanding the level of protection and safety boundary needed. However, due to the harsh environment and dynamic nature of an arc flash blast, it is difficult to provide a precise description and reliable measurement of pressure level. This paper explores different pressure measurement devices and techniques to obtain reliable results under harsh environment.

5.2.2 Basic of arc flash pressure measurement

The pressures from an arc are developed from two sources: the expansion of the metal in boiling, and the heating of the air by passage of the arc through it [64]. A high-pressure front is created as the expanding gases compress the surrounding air. “A phenomenon called ‘blast overpressure’ forms from the compression of air in front of a blast wave which heats and accelerates the movement of air molecules. [65]” The severity of the blast pressure depends on the initial peak pressure, the duration of the overpressure, the distance of individuals from the incident location [66].

Individuals may be injured or killed by blast pressures through three mechanisms:

1. Injuries which directly result from the pressure wave striking the body are known as primary blast injuries, such Air- and fluid-filled organs (i.e. lungs) injure, even cause brain injury like concussions or mild traumatic with a blow to the head.

2. Another kind of injuries results from flying debris propelled by the blast wind. Shrapnel wounds can occur anywhere, including the eye and head.

3. Moreover, the individual being thrown by the blast wind can also be fatal. Individuals may be injured by a fall or being propelled into a wall or equipment [67].

- Indirect measurement (Lee's Curve for Pressure)

Drouet and Nadeau conducted arc tests over a range of arc currents to measure the amplitudes of the pressure waves [68]. They did the test between 1 to 80kA for current ranging, measured the sound wave level at 3, 6 and 9m from the arcing point. At low arc power, the amplitude of the pressure waves is approximately proportional to the rate of change of arc power. The following formula might be used to estimate the amplitude of the pressure wave at a substation [68]:

$$Amplitude_{pressure} = 1.5 * \frac{I_{arc} * t}{d}$$

Where, I_{arc} is arcing current,

t is arc duration

d is distance from arc point

Based on the work of Drouet and Nadeau, Lee developed a set of pressure curves as shown in Figure 5-21. The curves are based on a pressure measurement of 0.19 atm for a 100 kA arc current [64].

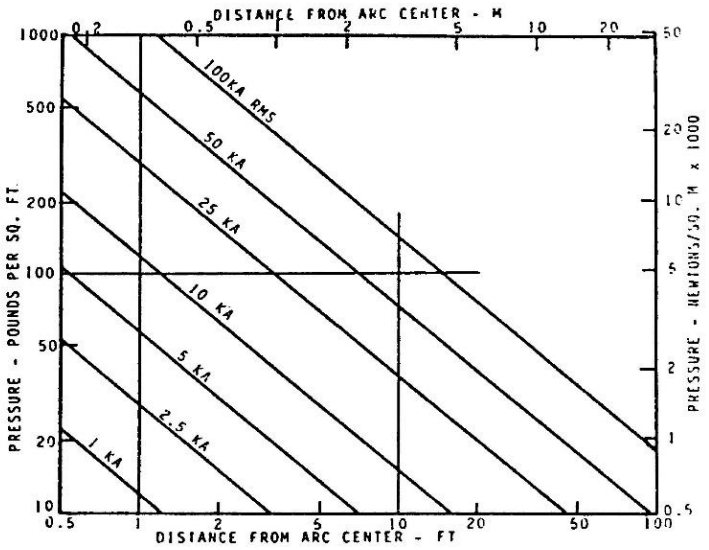

Figure 5- 21 Lee's Curves for Pressure versus Distance

This curve wildly used on previous arc flash hazards research and documentary for pressure estimation. However, Lee's curves developed from sound wave, and only fitted in the lower power arc flash. Because sound wave is only contains the low energy wave which has frequencies from about 20 Hz to 20,000 Hz. From physics point of view, sound wave has the essential difference with air pressure wave. Due to the speed of wave and energy transmittal length, sound wave could transmit long distance without loss of power. Based on this nature of sound wave, it may overestimate the pressure level in certain of distance. This theoretical results have been proved is too large to realize by recent tests performed by research team.

- Direct measurement

In 1993 and 1994, ten tests were conducted, following the test guidance in IEC Standard 298, Annex AA, to test an experimental latch and to compare the performance with a standard latch. Those test performed inside a closed equipment unit, which volume of the compartment is 1,578 inches and the door is approximately 14 x 13 inches. They

attached the pressure sensor inside the unit, and then measured the blast on door to estimate the pressure. Table 5-2 shows the results from their research.

Table 5- 2 Measured pressures for IEC tests [69]

Ibf (kA)	Peak (ms)	Pressure (psi)	Force on door (lbs)
51.5	6.7	4.94	711
25.0	5	4.04	576
66.0	5	6.26	901
67.8	5	7.55	1087
67.8	2	11.0	1584
67.8	8.3	9.15	1318
67.8	2.5	9.0	1296

However, recording accurate measurements using traditional direct pressure sensors is challenging due to the high magnetic flux and high temperature plasma gas during the arc event. Because the senor is easily damage by the arc blast, from the results list above, most of them are unreasonable and out of trend. Then a disappointed conclusion provided by them: “The uncontrollable and unpredictable variables such as arc characteristics, initiation conditions, propagation characteristics, dT/dt, etc. make it virtually impossible to accurately predict or duplicate test results.”

To ensure the accuracy of measurement result, a directly measurement is better to be performed during the arc flash tests. Pressure measurement devices typically use force collector to measure strain over a force area. However, the environments of arc flash events limited the function of traditional pressure measurement methods. The extremely harsh environment may impede the normal operation of the traditional pressure sensors. For example, high temperature may exceed the endurable range of most pressure sensors, molten metal may damage the mechanical components of pressure sensor, EMI/RFI may interfere the measurement signal, and direct contact of high voltage arcing plasma or induced voltage may bring fatal surge into sensor and damage the sensitive electronic components.

5.2.3 Design of arc flash pressure measurement system

5.2.3.1 Pressure transducers

A pressure transducer designed based on pressure sensors, such as gauge pressure sensor or vacuum pressure sensor. Pressure transducer generates a signal, such electrical signal.as a function of the pressure imposed [70].

Normal pressure transducer has a relatively slow speed of respond to the changes of pressure. In arc flash tests, the selected sensors need to have fast response to sudden changes in blast pressure level. Piezoelectric sensor, which designed to measure in a dynamic mode for capturing very high speed changes in pressure, has been used in the arc flash pressure measurement system. Piezoelectric sensor uses the piezoelectric effect, to measure changes in force by converting them to an electrical charge. Shown as Figure 5-22.

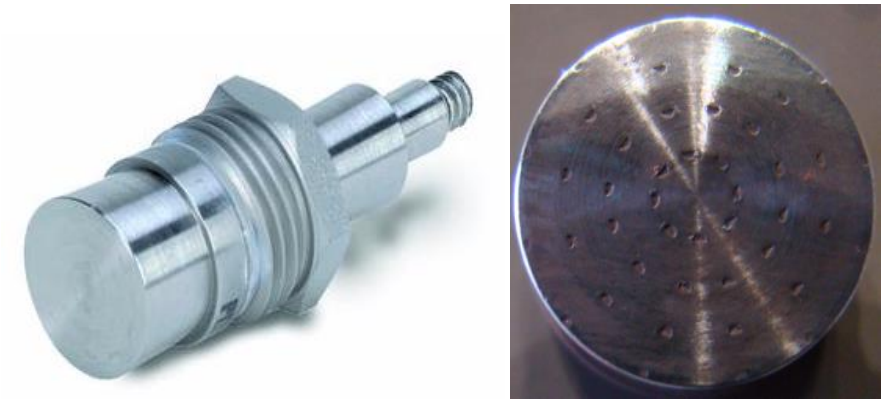

Figure 5- 22 Piezoelectric pressure transducer

Piezoelectric sensor has the very fast response to capture the peak pressure of arcing blast in milliseconds [71], but due to the structure of the sensing device, it can be damaged if it is placed in front of the plasma gas. To avoid the damage, piezoelectric sensor need to be placed on the side of arcing point during the test. However, side

measurement may affect the accuracy of results, one may even observe negative reading if it is located at the side of test set-up.

Also, because the direct contact with high voltage induced plasma, the large noise signal is observed obviously in the results, which also can reduce the accuracy of measurement, even burned the sensor. Figure 5-23 shows the negative recording with noise.

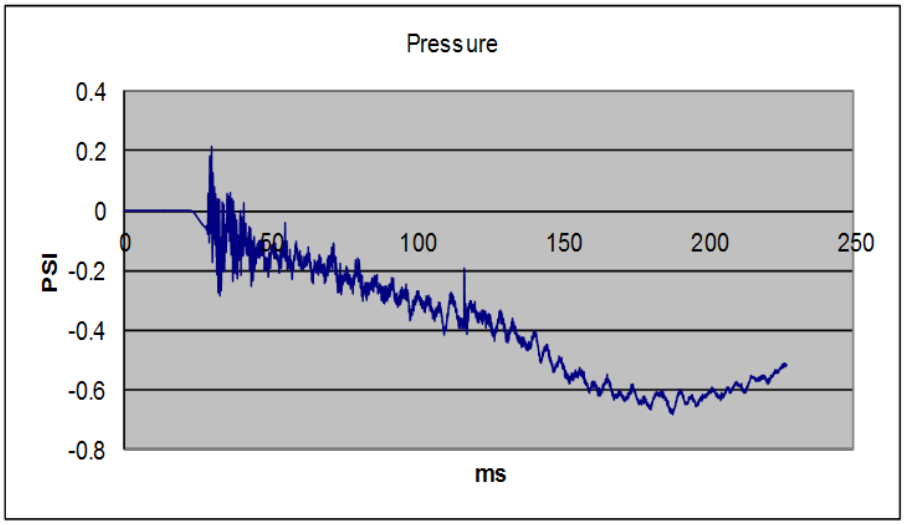

Figure 5- 23 Negative recording due to the side location of piezoelectric sensor

Then, to avoid the negative recording caused by location and increase the durability of measurement system, a specifically designed pressure sensor for harsh environment is selected after the previous unsuccessful attempt. A gauge based pressure sensor with isolated power supply and shield tube is incorporated in the design to avoid the interference and enhance its ability to handle the harsh environments. Gauge pressure is zero-referenced against ambient air pressure, so it is equal to absolute pressure minus atm pressure, and then the negative signs usually can be omitted [72].

To eliminate the loading effect and increase the compatibility with lab data acquisition system (DAQ), a buffer amplifier was designed to transfer the circuit from high

output impedance to low output impedance. Figure 5-24 illustrates a high input impedance operation amplifier (OP Amp) was used as core part of the buffer circuit.

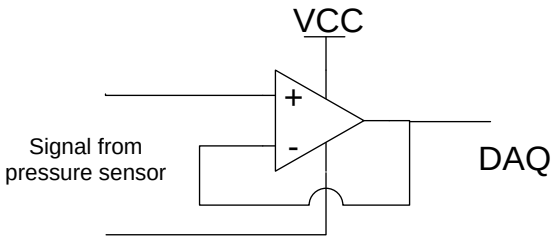

Figure 5- 24 Buffer circuit connect pressure sensor to DAQ

To ensure the accuracy of measurement results, a calibration system is fabricated. Figure 5-25 shows the pressure measurement system and calibration system.

However, the surface of sensor is still vulnerable for propel molten metal and hot plasma gas. For 14.3KV, 20kA test, one has to replace the sensor after 3 to 4 tests.

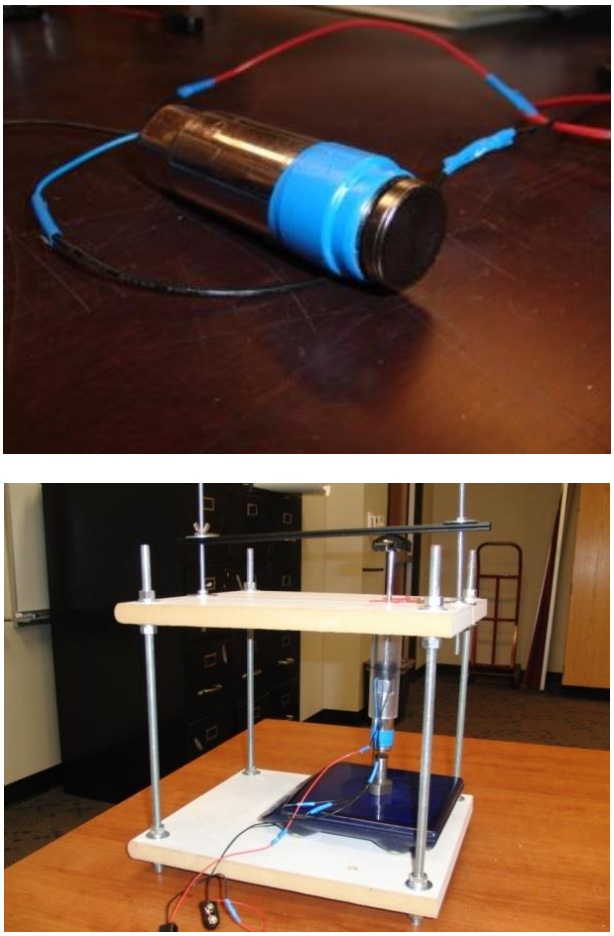

Figure 5- 25 Gauge sensor based pressure measurement system (upper) and calibration system (lower)

5.2.3.2 Pendulum system

Compare with previous attempt of directly utilization of pressure sensor, the pendulum system has its unique advantages:

1) Non-electrical interference. Whole system construct by insulated dummy components, in other words, it could neglect all kind of electrical interference at all.

2) Durable and high temperature resists. The part, which directly contact with blast air and plasma, to receive pressure is small plate, which shows on Figure 2-26. Hot plasma gas and propel metal cannot damage the system.

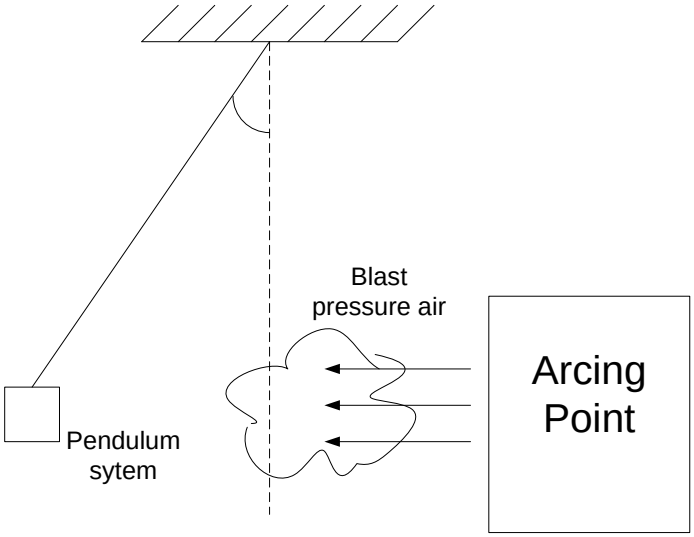

Figure 5- 26 Pendulum pressure measurement system

From kinetic equation of pendulum, the force from arcing blast can be easily to be calculated. Based on kinetic point of view, the momentum of pendulum can be expressed by equation:

$$M = -mgl\sin\theta$$

Where M is angular momentum,

m is mass,

g is acceleration of gravity,

l is length of pendulum,

θ is the vertical angle.

Based on angular momentum theory, the equation could be transformed as:

$$\frac{d^2\theta}{dt^2} + \frac{g}{l}\sin\theta = 0$$

Where $\frac{d^2\theta}{dt^2}$ is the angular acceleration.

Then, the force of pressure is able to be calculated from angular acceleration and mass of pendulum. The actual set up of pendulum system in arc flash shows on figure 5-27.

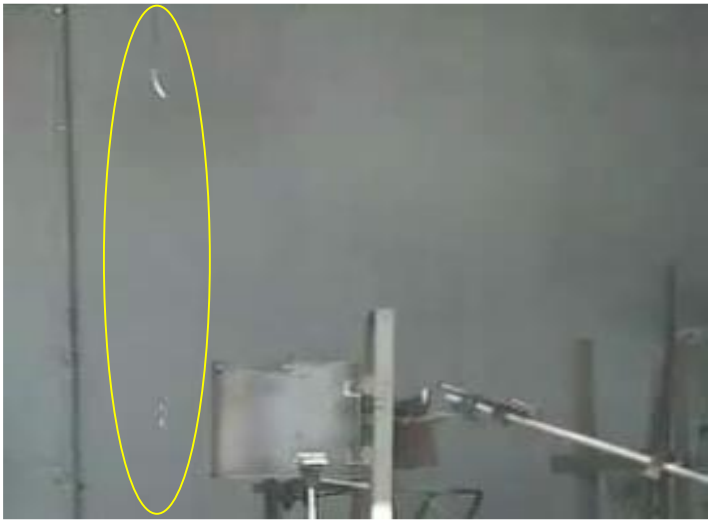

Figure 5- 27 Pendulum system applied in arc flash test for pressure measurement

However, system installs position and environment has specified requirement to enhance the accuracy of measurement result:

1) Place the metal plate at the maximum pressure point,

2) Remove objects in front of test set-up to avoid any possible air flow blockage to obtain accurate results.

5.2.3.3 LVDT pressure measurement system

Pendulum pressure measurement is a successful attempt to quantize arc blast pressure level from kinetic calculation. However, the requirement of installation has limited its application. After several tests and design, a linear variable displacement transducer (LVDT) based pressure measurement system has been developed.

LVDT is a type of transducer used for measuring linear displacement of an object [73]. It converts position information from a mechanical reference into a proportional electrical signal. The LVDT operation does not require an electrical contact between the moving part (probe) and the coil assembly, but instead relies on electromagnetic coupling. Figure 5-28 explained the work mechanism of LVDT.

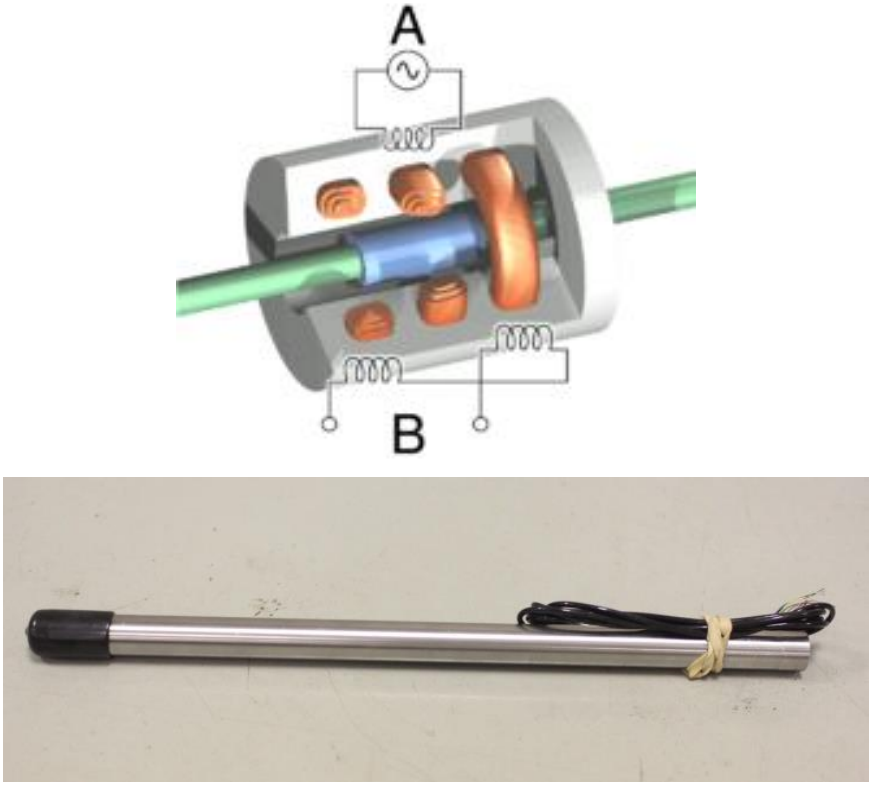

Figure 5- 28 LVDT working mechanism (upper) and typical LVDT device used in industry (lower).

LVDT pressure measurement system incorporate the advantages of pure mechanical structure based “kinetic to pressure” measurement system, with the idea of gauge sensor. This system overcomes the location limitation of pendulum, and eliminates the vulnerability of the sensor surface for force collection. Figure 5-29 provide the scheme of LVDT based pressure measurement system.

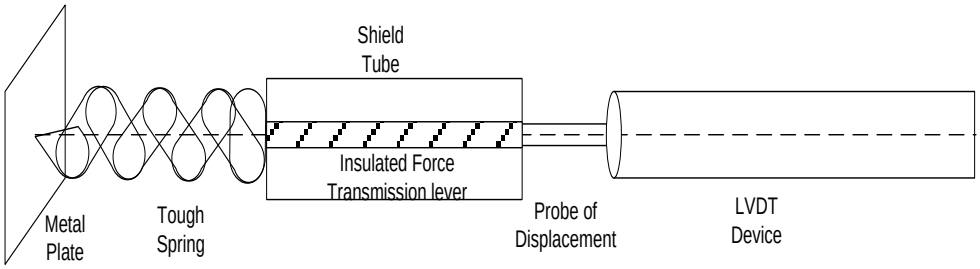

Figure 5- 29 Design scheme of LVDT based pressure measurement system

The proposed LVDT pressure measurement system consists of 4 major parts:

1) 2" x2" metal plate to collect force of arcing blast.

2) Tough spring to convert arcing pressure into distance (compress displacement of spring).

3) Insulated transmission lever with shield tube to transmit the displacement information to LVDT under non-interfere condition.

4) LVDT with probe to translate the displacement to readable electrical signal.

Based on Hooke's law and the characteristic of type of LVDT applied, it is easy to convert the displacement position into pressure measurement.

$$F = -kx$$

$$\Delta V = \frac{dv}{dl} \bullet x$$

$$\Pr essure = \frac{-k}{S} \bullet \frac{\Delta V}{\frac{dv}{dl}}$$

Where F is force from arcing blast

k is Hooke's coefficient

x is the extend or compress displacement of spring

$\frac{dv}{dl}$ is characteristic curve of LVDT

ΔV LVDT output for displacement of x

S is the area of force collect plate

There are several advantages of the LVDT based pressure measurement system. The metal plate can resist high temperature plasma and propel molten metal. An insulated displacement transmittal tube connected between the plate and LVDT can protect the electric component from high voltage plasma or induced voltage. Moreover, it can be placed in front of the calorimeters to safe the test cost. Figure 5-30 shows the pressure measurement system for arc flash test. Figure 5-31 illustrate the position of pressure measurement location during the arc flash test.

Figure 5- 30 LVDT pressure measurement system for arc flash test

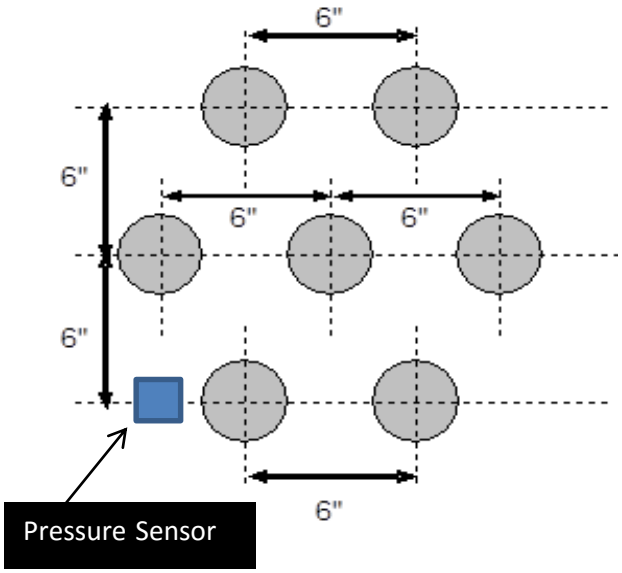

Figure 5- 31 Pressure measurement location during arc flash tests

5.2.4 Sample results of pressure measurement results

Figure 5-32 shows the recorded pressure level from LVDT based measurement system. The measurement system located at 18” from arcing point, under the 0.482 kV, vertical electrodes in cubic box (VCB in 20”x20”x20 box), 80.2 kA, 6-cycle, and 1.5” gap arc flash test.

From the recording, peak pressure produced 3.7V change for LVDT. Applied all calibrated parameter into the equation, the estimated pressure reached 0.715 psi (103 lbs/ ft^2) at working distance of 18”.

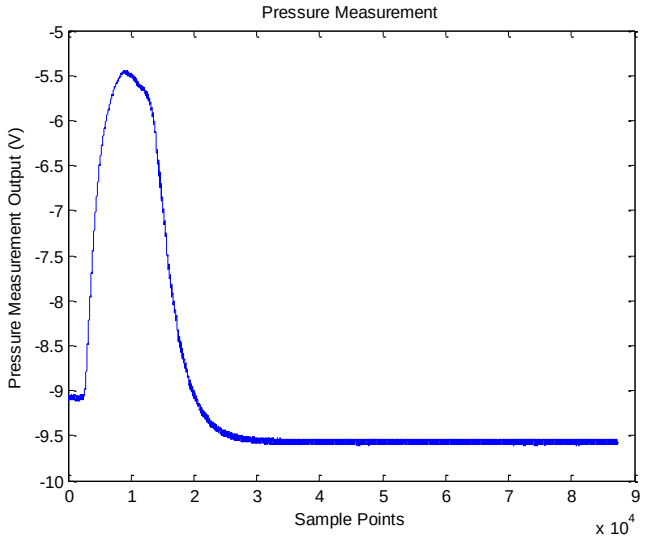

Figure 5- 32 LVDT output at 18” from 0.575kV VCB test with 80.2kA short circuit current arc flash test

5.2.5 Results comparison for indirect measurement method

High speed video as an indirectly measurement provides a reliable reference to verify the results of LVDT. Based on two consecutive high-speed video frames (1000 fps), the movement of the arc cloud can be used to estimate the pressure. Following is an example of a 2.7-kV, VCB (26”x26”x26” box size), 30 kA, 6 cycle, 3” gap arc flash test, which shows on Figure 5-33.

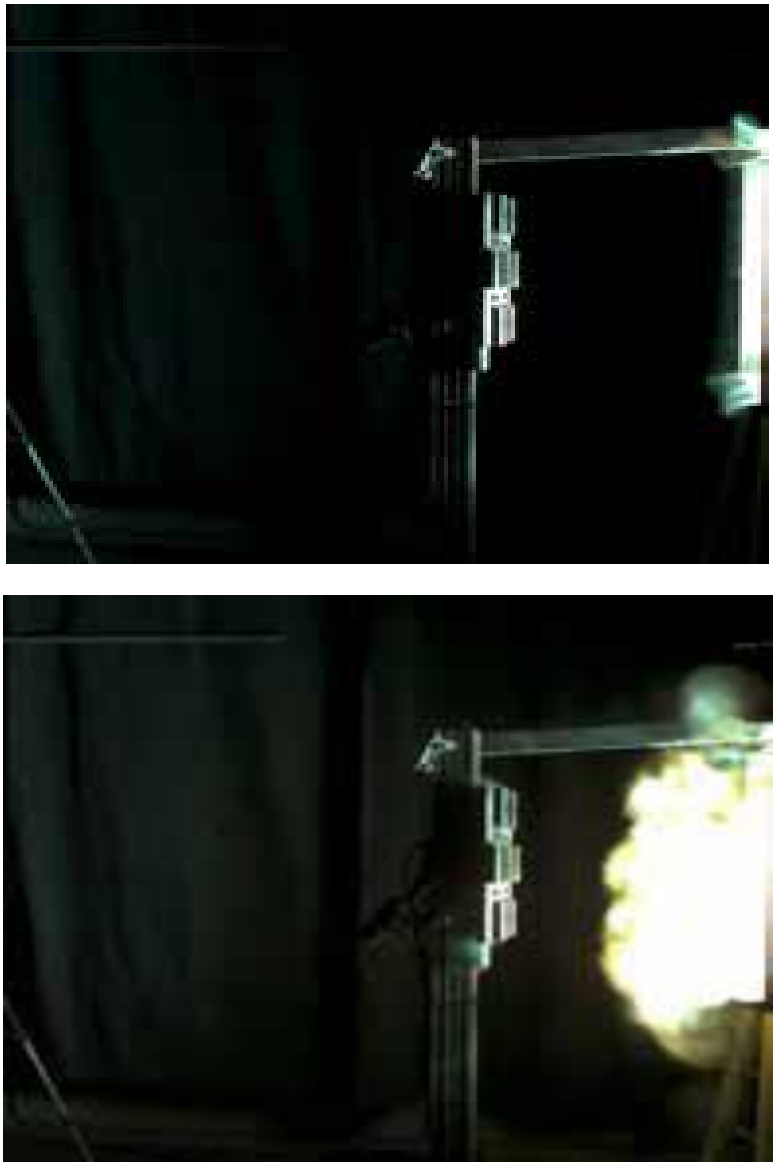

Figure 5- 33 Estimating Blast Pressure from Air Movement

From kinetic theory, the air pressure can be calculated based on air volume and moving distance. From this test recording, the estimated pressure reached 1.7 psi (245 lb/ft^2) at 24” away from arcing point. From the energy proportion point of view, when lower down voltage to 0.48kV and level up bolted fault current to 80.2kA, the pressure should be around 0.76 psi, which means LVDT has reasonable measurement.

Comparing the performance and their capability of handling the harsh environment, LVDT offers the best potential for arc blast pressure measurement. Though some other approaches may produce satisfactory results, they are either too expensive or not durable enough.

5.3 Sound hazards measurement

5.3.1 Basis of sound hazards

Every year, approximately 30 million people in the United States are occupationally exposed to hazardous noise. Noise related hearing loss has been listed as one of the most prevalent occupational health concerns in the United States for more than 25 years. Since 2004, the Bureau of Labor Statistics (BLS) has reported that nearly 125,000 workers have suffered significant, permanent hearing loss. In 2009 alone, BLS reported more than 21,000 hearing loss cases.

In the Code of Federal Regulations 1910.95(b)(2), it is stated, “Exposure to impulsive or impact noise should not exceed 140 dB peak sound pressure level.” When the potential peak sound pressure is 140 dB or greater, individuals should wear personal hearing protection devices (PHPDs) to reduce the exposure level within OSHA limits. And employers to have a hearing conservation program in place if workers are exposed to a time-weighted average (TWA) noise level of 85 decibels (dBA) or higher over an 8-hour work shift. Figure 5-34 provided the permissible noise exposure required by OSHA 1910.05.

Duration per day, hours	Sound level dBA slow response
8	90
6	92
4	95
3	97
2	100
1 1/2	102
1	105
1/2	110
1/4 or less	115

Figure 5- 34 Permissible noise exposure by OSHA [74]

According to OSHA, exposure to impulsive or impact noise should not exceed 140 dB peak sound pressure level. At 115 dB, OSHA's permissible noise exposure is 15 minutes or less daily [74].

Although using a PPE protective hood may attenuate the sound pressure level, since peak sound pressure is linked to the initial formation of the arc, the PPE categories which is defined base on incident energy exposure level, are not a good method for assessing the sound hazard.

5.3.2 Basic of sound pressure

Sound pressure is the local pressure deviation from the ambient atmospheric pressure, caused by a sound wave. The "loudness" of a given sound is related to the amplitude of the pressure wave striking the ear. The human ear actually perceives differing loudness from pressure waves of identical amplitudes created by different audible frequencies [75].

From the research, when the sound level approaches 100 dB, the ear's response to different frequencies becomes more linear [76]. Even for a single frequency, "loudness" is not simply a linear response; the response of the human ear to changes in

the amplitude of a pressure wave for a given frequency is roughly logarithmic. Therefore, the measure of loudness may be expressed as dB SPL (Sound Pressure Level),

dB SPL = 20 log (pressure wave amplitude / hearing threshold amplitude)

Figure 5-35 use noise exposures of carpenters as an example to illustrate the noise level received by human ears.

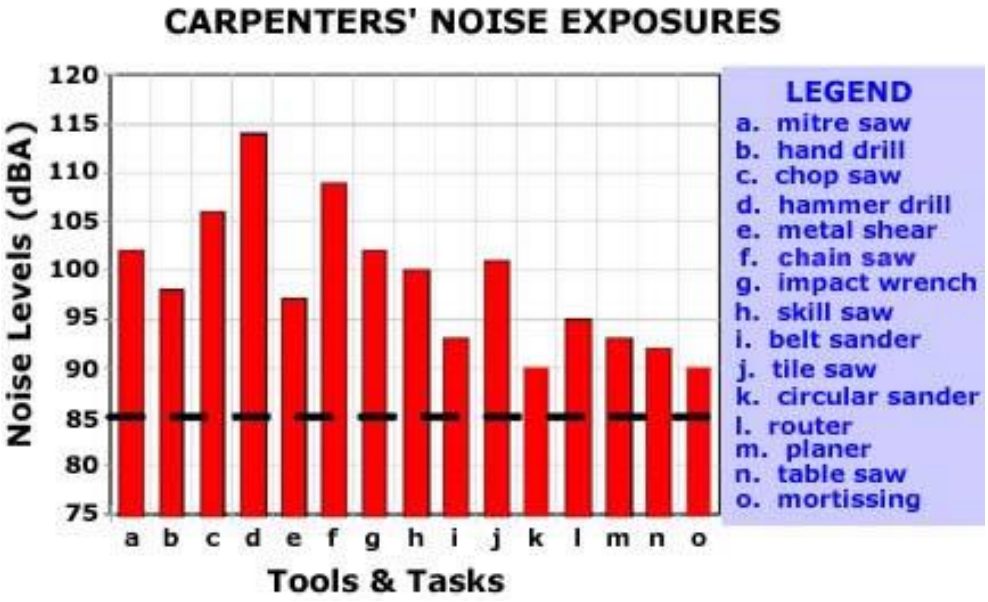

Figure 5- 35 Carpenters noise exposure level [77]

IEC 61672 defined the sound pressure level measurement as weighting, which is commonly used of a family of curves to identify. Four types of weighting are commonly used to assess sound pressure level [78].

A-weighting is applied to instrument-measured sound levels in effort to account for the relative loudness perceived by the human ear.

B-weighting and D-weighting is designed for use of high level aircraft noise level measurement, and sound frequency measurement

C-weighting is applied to class one sound level meters, which is only for testing purposes.

Figure 5-36 gives this family of weight curves defined by IEC 61672.

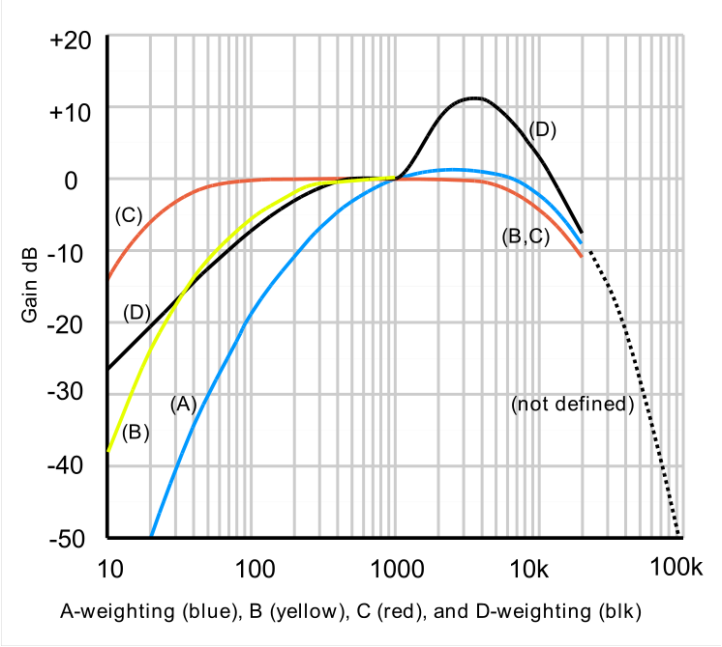

Figure 5- 36 Family of sound pressure weighting curves [78]

The amplitude of the threshold of hearing, 20 x 10^{-6} N/m^2, is the pressure amplitude of the softest 1 kHz sound that the average ear can detect. Table 5-3 lists a scale of relative pressures in N/m2 and dB for common sounds.

Table 5- 3 Relative pressures for common sounds [75]

Pressure (N/m^2)	Pressure Level (dB)	Example
0.00002 (reference)	0	Threshold of hearing
0.002	40	City noise at night
0.02	60	Conversational speech
0.2	80	Loud radio
20	120	Discomfort level, bad rock band
200	140	Pain level
2000	160	Mechanical damage to ear

Sound pressure can damage the ear because the sound wave is energy being transmitted to the human ear. Any mechanical wave, transferring energy through solids, liquids, or gases, may be considered a sound or acoustic wave. The intensity of the

pressure wave (W/m2) is the density of power being transmitted through a surface directly facing (i.e., perpendicular to) the pressure wave. The amplitude is the maximum air pressure change caused by the sound wave. According to basic pressure wave equations, the intensity is related to the square of the wave's amplitude; therefore, when the amplitude increases by a factor of two, the intensity increases by a factor of four. If the wave source is assumed to be a spherical source, the intensity of the wave decreases by the inverse square law; doubling the distance from the source decreases the energy by a factor of four [75] [79].

5.3.3 Sound pressure measurement

Acoustic sensors or sound meters, which are used to measure peak sound impulse level, are provided to measure the arc flash sound pressure level during the testing. One meter had been placed at 3 m, another one had been place at 4.5 m, and the last one had been placed at 6 m from arcing point.

All three meters comply with ANSI S1.4 and have the peak measurement level up to 180dB. Since the single arc flash testing is always less than 200ms, based on the weighting characteristics, type C-weighting is selected as the recording mode. Figure 5-37 shows the sound meters utilized in arc flash test.

Figure 5- 37 Sound meter utilized in arc flash test

From the tests, the measured sound pressure level exceeds 140dB in almost every single test. Even at 6m away from arcing point, the sound level can reach to 140dB. Figure 5-38 provides a sample result from one meter recording. The test was performed at 2.7kV arc flash test, and the meter was placed at 3 m away from arcing point.

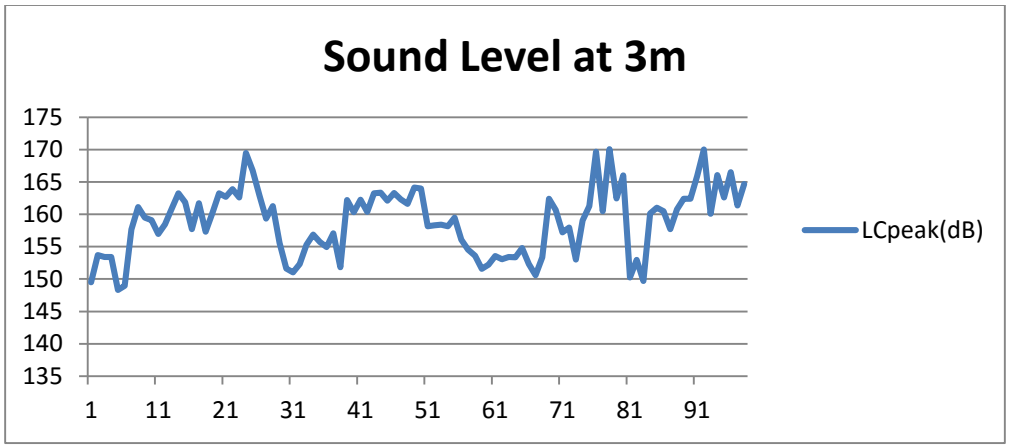

Figure 5- 38 Peak level of sound recorded in 2.7kV arc flash tests, which the meter placed at 3m away from arcing point

From the observation of tests, for example, in 2.7kV arc flash test, arcing currents from 5 to 40 kA, all sound pressures measured over 140 dB at a distance of 3 m away from the arcing point. Based on IEC's requirement, these results already passed the upper limits for the noise level exposure. Hearing protection should be included as part of PPE, which is distinct from incident energy PPE requirements.

Chapter 6

Conclusion and future work

Due to their random complex nature, accurately represent and correctly model all the real arc flash events are very difficult. In order to have a precise arc flash hazards assessment, approximately 2000 arc flash experiments had been conducted to investigate the arc flash behavior over extensive range of system voltage, bolted fault current, electrodes gap width, arc initiative configuration, and enclosure dimensions.

From thermal hazards modeling point of view, the works provide through the dissertation has performed a significant amount of testing and has developed models of arcing current and incident energy estimation. The methodology described in this dissertation has provided a reliable and rigid approach to estimate the arcing current and incident energy for arcs in three phase electrical systems between 208V and 15kV.

Previous researches, such as NFPA 70E and IEEE 1584-2002, arcing current and incident energy are based on either theoretical concepts or pure statistic models from very limited test data. The works from this dissertation derived sets of empirical models which combine the physical and statistical analysis approach from a significant amount of test data. These models overcame the weaknesses on previous modeling protocols, and bridged the gap between pure statistic models and physical representative models. Range of models fully cover the commonly used equipment conditions and arcing faults occur positions in common industrial practice. The results of incident energy estimation could be adopted to define risk category for hazards and determine PPE levels and safety working distance.

From non-thermal hazards analysis point of view, the novel measurement systems presented in this dissertation overcome the limitations of traditional approaches. Since the selected light sensor closely matches the $V(\lambda)$ photopic curve, the

measurement results from this dissertation could realistically represent the arcing light as perceived by human eyes. Moreover with the ND filter, the measurable brightness level range of the sensor system was greatly improved. Due to the harsh environment and dynamic nature of an arc flash blast, it is difficult to provide a reliable measurement of pressure level. This dissertation explores different pressure measurement devices and techniques to obtain reliable results under harsh environment. The sound measurement from this dissertation provides a solid evidence on the necessity to establish an essential non-thermal protection, especially for hearing protection in future NFPA 70E or other arc flash related standards.

From testing design point of view, the efforts and techniques to reliably protect the measurement systems in arc flash tests have offered valuable insight for future similar testing. The holistic isolation and grounding techniques and approaches ensure the measurement accuracy and survivability of the equipment under harsh testing environment.

The emphasis on electrical safety and recognition its potential risks and hazards have make significant improvement among industry to protect employees from arc flash hazards. Based on IEEE/NFPA collaborative efforts, the research and testing presented in this dissertation has provided deeper insight into arc flash phenomena and the hazards. This dissertation has reviewed the testing methodology, provided test equipment design, and established model development process for thermal related arc flash hazards. This has offered valuable information for the revision of IEEE Std. 1584. In addition to the thermal related hazard, it is possible to extend the knowledge gained from the initial research of this dissertation to establish practices and standards for non-thermal related hazards to further enhance the workplace safety.

In addition to these works, the relationship between arcing current and enclosure size need to be detail reviewed. In this model development process, the initial study of enclosure size is only considered on incident energy side. However, not the thermal transfer affects by box size but also arc column length may be determined by the size, which may have some unpredictable conditions for arcing current estimation.

Moreover, effect of back panel distance is another aspect of future works need to be studied. In test performed, there is only limited back panel distance has been selected, and it may affect the final incident energy level in enclosed vertical electrode configuration tests.

Low voltage arc flash analysis need to be emphasis on future study. Due to the dynamic nature of arc in low voltage tests, current model may have a reasonable prediction results based on certain of assumptions. However, it is essential to have a more detailed modeling process for low voltage arc, which in order to have a fully and precisely understanding in this special range then aided to current modeling equations.

Further thermal hazards modeling can be performed in association with or as a continuation of the short circuit study and protective device coordination study. Based on this, the protective device operation time in response to arcing currents could be applied into “real world” power systems.

Additionally, although the non-thermal hazards studies provided a reliable measurement approach and design for light hazards, pressure hazards and sound hazards analysis and industry standards development, the more tests on non-thermal part need to be performed. The future work would be focused on the non-thermal hazards modeling, based on a detailed and accurate measurement results, a similar modeling approach from thermal part could be utilized in non-thermal analysis. This important work may become for foundation of industry standards development.

Appendix A

Results comparison between test recording and model estimation

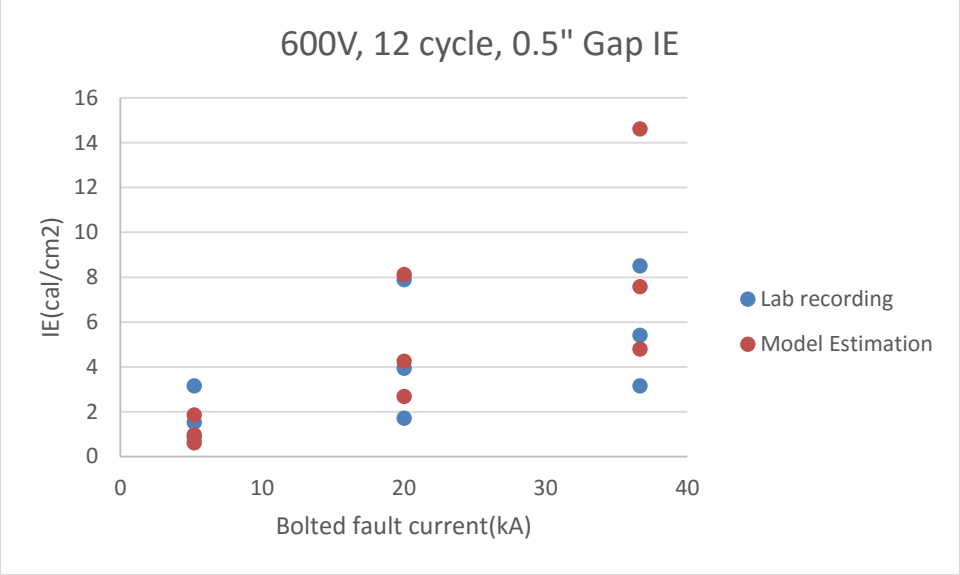
600V, 12 cycle, 0.5" Gap IE
IE(cal/cm2)
16
14
12
10
8
6
4
2
0
0
10
20
30
40
Bolted fault current(kA)
Lab recording
Model Estimation

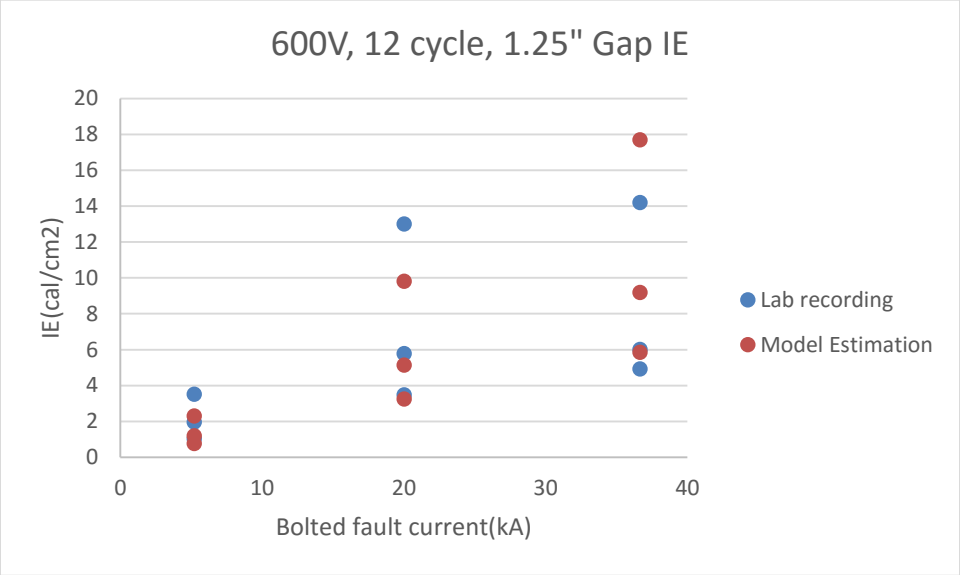
600V, 12 cycle, 1.25" Gap IE
IE(cal/cm2)
20
18
16
14
12
10
8
6
4
2
0
0
10
20
30
40
Bolted fault current(kA)
Lab recording
Model Estimation

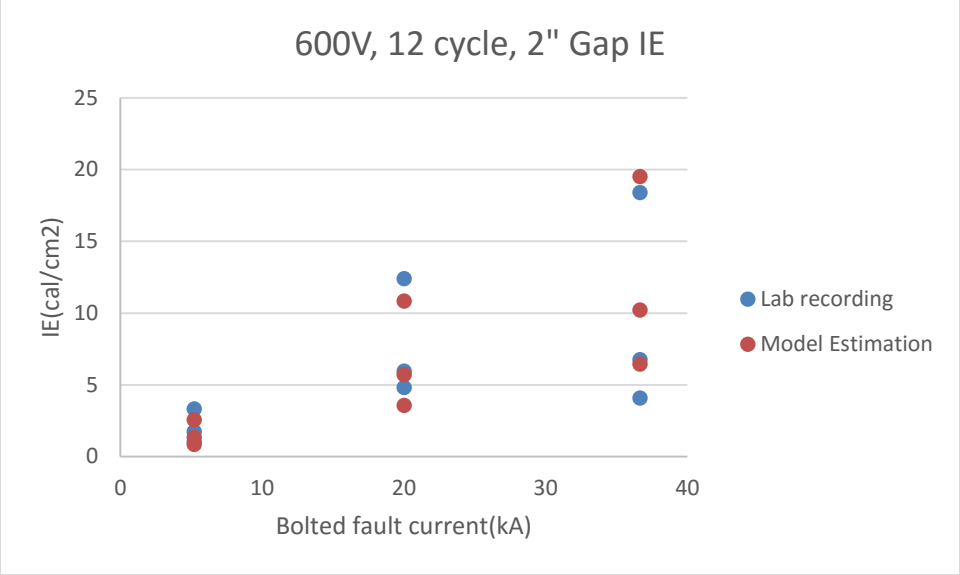
600V, 12 cycle, 2" Gap IE
IE(cal/cm2)
25
20
15
10
5
0
0
10
20
30
40
Bolted fault current(kA)
Lab recording
Model Estimation

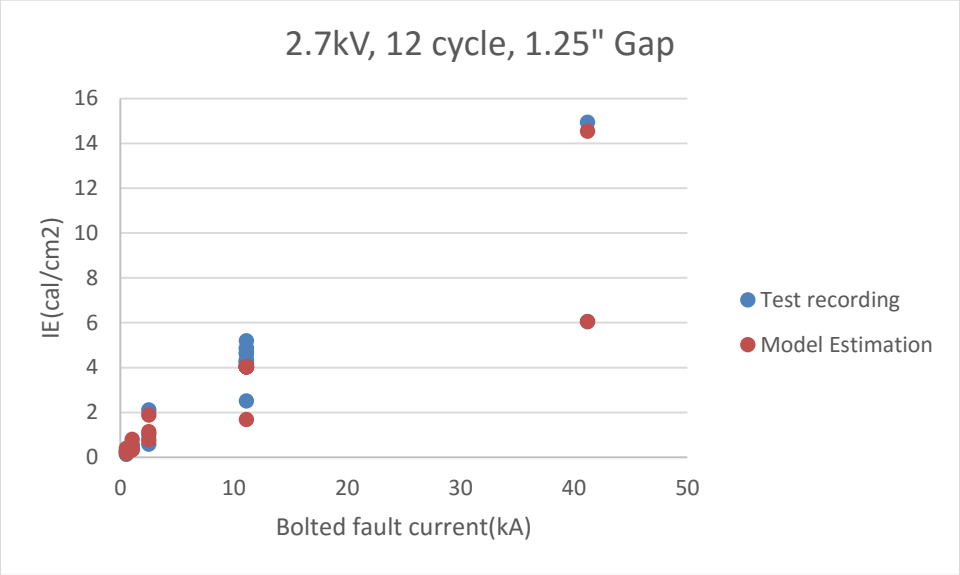
2.7kV, 12 cycle, 1.25" Gap
IE(cal/cm2)
16
14
12
10
8
6
4
2
0
0
10
20
30
40
50
Bolted fault current(kA)
Test recording
Model Estimation

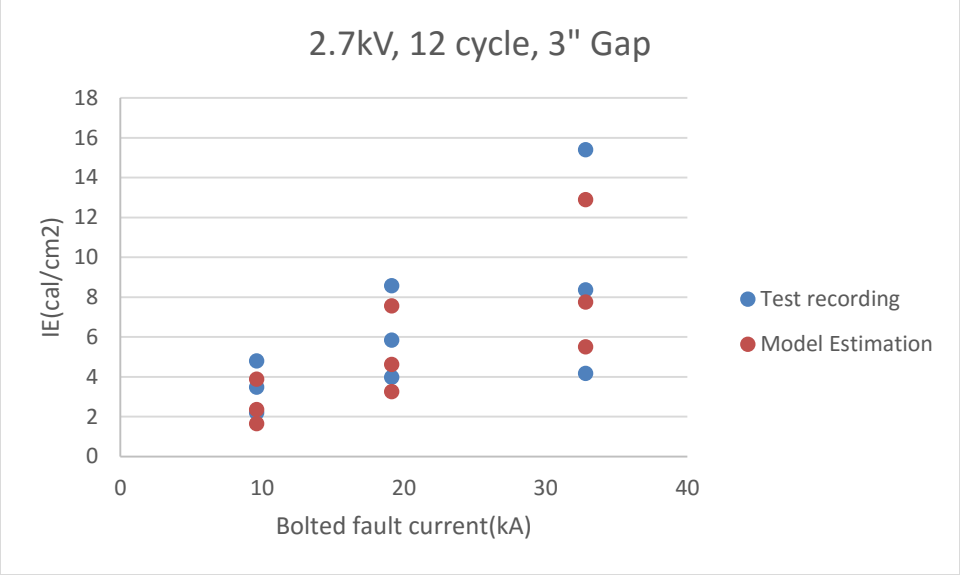
2.7kV, 12 cycle, 3" Gap
IE(cal/cm2)
Bolted fault current(kA)
Test recording
Model Estimation

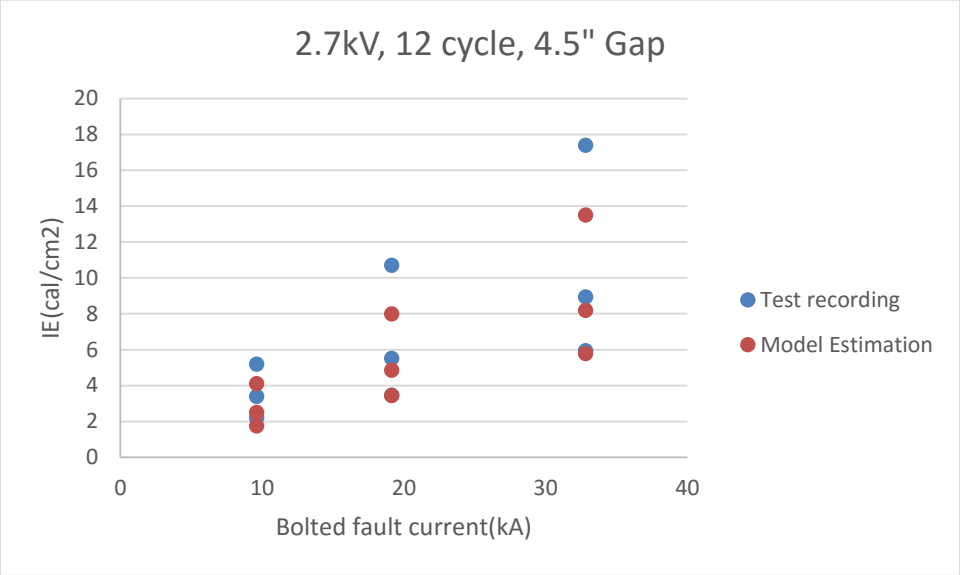
2.7kV, 12 cycle, 4.5" Gap
IE(cal/cm2)
Bolted fault current(kA)
Test recording
Model Estimation

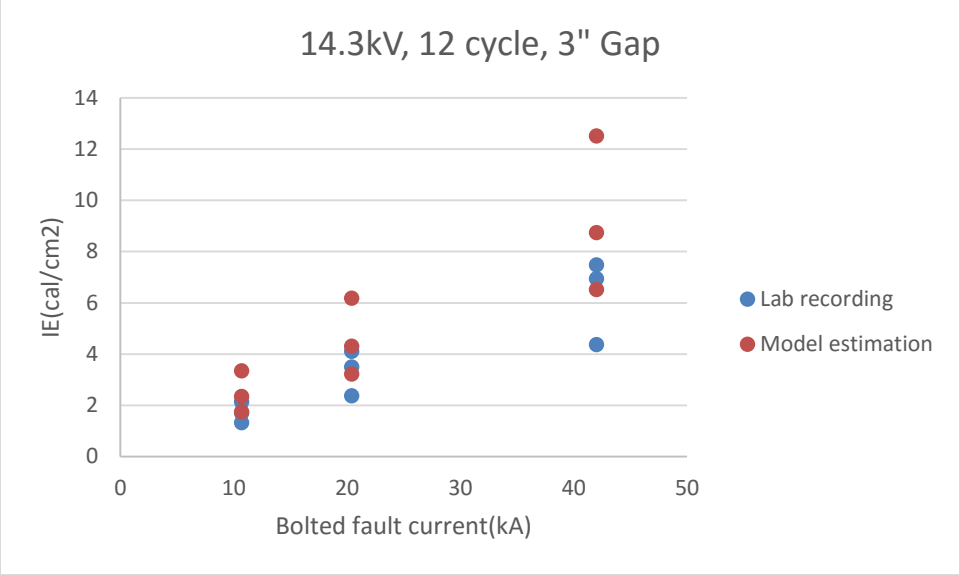
14.3kV, 12 cycle, 3" Gap
IE(cal/cm2)
Bolted fault current(kA)
Lab recording
Model estimation

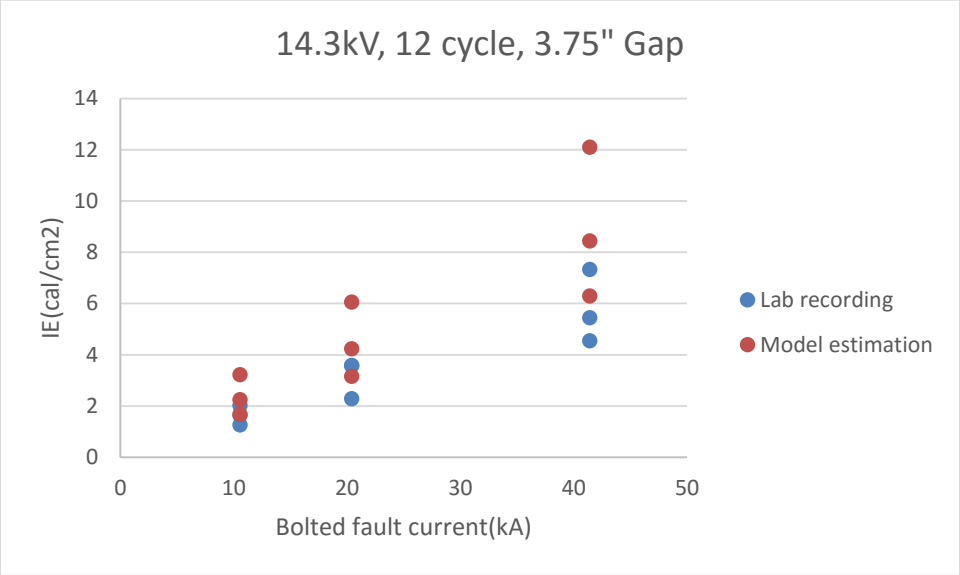
14.3kV, 12 cycle, 3.75" Gap
IE(cal/cm2)
Bolted fault current(kA)
Lab recording
Model estimation

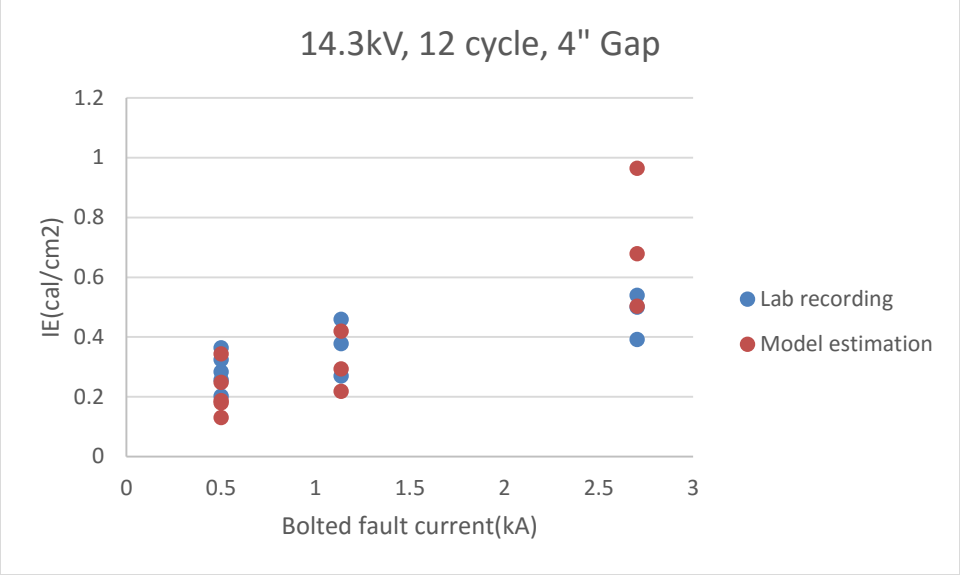
14.3kV, 12 cycle, 4" Gap
IE(cal/cm2)
1.2
1
0.8
0.6
0.4
0.2
0
0
0.5
1
1.5
2
2.5
3
Bolted fault current(kA)
Lab recording
Model estimation

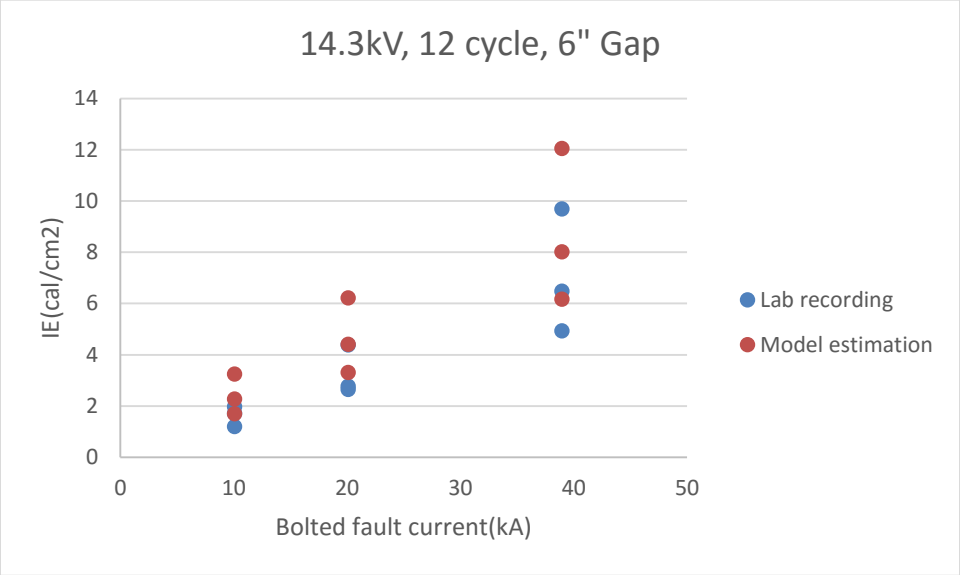
14.3kV, 12 cycle, 6" Gap
IE(cal/cm2)
14
12
10
8
6
4
2
0
0
10
20
30
40
50
Bolted fault current(kA)
Lab recording
Model estimation

References

[1] S. D. A. D. P. Richard B. Campbell, “Occupational Injuries From Electrical Shock and Arc Flash Events,” Fire Protection Research Foundation , March 2015.

[2] T. N. M. Lang, “Arc flash basics: testing update,” *Proceedings of the 8th International Conference on Electric Fuses and their Applications*, Clermont-Ferrand, France, Sept. 2007.

[3] “Victim of an Arc Flash at an Electric Meter,” [Online]. Available: https://www.nachi.org/bbsystem/viewtopic.php?t=5145&PHPSESSID=68ded59e609759dc8b34a0034a55af1e.

[4] ABB, “Protection against electric arc,” ABB, 2011.

[5] “NFPA/IEEE Research and Testing Planning Committee (RTPC), Final Report,” July 28, 2005.

[6] T. E. N. a. R. F. Parry, “Specialized PPE Testing for Electric Arc Hazards Beyond Heat Exposure,” *Conference Record of the IEEE IAS I&CPS*, May 2004.

[7] “IEEE Standard 1584-Guide for Performing Arc Flash Calculations,” IEEE, 2002.

[8] A. S. D. Stokes, “Electric arcing burn hazards,” *IEEE Transactions on Industry Applications,* vol.42, no.1, pp. 134-141, 2006.

[9] Wikipedia, “High voltage,” [Online]. Available: https://en.wikipedia.org/wiki/High_voltage.

[10] E. S. F. I. (ESFI), “ Electrical Safety in the Workplace Fact Sheet”.

[11] “Improved Safety During Infrared Inspections of Electrical Equipment,” [Online]. Available: http://www.thermal-cameras.com/wp-improved_safety.html.

[12] p. B. Koch, “Characterization of Secondary Arcing Faults Part 1: General Characteristics.,” Canadian Electrical Association, 1989.

[13] J. M. Somerville, The Electric Arc, New York: John Wiley & Sons, 1958.

[14] A. E. Guile, “Arc-electrode phenomena,” *Proceeding of IEE,* vol.118, no.9R, pp. 1131-1154, Sept. 1971.

[15] T. H. Lee, “Plasma physics and the interruption of an electric circuit,” *Proceedings of the IEEE,* vol.57, no.3, pp. 307-323, Mar. 1969.

[16] e. T. E.Browne, “Circuit Interruption.,” Marcel Dekker, Inc., New York, 1984.

[17] R. Holm, “The vaporization of the cathode in the electric arc,” *Journal of Applied Physics,* vol.20, pp. 715-716, July 1949.

[18] W. R. Wilson, “High-current arc erosion of electric contact materials,” *AIEE Transactions,* pp. 657-664, Aug. 1955.

[19] J. J. Lowke, “Simple theory of free-burning arcs,” *Journal of Physics D: Applied Physics,* vol.12, pp. 1873-1886, 1979.

[20] NFPA, NFPA 70E-Electrical Safety in Workplace, 2012.

[21] J. M. T. A. L. Stanford, Physics for Students of Science and Engineering, New York: Harcourt Brace Jovanovich, 1985.

[22] M. A. B. Y. A. Çengel, Thermodynamics: An Engineering Approach, Third Edition, New York: McGraw-Hill Companies, Inc, 1998.

[23] L. S. D. Pitts, Schaum’s Outline of Heat Transfer, Second Edition, New York: McGraw-Hill Companies, Inc., 1998.

[24] A. H. B. a. R. L. D. T. E. Neal, “Protective clothing guidelines for electric arc exposure,” *IEEE Transactions on Industry Applications,* vol.33, no.4, pp. 1041-1054, July/Aug. 1997.

[25] M. A. a. M. L. R. Wilkins, “Calculating hazards,” *IEEE Industry Applications Magazine,* pp. 40-48, May/June 2005.

[26] M. A. a. M. L. R. Wilkins, “Time-domain analysis of 3-phase arc flash hazard,” *Proceedings of the Seventh International Conference on Electric Fuses and their Applications*, Gdansk, Poland, Sept. 2003.

[27] “UNDERSTANDING THE STOLL CURVE,” OBERON, 2005. [Online]. Available: http://csaz462.ca/data/1/rec_docs/102_Oberon_WP_Understanding_the_Stoll_Curve.pdf.

[28] A. H. B. a. R. L. D. T. E. Neal, “Protective clothing guidelines for electric arc exposure,” *IEEE Transactions on Industry Applications,* vol.33, no.4, pp. 1041-1054, July/Aug. 1997.

[29] R. Lee, “The other electrical hazard: Electrical arc blast burns,” *IEEE Trans. Ind. Appl.,* vol.%1，共 %2 vol. 1A-18, no.3, pp. 246-251, May/June 1982.

[30] T. E. N. a. H. L. F. I. R. L. Doughty, “Predicting incident energy to better manage the electric arc hazard on 600V power distribution systems,” *IEEE Transactions on Industry Applications,* vol.36, no.1, pp. 257-269, Jan./Feb. 2000.

[31] D. K. S. A. D. Stokes, “Electric arcing burn hazards,” *IEEE Transactions on Industry Applications,* vol.42, no.1, pp. 134-141, Jan./Feb. 2006.

[32] A. C2, National Electric Safety Code, 2007.

[33] IEEE, IEEE Std 1427-2006, 2007.

[34] “What is data acquisition,” National Instruments, [Online]. Available: http://www.ni.com/data-acquisition/what-is/.

[35] R. H. Lee, “Grounding of computers and other similar sensitive equipment,” *IEEE Transactions on Industry Applications,* vol.3, pp. 408-411, 1987.

[36] “Isolation Technologies for Reliable Industrial Measurements,” National Instrument, [Online]. Available: http://sine.ni.com/np/app/main/p/ap/daq/lang/en/pg/1/sn/n17:daq,n21:41/fmid/2871/.

[37] “AN103 Application Note,” Dataforth Corporation, [Online]. Available: http://www.dataforth.com/catalog/pdf/an103.pdf.

[38] “Data Acquisition Handbook, Chapter 5,” Measurement Computing, [Online]. Available: http://www.mccdaq.com/handbook/chapt_5.aspx.

[39] “MT-042 Tutorial, Op Amp Common-Mode Rejection Ratio,” Analog Devices, [Online]. Available: http://www.analog.com/static/imported-files/tutorials/MT-042.pdf.

[40] W. H. Paul Horowitz, “The Art of Electronics, Second Edition,” Cambridge, 1989, pp. 462-464.

[41] “Different Types of Isolation,” National Instrument, [Online]. Available: http://digital.ni.com/public.nsf/allkb/CF71091043A6193B862573D70077138B.

[42] M. A. M. M. A. Mohd, “Fiber optics: an antidote to electromagnetic interference (EMI),” *IEEE Southcon/94. Conference Record*, 1994.

[43] G. B. Stanley E. Zocholl, “HOW MICROPROCESSOR RELAYS RESPOND TO HARMONICS, SATURATION, AND OTHER WAVE DISTORTIONS,” Schweitzer

Engineering Laboratories, Inc., Pullman, 1998.

[44] “PARTIAL REGRESSION PLOT,” National Institute of Standards and Technology, [Online]. Available: http://www.itl.nist.gov/div898/software/dataplot/refman1/auxillar/partregr.htm.

[45] C. S. P. D. C. R. L. S. S. Chet Davis, “Practical Solution Guide to Arc Flash Hazards,” ESA, Inc., 2003.

[46] T. Gammon, ““electric arc” key term,” *unpublished analysis of OSHA records,* Sept. 2008.

[47] J. D. Teresi, “A review of research on flash blindness,” Radiological Defense Laboratory, San Francisco, California, 1968.

[48] L. L. H. M. Luckiesh, “Glare and Visibility,” *Transactions of the Illuminating Engineering Society,* vol.20, pp. 221-252, 1925.

[49] R. H. J. K. S. G. R. A. Wilson, “Tripping with the speed of light: arc flash protection,” *Proceedings of the 60th Annual Conference for Protective Relay Engineers*, College Station, Texas, 2007.

[50] “Electro Magnetic Spectrum and light,” [Online]. Available: http://9-4fordham.wikispaces.com/Electro+Magnetic+Spectrum+and+light.

[51] Crawford, “The scotopic visibility function,” *Proceedings of the Physical Society*, 1949.

[52] “CIE Proceedings,” Bureau Central de la CIE, Paris, 1951.

[53] G. &. S. W. S. Wyszecki, Color Science: concepts and methods, quantitative data and formulae. (2nd ed.), New York: Wiley, 1982.

[54] T. G. Z. Z. B. J. a. S. V. Wei-Jen Lee, “IEEE/NFPA Collaboration on Arc Flash Phenomena Research Project,” *IEEE-PES, T&D Expo*, Orlando, May 2012.

[55] “Light Sensors,” [Online]. Available: http://www.electronics-utorials.ws/io/io_4.html.

[56] A. V. W. K. Christine Rüth, “Ambient Light Sensors General Application Note,” 2006.

[57] “Construction and Characteristics of CdS Cells,” [Online]. Available: http://www.selcoproducts.com/pdfs/Photocell%20Contstruction%20and%20Characteristics.pdf.

[58] A. V. Christine Rüth, “Application Note for High accuracy Ambient Light Sensor,” 2006.

[59] J. Das, *Arc Flash Hazardanalysis And Mitigation*, John Wiley & Sons, Inc., 2012, pp. 306-314,.

[60] “SFH5711 Datasheet,” [Online]. Available: http://www.osram-os.com/.

[61] R. Hanke, “Filter-Faszination,” Monheim/Bayern, p. 70.

[62] “Camera Lens Filters,” [Online]. Available: http://www.cambridgeincolour.com/tutorials/camera-lens-filters.htm.

[63] R. H. Lee, “Pressures developed by arcs,” *IEEE Transactions on Industry Applications,* vol.%1，共 %2 vol. IA-23, no.4, pp. 760-764, July/Aug. 1987.

[64] G. L. Wallace, “Blast injury basics: A guide for the medical speech-language pathologist,” *The ASHA Leader,* vol.11, no.9, pp. 26-28.

[65] Wikipedia, “Blast injury,” [Online]. Available: http://en.wikipedia.org/wiki/ Blast_injury.

[66] “Explosions and blast injuries: A primer for clinicians,” Center for Disease Control,

May 9, 2003.

[67] M. D. a. F. Nadeau, “Pressure waves due to arcing faults in a substation,” *IEEE Transactions on Power Apparatus and Systems,* vol.98, no.5, pp. 1632-1635, 1979.

[68] J. J. A. H. a. R. A. E. G. E. Heberlein, “Report on enclosure internal arcing tests,” *IEEE Industry Applications Magazine,* vol.2, no.3, pp. 35-42, May/June 1996.

[69] Wikipedia, “Pressure sensor,” [Online]. Available: http://en.wikipedia.org/wiki/Pressure_sensor.

[70] Wikipedia, “Piezoelectric sensor,” [Online]. Available: https://en.wikipedia.org/wiki/Piezoelectric_sensor.

[71] Wikipedia, “Pressure measurement,” [Online]. Available: https://en.wikipedia.org/wiki/Pressure_measurement#Absolute.2C_gauge_and_differential_pressures_-_zero_reference.

[72] Wikipedia, “Linear variable differential transformer,” [Online]. Available: https://en.wikipedia.org/wiki/Linear_variable_differential_transformer.

[73] OSHA, “Permissible noise exposure (29 CFR1910.25)”.

[74] A. L. J. M. T. Stanford, Physics for Students of Science and Engineering, New York: Harcourt Brace Jovanovich, 1985.

[75] [Online]. Available: http://www.ptme.com/et/audio/reference/sound/dB-SPL.htm.

[76] C. f. D. C. a. Prevention, “NOISE AND HEARING LOSS PREVENTION,” [Online]. Available: http://www.cdc.gov/niosh/topics/noise/chart-carpenters.html.

[77] Wikipedia, “A-weighting,” [Online]. Available: https://en.wikipedia.org/wiki/A-weighting.

[78] “Understanding Decibels,” [Online]. Available: ccms.ntu.edu.tw/~karchung/decibels/decibels1.ppt.

[79] Wikipedia, “Paschen’s law,” [Online]. Available: http://en.wikipedia.org/wiki/Paschen%27s_law.

[80] M. T. C. F. G. R. Jones, “The physics of high-power arcs,” *Reports on Progress in Physics,* vol.43, pp. 1416-1465, 1980.

[81] R. Wilkins, “Simple Improved Equations for Arc Flash Hazard Analysis,” July 2004.

[82] M. M. L. R. Wilkins, “Improved Method for Arc Flash Hazard Analysis,” *IEEE Industrial and Commercial Power Systems Technical Conference*, Clearwater Beach, Florida, USA, 2004.

Biographical Information

Zhenyuan Zhang received Ph.D. degree in electrical engineering at the Energy Systems Research Center, Department of Electrical Engineering, the University of Texas at Arlington, Arlington, Texas, USA, in 2015, and the B.S degree from Chang'an University, Xi'an, China, in 2007. His focus lies in arc flash research, but he has also been involved in hybrid energy storage, smart grids, renewable energy, electrical safety analysis, and power systems analysis. Since 2010 Zhenyuan has served as the project associate for the IEEE/NFPA Arc Flash Research Project.